CHAPTER 4

REACTOR

4.1 SUMMARY DESCRIPTION

•→10
The reactor assembly consists of the reactor vessel, its internal components consisting of the core, shroud, steam separator and dryer assemblies, and jet pumps. Also included in the reactor assembly are the control rods, the control rod drives (CRD), and the CRD housings. Fig. 3.9B-7 shows the arrangement of reactor assembly components. A summary of the important design and performance characteristics is given in Section 1.3.1. Loading conditions for reactor assembly components are specified in Section 3.9.5.2B.
10←•

4.1.1 Reactor Vessel

The reactor vessel design and description are covered in Section 5.3.

4.1.2 Reactor Internal Components

The major reactor internal components are the core (fuel, channels, control blades, and instrumentation), the core support structure (including the shroud, top guide, and core plate), the shroud head and steam separator assembly, the steam dryer assembly, the feedwater spargers, the core spray spargers, and the jet pumps. Except for the Zircaloy in the reactor core, these reactor internals are stainless steel or other corrosion-resistant alloys. The fuel assemblies (including fuel rods and channel), control blades, incore instrumentation, shroud head and steam separator assembly, and steam dryers are removable when the reactor vessel is opened for refueling or maintenance.

4.1.2.1 Reactor Core

4.1.2.1.1 General

The design of the boiling water reactor (BWR) core, including fuel, is based on the proper combination of many design variables and operating experience. These factors contribute to the achievement of high reliability.

A number of important features of the BWR core design are summarized in the following paragraphs:

1. The BWR core mechanical design is based on conservative application of stress limits, operating experience, and experimental test results. The moderate pressure level characteristics of a direct cycle reactor (approximately 1,000 psia) result in moderate cladding temperatures and stress levels.

2. The low coolant saturation temperature, high heat transfer coefficients, and neutral water chemistry of the BWR are significant, advantageous factors in minimizing Zircaloy temperature and associated temperature-dependent corrosion and hydride buildup.

   The relatively uniform fuel cladding temperatures throughout the core minimize migration of the hydrides to cold cladding zones and reduce thermal stresses.

3. The basic thermal and mechanical criteria applied in the design have been proven by irradiation of statistically significant quantities of fuel. The design heat transfer rates and linear heat generation rates (LHGR) are similar to values proven in fuel assembly irradiation.

4. The design power distribution used in sizing the core represents a worst expected state of operation.

•→15

5. The GNF thermal analysis basis, GETAB, with revised methodology and improved uncertainties utilizing the GEXL-Plus critical power correlations as described in GESTAR (Reference 12) is applied to assure that more than 99.9 percent of the fuel rods in the core are expected to avoid boiling transition for the most severe moderate frequency transient described in Chapter 15. The possibility of boiling transition occurring during normal reactor operation is insignificant.

15←•

6. Because of the large negative moderator density coefficient of reactivity, the BWR has a number of inherent advantages. These are the uses of coolant flow for load following, the inherent self-flattening of the radial power distribution, the ease of control, the spatial xenon stability, and the ability to override xenon in order to follow load.

BWRs do not have instability problems due to xenon. This has been demonstrated by special tests which have been conducted on operating BWRs in an attempt to force the reactor into xenon instability and by calculations. No xenon instabilities have ever been observed in the test results. All of these indicators have proven that xenon transients are highly damped in a BWR due to the large negative power coefficient of reactivity(1).

Important features of the reactor core arrangement are as follows:

•→8

1. The bottom-entry cruciform control rod blades (CRBs) are a mix of the General Electric original equipment (OE) CRBs and functional equivalents. Figure 4.2-5 shows CRBs currently utilized at RBS.

8←•

•→8

The OE control rods consist of boron carbide (B_4C) in longitudinal stainless steel tubes surrounded by a stainless steel sheath. Rods of this design have been irradiated for more than 8 years in the Dresden-1 reactor and have accumulated thousands of hours of service without significant failure in operating BWRs.

Both the GE Marathon control rod and GE Marathon Ultra HD control rod were designed to be a direct replacement for any BWR/6 control rod.

The ABB CR-82M control rods are equivalent to the OE control rods, with some internal design characteristics that differ from the OE control blades. The ABB control blades use both (B_4C) and Hafnium as the absorber material that is added in horizontal holes in the blade of the control rod. Other differences include a lower weight, use of 316L SS in the rod wing and handle, and less Stellite on the wear surfaces.

•←8

2. The fixed incore fission chambers provide continuous power range neutron flux monitoring. A guide tube in each incore assembly provides for a traversing ion chamber for calibration and axial detail. Source and intermediate range detectors are located incore and are axially retractable. The incore location of the startup and source range instruments provides coverage of the large reactor core and provides an acceptable signal-to-noise ratio and neutron-to-gamma ratio. All incore instrument leads enter from the bottom, and the instruments are in service during refueling. Incore instrumentation is discussed in Section 7.6.1.3.

3. As shown by experience obtained at Dresden-1 and other plants, the operator, utilizing the incore flux monitor system, can maintain the desired power distribution within a large core by proper control rod scheduling.

•→15 •→10

4. The Zircaloy-2, Zircaloy-4, and NSF reusable channels provide a fixed flow path for the boiling coolant, serve as a guiding surface for the control rods, and protect the fuel during handling operations.

10←• 15←•

5. The mechanical reactivity control permits criticality checks during refueling and provides maximum plant safety. The core is designed to be subcritical at any time in its operating history with any one control rod fully withdrawn.

6. The selected control rod pitch represents a practical value of individual control rod reactivity worth and allows adequate clearance below the pressure vessel between CRD mechanisms for ease of maintenance and removal.

4.1.2.1.2 Core Configuration

•→15 •→1
The reactor core is arranged as an upright circular cylinder containing a large number of fuel cells and is located within the reactor vessel. The coolant flows upward through the core. The reload core loading pattern is given in Reference 27 of Appendix 15B. The lattice details are given in Reference 12, Section 2, Reference 13, and Reference 19 for GE fuel.

4.1.2.1.3 Fuel Assembly Description

As can be seen from the above references and appendix, the BWR core is composed of essentially two components -- fuel assemblies and control rods. The control rod mechanical configurations, Fig. 4.2-4, are basically the same as used in Dresden-1 and in all subsequent GE BWRs. The reload fuel assembly configuration is given in Reference 13 for GE fuel.
1←• 15←•

4.1.2.1.4 Assembly Support and Control Rod Location

A few peripheral fuel assemblies are supported by the core plate. Otherwise, individual fuel assemblies in the core rest on fuel support pieces mounted on top of the control rod guide tubes. Each guide tube, with its fuel support piece, bears the weight of four assemblies and is supported by a CRD penetration nozzle in the bottom head of the reactor vessel. The core plate provides lateral support and guidance at the top of each control rod guide tube.
•→8
The top guide, mounted on top of the shroud, provides lateral support and guidance for the top of each fuel assembly. The reactivity of the core is controlled by cruciform control rods, containing neutron absorber materials, and their associated mechanical hydraulic drive systems. The control rods occupy alternate spaces between fuel assemblies. Each independent drive enters the core from the bottom and can accurately position its associated control rod during normal operation and yet exert approximately 10 times the force of gravity to insert the control rod during the scram mode of operation. Bottom entry allows optimum power shaping in the core, ease of refueling, and convenient drive maintenance.
•←8

4.1.2.2 Shroud

The information on the shroud is contained in Section 3.9.5.1.1.1B.

4.1.2.3 Shroud Head and Steam Separators

The information on the shroud head and steam separators is contained in Section 3.9.5.1.1.3B.

4.1.2.4 Steam Dryer Assembly

The information on the steam dryer assembly is contained in Section 3.9.5.1.1.9B.

4.1.3 Reactivity Control Systems

4.1.3.1 Operation

The control rods perform dual functions of power distribution shaping and reactivity control. Power distribution in the core is controlled during operation of the reactor by manipulation of selected patterns of rods. The rods, which enter from the bottom of the near-cylindrical reactor core, are positioned in such a manner as to counterbalance steam voids in the top of the core and affect significant power flattening.

These groups of control elements, used for power flattening, experience a somewhat higher duty cycle and neutron exposure than the other rods in the control system.

The reactivity control function requires that all rods be available for either reactor scram (prompt shutdown) or reactivity regulation. Because of this, the control elements are mechanically designed to withstand the dynamic forces resulting from a scram. They are connected to bottom-mounted, hydraulically actuated drive mechanisms which allow either axial positioning for reactivity regulation or rapid scram insertion. The design of the rod-to-drive connection permits each blade to be attached or detached from its drive without disturbing the remainder of the control system. The bottom-mounted drives permit the entire control system to be left intact and operable for tests with the reactor vessel open.

4.1.3.2 Description of Control Rods

•→8
The General Electric original equipment (OE) cruciform shaped control rods contain 72 stainless steel tubes (18 tubes in each wing of the cruciform) filled with vibration compacted B_4C powder. The tubes are seal welded with end plugs on either end. Stainless steel balls are used to separate the tubes into individual compartments. The stainless steel balls are held in position by a slight crimp in the tube. The individual tubes provide containment of the helium gas released by the boron-neutron capture reaction.
8←•
The tubes are welded in a cruciform array. Some models have a stainless steel sheath extending the full length of the tubes. A top handle, shown on Fig. 4.2-4, aligns the tubes and provides structural rigidity at the top of the control rod. Rollers housed in the handle provide guidance for control rod insertion and withdrawal. A bottom casting is also used to provide structural rigidity and contains positioning rollers and a

parachute-shaped velocity limiter. The handle and lower casting are welded into a single structure by means of a small cruciform post located in the center of the control rod. The control rods can be positioned at 6-in steps and have a nominal withdrawal and insertion speed of 3 in/sec.

The velocity limiter is a device which is an integral part of the control rod and protects against the low probability of a rod drop accident. It is designed to limit the free fall velocity and reactivity insertion rate of a control rod so that minimum fuel damage would occur. It is a one-way device, in that control rod scram time is not significantly affected.

Both the GE Marathon control rod and GE Marathon Ultra HD control rod were designed to be a direct replacement for any BWR/6 control rod.

•→8
The ABB CR-82M control blades contain 547 horizontal holes of B_4C and 24 horizontal holes of Hafnium absorber material in the 316L stainless steel control rod blade. The velocity limiter, top handle, and positioning rollers for the ABB control rods are the same in design and function as those for the OE control rods.
•←8
Control rods are cooled by the core leakage (bypass) flow. The core leakage flow is made up of recirculation flow that leaks through the several leakage flow paths shown on Fig. 4.4-1, the most important of which are:

1. The area between the fuel channel and the fuel assembly lower tie plate

2. Holes in the lower tie plate

3. The area between the fuel assembly lower tie plate and the fuel support piece

4. The area between the fuel support piece and the control rod guide tube

5. The area between the control rod guide tube and the core support plate

6. The area between the core support plate and the shroud.

4.1.3.3 Supplementary Reactivity Control

The initial and reload core control requirements are met by use of the combined effects of the movable control rods, supplementary burnable poison, and variation of reactor coolant flow. The supplementary burnable poison is gadolinia (Gd_2O_3) mixed with UO_2 in selected fuel rods in each fuel bundle.

4.1.4 Analysis Techniques

4.1.4.1 Reactor Internal Components

•→6
Computer codes used for the analysis of the internal components are as follows:

1. MASS
2. SNAP (MULTISHELL)
3. GASP
4. NOHEAT
5. FINITE
6. DYSEA
7. SHELL 5
8. HEATER
9. FAP-71
10. CREEP-PLAST
11. ANSYS
12. ANSYS05V

6←•
Detail descriptions of these programs are given in the following sections.

4.1.4.1.1 MASS (Mechanical Analysis of Space Structure)

4.1.4.1.1.1 Program Description

The program, proprietary to GE, is an outgrowth of the PAPA (plate and panel analysis) program originally developed by L. Beitch in the early 1960s. The program is based on the principle of the finite element method. Governing matrix equations are formed in terms of joint displacements using a "stiffness-influence-coefficient" concept originally proposed by L. Beitch (2). The program offers curved beam, plate, and shell elements. It can handle mechanical and thermal loads in a static analysis and predict natural frequencies and mode shapes in a dynamic analysis.

4.1.4.1.1.2 Program Version and Computer

•→1
GE is using a past revision of MASS. This revision is identified as Revision 0 in the computer production library. The program operates on the Honeywell 6000 computer.
1←•

4.1.4.1.1.3 History of Use

Since its development in the early 1960s, the program has been successfully applied to a wide variety of jet engine structural problems, many of which involve extremely complex geometries. The use of the program by GE started shortly after its development.

4.1.4.1.1.4 Extent of Application

•→1
Besides the nuclear and aircraft engine divisions, the missile and space division, the appliance division, and the turbine division of GE have also applied the program to a wide range of engineering problems. The GE nuclear division uses it mainly for piping and reactor internals analyses.
1←•

4.1.4.1.2 SNAP (MULTISHELL)

4.1.4.1.2.1 Program Description

The SNAP program, also called MULTISHELL, is the GE code which determines the loads, deformations, and stresses of axisymmetric shells of revolution (cylinders, cones, discs, toroids, and rings) for axisymmetric thermal boundary and surface load conditions. Thin shell theory is inherent in the solution of E. Peissner's differential equations for each shell's influence coefficients. Surface loading capability includes pressure, average temperature, and linear through-wall gradients; the latter two may be linearly varied over the shell meridian. The theoretical limitations of this program are the same as those of classical theory.

4.1.4.1.2.2 Program Version and Computer

•→1
The current version, maintained by the GE aircraft engine division at Evandale, Ohio, is being used on the Honeywell 6000 computer.

4.1.4.1.2.3 History of Use

The initial version of the shell analysis program was completed by the aircraft engine division in 1961. Since then, a considerable amount of modification and addition has been made to accommodate its broadening area of application. Its application in the GE nuclear division has a history longer than 10 yr.

4.1.4.1.2.4 Extent of Application

The program has been used to analyze jet engine, space vehicle, and nuclear reactor components. Because of its efficiency and economy, in addition to reliability, it has been one of the main shell analysis programs in GE.
1←•

4.1.4.1.3 GASP

4.1.4.1.3.1 Program Description

GASP is a finite element program for the stress analysis of axisymmetric or plane two-dimensional geometries. The element representations can be either quadrilateral or triangular. Axisymmetric or plane structural loads can be input at nodal points. Displacements, temperatures, pressure loads, and axial inertia can be accommodated. Effective plastic stress and strain distributions can be calculated using a bilinear stress-strain relationship by means of an iterative convergence procedure.

4.1.4.1.3.2 Program Version and Computer

The GE version, originally obtained from the developer, Professor E. L. Wilson, operates on the Honeywell 6000 computer.

4.1.4.1.3.3 History of Use

•→1
The program was developed by E. L. Wilson in 1965[3]
The present version in GE has been in operation since 1967.

4.1.4.1.3.4 Extent of Application

The application of GASP in GE is mainly for elastic analysis of axisymmetric and plane structures under thermal and pressure loads. The GE version has been extensively tested and used by GE engineers.
1←•

4.1.4.1.4 NOHEAT

4.1.4.1.4.1 Program Description

The NOHEAT program is a two-dimensional and axisymmetric, transient, nonlinear temperature analysis program. An unconditionally stable numerical integration scheme is combined with an iteration procedure to compute temperature distribution within the body subjected to arbitrary time-and temperature-dependent boundary conditions.

This program utilizes the finite element method. Included in the analysis are the three basic forms of heat transfer - conduction, radiation, and convection - as well as internal heat generation. In addition, cooling pipe boundary conditions are also treated. The output includes temperature of all the nodal points for the time instants specified by the user. The program can handle multitransient temperature input.

4.1.4.1.4.2 Program Version and Computer

The current version of the program is an improvement of the program originally developed by I. Farhoomand and Professor E. L. Wilson of the University of California at Berkeley[4]. The program operates on the Honeywell 6000 computer.

4.1.4.1.4.3 History of Use

The program was developed in 1971 and installed in the GE Honeywell computer by one of its original developers, I. Farhoomand, in 1972. A number of heat transfer problems related to the reactor pedestal have been satisfactorily solved using the program.

4.1.4.1.4.4 Extent of Application

The program using finite element formulation is compatible with the finite element, stress-analysis computer program GASP. Such compatibility simplifies the connection of the two analyses and minimizes human error.

4.1.4.1.5 FINITE

4.1.4.1.5.1 Program Description

FINITE is a general-purpose, finite element computer program for elastic stress analysis of two-dimensional structural problems, including 1) plane stress, 2) plane strain, and 3) axisymmetric structures. It has provision for thermal, mechanical, and body force loads. The materials of the structure may be homogeneous or nonhomogeneous and isotropic or orthotropic. The development of the FINITE program is based on the GASP program (Section 4.1.4.1.3).

4.1.4.1.5.2 Program Version and Computer

•→1
The present version of the program at GE nuclear division was obtained from the developer, J. E. McConnelee, of the GE gas turbine department in 1969[5]. The program is used on the Honeywell 6000 computer.

4.1.4.1.5.3 History of Use

Since its completion in 1969, the program has been widely used in the gas turbine and the aircraft engine departments of GE for the analysis of turbine components.
1←•

4.1.4.1.5.4 Extent of Usage

•→1
The program is used in the analysis of axisymmetric or nearly axisymmetric BWR internals.
1←•

4.1.4.1.6 DYSEA (Dynamic and Seismic Analysis)

4.1.4.1.6.1 Program Description

The DYSEA program is a GE proprietary program developed specifically for seismic and dynamic analysis of the reactor pressure vessel (RPV) and internals/building system. It calculates the dynamic response of linear structural systems by either temporal modal superposition or response spectrum method. Fluid-structure interaction effect in the RPV is taken into account by way of hydrodynamic mass.

Program DYSEA was based on program SAPIV, with added capability to handle the hydrodynamic mass effect. Structural stiffness and mass matrices are formulated similarly to SAPIV. Solution is obtained in time domain by calculating the dynamic response mode by mode. Time integration is performed by using Newmark's B-method. Response spectrum solution is also available as an option.

4.1.4.1.6.2 Program Version and Computer

•→1
The DYSEA version now operating on the Honeywell 6000 computer was developed at GE by modifying the SAPIV program. Capability was added to handle the hydrodynamic mass effect due to fluid-structure interaction in the reactor. It can handle three-dimensional dynamic problems with beam, trusses, and springs. Both acceleration time histories and response spectra may be used as input.
1←•

4.1.4.1.6.3 History of Use

The DYSEA program was developed in the summer of 1976. It has been adopted as a standard production program since 1977 and has been used extensively in all dynamic and seismic analyses of the RPV and internals/building system.

4.1.4.1.6.4 Extent of Application

The current version of DYSEA has been used in all dynamic and seismic analyses since its development. Results from test problems were found to be in close agreement with those obtained from either verified programs or analytic solutions.

4.1.4.1.7 SHELL 5

4.1.4.1.7.1 Program Description

SHELL 5 is a finite shell element program used to analyze smoothly curved thin shell structures with any distribution of elastic material properties, boundary constraints, and mechanical thermal and displacement loading conditions. The basic element is triangular whose membrane displacement fields are linear polynomial functions and whose bending displacement field is a cubic polynomial function[6]. Five degrees of freedom (three displacements and two bending rotations) are obtained at each nodal point. Output displacements and stresses are in a local (tangent) surface coordinate system.

Due to the approximation of element membrane displacements by linear functions, the in-plane rotation about the surface normal is neglected. Therefore, the only rotations considered are due to bending of the shell cross section, and application of the method is not recommended for shell intersection (or discontinuous surface) problems where in-plane rotation can be significant.

4.1.4.1.7.2 Program Version and Computer

•→1
SHELL 5 operates on the UNIVAC 1108 computer.
1←•

4.1.4.1.7.3 History of Use

SHELL 5 is a program developed by Gulf General Atomic Incorporated in 1969[7]. The program has been in production status at Gulf General Atomic, GE, and other major computer operating systems since 1970.

4.1.4.1.7.4 Extent of Application

SHELL 5 has been used at GE to analyze reactor shroud support and torus. Satisfactory results were obtained.

4.1.4.1.8 HEATER

4.1.4.1.8.1 Program Description

HEATER is a computer program used in the hydraulic design of feedwater spargers and their associated delivery headers and piping. The program utilizes test data obtained by GE using full scale mockups of feedwater spargers combined with a series of models which represent the complex mixing processes obtained in the upper plenum, downcomer, and lower plenum. Mass and energy balances throughout the nuclear steam supply system are modeled in detail[8].

4.1.4.1.8.2 Program Version and Computer

•→1
This program was developed at GE in FORTRAN IV for the Honeywell 6000 computer.

4.1.4.1.8.3 History of Use

The program was developed by various individuals in GE beginning in 1970. The present version of the program has been in operation since January 1972.
1←•
4.1.4.1.8.4 Extent of Application

The program is used in the hydraulic design of the feedwater spargers for each BWR plant, in the evaluation of design modifications, and in the evaluation of unusual operational conditions.

4.1.4.1.9 FAP-71 (Fatigue Analysis Program)

4.1.4.1.9.1 Program Description

The FAP-71 computer code is a stress analysis tool used to aid in performing ASME III Boiler and Pressure Vessel Code structural design calculations. Specifically, FAP-71 is used in determining the primary plus secondary stress range and number of allowable fatigue cycles at points of interest. For structural locations at which the 3S (P+Q) ASME Code limit is exceeded, the program can perform either (or both) of two elastic-plastic fatigue life evaluations: 1) the method reported in ASME Paper 68-PVP-3, or 2) the present method documented in Paragraph NB-3228.3 of the 1971 Edition of the ASME Section III Boiler and Pressure Vessel Code. The program can accommodate up to 25 transient stress states of as many as 20 structural locations.

4.1.4.1.9.2 Program Version and Computer

•→1
The present version of FAP-71 was completed by L. Young of GE in 1971[9]. The program currently is on the Honeywell 6000 computer.
1←•
4.1.4.1.9.3 History of Use

Since its completion in 1971, the program has been applied to several design analyses of GE BWR vessels.

4.1.4.1.9.4 Extent of Use

The program is used in conjunction with several shell analysis programs in determining the fatigue life of BWR mechanical components subject to thermal transients.

4.1.4.1.10 CREEP/PLAST

4.1.4.1.10.1 Program Description

A finite element program is used for the analysis of two-dimensional (plane and axisymmetric) problems under conditions of creep and plasticity. The creep formulation is based on the memory theory of creep in which the constitutive relations are cast in the form of hereditary integrals. The material creep properties are built into the program, and they represent annealed 304 stainless steel. Any other creep properties can be included if required.

The plasticity treatment is based on kinematic hardening and von Mises yield criterion. The hardening modulus can be constant or a function of strain.

4.1.4.1.10.2 Program Version and Computer

The program can be used for elastic-plastic analysis with or without the presence of creep. It can also be used for creep analysis without the presence of instantaneous plasticity. A detailed description of theory is given in Reference 11. The program is operative on Univac-1108.

4.1.4.1.10.3 History of Use

This program was developed by Y. R. Rashid in 1971[11] It underwent extensive program testing before it was put on production status.

4.1.4.1.10.4 Extent of Application

•→1
The program is used at GE in the channel cross section mechanical analysis.
1←•

4.1.4.1.11 ANSYS

4.1.4.1.11.1 Program Description

ANSYS is a general-purpose finite element computer program designed to solve a variety of problems in engineering analysis.

The ANSYS program features the following capabilities:

1. Structural analysis, including static elastic, plastic and creep, dynamic, seismic and dynamic plastic, and large deflection and stability analysis.

2. One-dimensional fluid flow analyses.

3. Transient heat transfer analysis, including conduction, convection, and radiation with direct input to thermal-stress analyses.

4. An extensive finite element library, including gaps, friction interfaces, springs, cables (tension only), direct interfaces (compression only), curved elbows, etc. Many of the elements contain complete plastic, creep, and swelling capabilities.

5. Plotting - Geometry plotting is available for all elements in the ANSYS library, including isometric and perspective views of three-dimensional structures.

6. Restart Capability - The ANSYS program has restart capability for several types of analysis. An option is also available for saving the stiffness matrix once it is calculated for the structure and using it for other loading conditions.

4.1.4.1.11.2 Program Version and Computer

The program is maintained current by Swanson Analysis Systems, Inc of Pittsburgh, Pennsylvania, and is supplied to GE for use on the Honeywell 6000.

4.1.4.1.11.3 History of Use

The ANSYS program has been used for productive analysis since early 1970. Users now include the nuclear, pressure vessels and piping, mining, structures, bridge, chemical, and automotive industries, as well as many consulting firms.

4.1.4.1.11.4 Extent of Application

•→1

ANSYS is used extensively in GE for elastic and elastic-plastic analysis of the RPV, core support structures, reactor internals, and fuel.

•→6

4.1.4.1.12 ANSYS05V

4.1.4.1.12.1 Program Description

The ANSYS engineering analysis system, developed by Swanson Analysis Systems, Inc., is a fully warranted and documented computer program available at General Electric Nuclear Energy (GENE), where it is renamed ANSYS05V.

The ANSYS computer program, which has been used for production analysis since early 1970, is a large-scale, general-purpose computer program for the solution of several classes of engineering analysis problems. Analysis capabilities include: static and dynamic; plastic, creep, and swelling; small and large deflections; steady-state and transient heat transfer; and steady-state flow.

1←• 6←•

•→6 •→1
The matrix displacement method of analysis, based upon finite element idealization, is employed throughout the program. The library of finite elements available contains more than 30 elements for static and dynamic analyses and more than 210 for heat transfer and fluid flow analyses. This variety of elements gives the ANSYS05V program the capability of analyzing frame structures (two-dimensional frames, grids, and three-dimensional frames), piping systems, two-dimensional plane and axisymmetric solids, flat plates, three-dimensional solids, axisymmetric and three-dimensional shells and nonlinear problems, including interfaces and cables.

Loading on the structure may be forces, displacements, pressure, temperatures, or response spectra. Loadings for heat transfer analyses include: internal heat generation, convection, and radiation boundaries and specified temperatures or heat flow.

4.1.4.1.12.2 Extent of Use

ANSYS05V was used to determine temperature distributions, thermal stresses and pressure stresses for the stress and fatigue analysis of the replacement safe end and thermal sleeve. The heat transfer (KAN = -1) and static (KAN = 0) analysis options, and the 2-d axisymmetric solid thermal (STIF 55) and structural (STIF 42) element types used in the analysis are acceptable for design use and have been verified consistent with the GE approved quality assurance (QA) program (which also complies with 10 CFR 50 Appendix B).

4.1.4.1.12.3 Program Qualification

Qualification of ANSYS05V was performed by GENE and consisted of running the 203 verification problems provided by Swanson Analysis Systems, Inc. The problems are extracted from text books in which classical or theoretical solutions are published or can be readily obtained by simple hand calculations. Comparisons were made among the theoretical results, the verification problem solutions provided by Swanson Analysis Systems, Inc. and the ANSYS05V solutions. The 203 verification problems were used as the basis of the verification. A summary of the results of the verification is contained in Ref 14.

Close agreements (differences of less than 0.1%) were found between the solutions provided by Swanson Analysis Systems, Inc. and ANSYS05V, thereby demonstrating that ANSYS05V is technically acceptable and properly installed at GENE and has been verified consistent with the GE approved QA program.
6←•
4.1.4.2 Fuel Rod Thermal Analysis
•→15
Reference to fuel rod thermal design analyses are given in Section 2 of Reference 12 and in Reference 17.
1←• 15←•

4.1.4.3 Reactor Systems Dynamics

•→15 •→10

The analysis techniques and computer codes used in reactor system dynamics are described in Section 5 of Reference 10 for the initial cycle and Reference 16 for the current cycle. Section 4.4.4.6 also provides a complete stability analysis for the reactor coolant system.

10←• 15←•

4.1.4.4 Nuclear Engineering Analysis

The analysis techniques are described and referenced in Section 4.3.3. The codes used in the analysis are:

Computer Code	Function
Lattice physics model	Calculates average few-group cross sections, bundle reactivities, and relative fuel rod powers within the fuel bundle.
BWR reactor simulator	Calculates three-dimensional nodal power distributions, exposures, thermal-hydraulic characteristics as burnup progresses.

4.1.4.5 Neutron Fluence Calculations

•→4

Neutron vessel fluence calculations were carried out using a two-dimensional, discrete ordinates, S_n transport code with general anisotropic scattering.

This code is a widely used discrete ordinates code which will solve a wide variety of radiation transport problems. The program will solve both fixed source and multiplication problems. Slab, cylinder, and spherical geometries are allowed with various boundary conditions. The fluence calculations incorporate, as an initial starting point, neutron fission distributions prepared from core physics data as a distributed source. Anisotropic scattering was considered for all regions. The cross sections were prepared with 1/E flux weighted, P_1 matrices for anisotropic scattering but did not include resonance self-shielding factors.

Fast neutron fluxes at locations other than the core midplane were calculated using a second two-dimensional, discrete ordinate code. This second two-dimensional code is used to solve smaller sized problems, and is similar to the two-dimensional code used for the vessel neutron fluence calculations.

The fast neutron flux calculations are used to establish the ratio of flux between the surveillance capsule locations and the location of peak vessel inside surface flux, known as the lead factor. Use of the lead factor is discussed in Section 4.3.2.8.

4←•

Additional vessel fluence calculations, which comply with the requirements of Regulatory Guide 1.190, are described in Section 4.3.2.8.

4.1.4.6 Thermal-hydraulic Calculations

The digital computer program uses a parallel flow path model to perform the steady-state BWR reactor core thermal-hydraulic analysis. Program input includes the core geometry, operating power, pressure, coolant flow rate and inlet enthalpy, and power distribution within the core. Output from the program includes core pressure drop, coolant flow distribution, critical power ratio, and axial variations of quality, density, and enthalpy for each channel type.

References - 4.1

1. Crowther, R. L. Xenon Considerations in Design of Boiling Water Reactors, APED-5640, June 1968.

2. Beitch, L. Shell Structures Solved Numerically by Using a Network of Partial Panels, AIAA Journal, Volume 5, No. 3, March 1967.

3. Wilson, E. L. A Digital Computer Program For the Finite Element Analysis of Solids With Non-Linear Material Properties, Aerojet General Technical Memo No. 23, Aerojet General, July 1965.

4. Farhoomand, I. and Wilson, E. L. Non-Linear Heat Transfer Analysis of Axisymmetric Solids, SESM Report SESM71-6, University of California at Berkeley, Berkeley, California, 1971.

5. McConnelee, J. E. Finite-Users Manual, General Electric TIS Report DF 69SL206, March 1969.

6. Clough, R. W. and Johnson, C. P. A Finite Element Approximation For the Analysis of Thin Shells, International Journal Solid Structures, Vol. 4, 1968.

7. A Computer Program For the Structural Analysis of Arbitrary Three-Dimensional Thin Shells, Report No. GA-9952, Gulf General Atomic.

8. Burgess, A. B. User Guide and Engineering Description of HEATER Computer Program, March 1974.

9. Young, L. J., FAP-71 (Fatigue Analysis Program) Computer Code, GE/NED Design Analysis Unit R. A. Report No. 49, January 1972.

10. Carmichael, L. A. and Scatena, G. J. Stability and Dynamic Performance of the General Electric Boiling Water Reactor, January 1977 (NEDO-21506).

11. Rashid, Y. R. Theory Report for Creep-Plast Computer Program, GEAP-10546, AEC Research and Development Report, January, 1972.

•→6 •→3 •→1

12. General Electric Standard Application for Reactor Fuel, NEDE-24011-P-A, latest approved revision.

13. G. E. Fuel Bundle Designs, NEDE-31152P, latest approved revision.

14. Fujikawa, K. K. "ANSYSO5V Engineering Computer Program Software Test Report". GE-NE-523-145-1291. January 1992, contains GE proprietary information.

1←• 3←• 6←•

•→15
15. DELETED

16. NEDC-32339P-A, Supplement 1, "Reactor Stability Long-Term Solution: ODYSY Application to E1A," GE, December, 1996.

17. DELETED

18 DELETED
15←•
19. 003N9292, Revision 0, "Fuel Bundle Information Report for River Bend Station - Unit 1 Reload 19 Cycle 20," Global Nuclear Fuel - Americas, LLC, November, 2016. (Entergy Report # ECH-NE-16-00038, Revision 0).

•→1
4.2 FUEL SYSTEM DESIGN

4.2.1 Design Bases

•→15
The fuel mechanical design bases are provided in Subsection 2.2 of Reference 1. The fuel design basis establishes Linear Heat Generation Rate (LHGR) limits which shall not be exceeded during steady state operation.

Control rod design bases are covered in Subsection 4.2.1.1, and control rod reactivity is discussed in Subsection 4.3.1 and in Reference 2.
15←•

4.2.1.1 Control Assembly and Its Components

4.2.1.1.1 Safety Design Bases

The reactivity control mechanical design shall include control rods and gadolinia burnable poison in selected fuel rods within fuel assemblies and shall meet the following safety design bases.

1. The control rods shall have sufficient mechanical strength to prevent displacement of their reactivity control material.

2. The control rods shall have sufficient strength and be so designed as to prevent deformation that could inhibit their motion.

3. Each control rod shall have a device to limit its free fall velocity sufficiently to avoid damage to the nuclear system process barrier by the rapid reactivity increase resulting from a free fall of the control rod from its fully inserted position to the position where the drive was withdrawn.

The design basis of the initial core supplementary fuel/reactivity control rods $(UGd)_2$ is the same as UO_2 fuel rods. Additional information on urania-gadolinia physical and irradiation characteristics and material properties is provided in Reference 3.

4.2.1.1.2 Design Acceptability

The acceptability of the control rod and CRD under scram loading condition is demonstrated by functional testing instead of analysis of adherence to formally defined stress limits.
1←•

•→1
4.2.1.1.3 Control Rod Clearances

The basis of the mechanical design of the control rod clearances is that there shall be no interference which will restrict the passage of the control rod.

Layout studies are performed to assure that, given the worst combination of extreme detail part tolerance ranges at assembly, no interference exists which will restrict the passage of control rods. In addition, preoperational verification is made on each control rod system to demonstrate that the acceptable levels of operational performance are met.

4.2.1.1.4 Mechanical Insertion Requirements

Mechanical insertion requirements during normal operation are selected to provide adequate operability and load following capability, and to be able to control the reactivity addition resulting from burnout of peak shutdown xenon at 100 percent power.

Scram insertion requirements are chosen to provide sufficient negative reactivity to meet all safety criteria for plant operational transients.

4.2.1.1.5 Material Selection

•→8
The selection of materials for use in the control rod design is based upon their in-reactor properties. The irradiated properties of Type 304 and 316L austenitic stainless steel, which comprise the major portions of the assembly, B_4C and Hafnium powder, Alloy X-750, and Stellite are well known and are taken into account in establishing the design of the control rod components. The Marathon design uses a high purity stabilized enhanced type 304 stainless steel, referred to as RAD RESIST 304S, to provide high resistance to irradiation-assisted corrosion cracking. Niobium and Tantalum are added to the high purity 304 stainless steel to provide greater protection against stress corrosion cracking. HP348 stainless steel of similar property has been demonstrated successfully in both control rod absorber tube and fuel cladding applications. HP348 stainless steel absorber tube material has achieved approximately 3% cladding strain at 100% burnup without failure. The basic cruciform control rod design and materials have been operating successfully in all GE reactors.
8←•

4.2.1.1.6 Radiation Effects

The radiation effects on B_4C powder include the release of gaseous products and swelling.

The B_4C cladding is designed to sustain the resulting internal pressure buildup due to gaseous products and the lifetime of the control rod has been established to minimize the effects of swelling. The corrosion rate and the physical properties, e.g., density, modulus of elasticity, dimensional aspects, etc., of austenitic stainless steel, and Alloy X-750 are essentially unaffected by the irradiation experienced in the BWR reactor core. The effects upon the mechanical properties, i.e., yield strength, ultimate tensile strength, percent elongation, and ductility on the 304 stainless steel cladding also are well known and are considered in mechanical design.
1←•

• →1

4.2.1.1.7 Positioning Requirements

Rod positioning increments (not lengths) are selected to provide adequate power shaping capability. The combination of rod speed and notch length must also meet the limiting reactivity addition rate criteria.

4.2.2 Description and Design Drawings

• →15 • →10 • →6 • →4

The fuel assemblies are described in Subsection 2.1 of Reference 1 for GE fuel. Fuel bundle specific information is provided in Reference 4 and Chapter 15B. The reactivity control assembly is discussed below.

4←• 6←• 10←• 15←•

4.2.2.1 Reactivity Control Assembly

• →8

4.2.2.1.1.1 GE Original Equipment Control Rods

• →10

The GE original equipment control rods perform the dual function of power shaping and reactivity control. A design drawing of the control blade is seen in Fig. 4.2-4. Power distribution in the core is controlled during operation of the reactor by manipulating selected patterns of control rods. Control rod displacement tends to counterbalance steam void effects at the top of the core and results in significant power flattening.

10←• 8←•

The control rod consists of a cruciform array of stainless steel tubes filled with B_4C powder. The control rods are 9.804-nominal span and are separated uniformly through the core on a 12-inch pitch maximum. Each control rod is surrounded by four fuel assemblies.

The main structural member of a control rod is made of Type 304 stainless steel and consists of a top handle, a bottom casting with a velocity limiter and CRD coupling, a vertical cruciform center post, and on some models, four U-shaped absorber tube sheaths. The top handle, bottom casting, and center post are welded into a single skeletal structure.

The U-shaped sheaths are resistance welded to the center post, handle, and castings to form a rigid housing to contain the B_4C-filled absorber rods. Rollers at the top and bottom of the control rod guide the control rod as it is inserted and withdrawn from the core. The control rods are cooled by the core bypass flow. The U-shaped sheaths are perforated to allow the coolant to circulate freely about the absorber tubes. Operating experience has shown that control rods constructed as described above are not susceptible to dimensional distortions.

1←•

•→1
The B_4C powder in the absorber tubes is compacted to about 70 percent of its theoretical density. The B_4C contains a minimum of 76.5 percent by weight natural boron. The boron-10 (B-10) minimum content of the boron is 18 percent by weight. Absorber tubes are made of Type 304 stainless steel. Each absorber tube is 0.220 inches in outside diameter and has a 0.027-in wall thickness. Absorber tubes are sealed by a plug welded into each end. The B_4C is longitudinally separated into individual compartments by stainless steel balls at approximately 17-in intervals. The steel balls are held in place by a slight crimp of the tube. Should B_4C tend to compact further in service, the steel balls will distribute the resulting voids over the length of the absorber tube.
•→8
4.2.2.1.1.2 ABB CR-82M and CR-82M-1 Control Rods

The ABB CR-82M control rods, Figure 4.2-5A, are equivalent to the GE original equipment control rods, with some internal design characteristics that differ from the OE control blades. The ABB control blades use both (B_4C) and Hafnium as the absorber material that is added in horizontal holes of B_4C and 24 horizontal holes of Hafnium of absorber material in the 316L stainless steel control rod blades. The velocity limiter, top handle, and positioning rollers for the ABB control rods are the same in design and function as those for the OE control rods. Other differences include a lower weight, use of 316L SS in the rod wing and handle, and less Stellite on the wear surfaces. The CR82M-1 blade model is a revision to the CR82M model, with some differences in the absorber tube sizes and pitch being the difference between the two blade models (Figure 4.2-5).
•←8
4.2.2.1.1.3 GE Marathon Control Rods

The GE Marathon control rod, Figure 4.2-5B, was designed to be compatible with, and a direct replacement for, any of the current control rod assemblies in the BWR/6 S lattice core configurations. The envelope dimensions within the core for the Marathon control rods are the same as the original equipment control rods and the initial reactivity worth is approximately equal to the original equipment control rods. The structural material used in the Marathon control rod is HP304S stainless steel. This material is less susceptible to Irridiation Assisted Corrosion Cracking. The absorbing material contained in the GE Marathon rods consistes of both B4C and hafnium which provides a 20% higher boron-10 capture level than the GE original equipment design.

4.2.2.1.2 Velocity Limiter

The control rod velocity limiter (Fig. 4.2-6) is an integral part of the bottom assembly of each control rod. This engineered safeguard limits the amount and rate of reactivity insertion in the event of a control rod drop accident in such a way that the peak fuel pellet enthalpy is less than the 280 cal/gm design limit. It is a one-way device in that the control rod scram velocity is not significantly affected but the control rod dropout velocity is reduced to a permissible limit.

The velocity limiter is in the form of two nearly mated, conical elements that act as a large clearance piston inside the control rod guide tube. The lower conical element is separated from the upper conical element by four radial spacers 90 degrees apart and is at a 15-degree angle relative to the upper conical element, with the peripheral separation less than the central separation.
1←•

•→1
The hydraulic drag forces on a control rod are proportional to approximately the square of the rod velocity and are negligible at normal rod withdrawal or rod insertion speeds. However, during the scram stroke the rod reaches high velocity, and the drag forces must be overcome by the drive mechanism. To limit control rod velocity during dropout, but not during scram, the velocity limiter is provided with a streamlined profile in the scram (upward) direction. Thus, when the control rod is scrammed, water flows over the smooth surface of the upper conical element into the annulus between the guide tube and the limiter. In the dropout direction, however, water is trapped by the lower conical element and discharged through the annulus between the two conical sections. Because the water is jetted in a partially reversed direction into water flowing upward in the annulus, a severe turbulence is created, thereby slowing the descent of the control rod assembly to less than 3.11 ft/sec.

The Marathon control rod is supplied with either the original velocity limiter design or the weight optimized design. The Marathon design is directly interchangeable with existing control assemblies.

4.2.3 Design Evaluation

•→15
The fuel mechanical design evaluations are provided in Subsection 2.2 of Reference 1 and in Reference 4 for GE fuel. Reference 7 provides the fuel design evaluations for FRA-ANP fuel. Control rod reactivity is discussed below and in Reference 2.
15←•

4.2.3.1 Reactivity Control Assembly Evaluation (Control Rods)

4.2.3.1.1 Materials Adequacy Throughout Design Lifetime

•→8
The adequacy of the GE original, ABB CR-82M and ABB CR-82M-1 control rod and GE Marathon control rod materials throughout the design life was evaluated in the design of the control rods. The primary materials, B_4C powder, 304, HP304S and 316L austenitic stainless steel, have been found to perform adequately for the lifetime of the control rods.
8←•

4.2.3.1.2 Dimensional and Tolerance Analysis

Layout studies are done to assure that, given the worst combination of extreme detail part tolerance ranges at assembly, no interference exists which will restrict the passage of control rods. The envelope dimensions within the core for the Marathon control rod, a direct replacement of the BWR/6 control rod, are the same as the original equipment control rods. In addition, preoperational verification is made on each control rod system to show that the acceptable levels of operational performance are met.

•→8
ABB CR-82M and ABB CR-82M-1 Guide button thickness tolerance will allow for a larger gap (≤ 13 mils) at the button location. The potential for creating new flow-induced vibration related problems by insertion of the control rods has been evaluated and is not expected due to low bypass flow velocities in GE BWRs and a gap size smaller than that caused by channel bow in which no flow-induced vibration has been seen.
1←• 8←•

•→1
4.2.3.1.3 Thermal Analysis of the Tendency to Warp
•→10
The various parts of the control rod assembly remain at approximately the same temperature during reactor operation, negating the problem of distortion or warpage. Mechanical design allows for what little differential thermal growth can exist. A minimum axial gap is maintained between absorber rod tubes and the control rod frame assembly for the purpose. In addition, to further this end, dissimilar metals are avoided.
10←•
4.2.3.1.4 Forces for Expulsion

An analysis has been performed which evaluates the maximum pressure forces which could tend to eject a control rod from the core.

If the collet remains open, which is unlikely, calculations indicate that the steady-state control rod withdrawal velocity would be 2 ft/sec for a pressure-under line break, the limiting case for rod withdrawal.

4.2.3.1.5 Effect of Fuel Rod Failure on Control Rod Channel Clearances

The control rod drive mechanical design ensures a sufficiently rapid insertion of control rods to preclude the occurrence of fuel rod failures which would hinder reactor shutdown by causing significant distortions in channel clearances.

4.2.3.1.6 Effect of Blowdown Loads on Control Rod Channel Clearances

The fuel channel load resulting from an internally applied pressure is evaluated utilizing a fixed beam analytical model under a uniform load. Tests to verify the applicability of the analytical model indicate that the model is conservative. A roller at the top of the control rod guides the blade as it is inserted. If the gap between channels is less than the diameter of the roller, the roller deflects the channel walls as it makes its way into the core. The friction force is a small percentage of the total force available to the CRDs for overcoming such friction, and it is concluded that the main steam line break accident does not impede the insertability of the control rod.
•←1

•→|
4.2.3.1.7 Mechanical Damage

Analysis has been performed for all areas of the control system showing that system mechanical damage does not affect the capability to continuously provide reactivity control.

The following discussion summarizes the analysis performed on the control rod guide tube.

The guide tube can be subjected to any or all of the following loads:

1. Inward load due to pressure differential

2. Lateral loads due to flow across the guide tube

3. Dead weight

4. Seismic (vertical and horizontal)

5. Vibration.

In all cases analyses were performed considering both a recirculation line break and a steam line break, events which result in the largest hydraulic loadings on a control rod guide tube.

Two primary modes of failure were considered in the guide tube analysis: exceeding allowable stress and excessive elastic deformation. It was found that the allowable stress limit will not be exceeded and that the elastic deformations of the guide tube never are great enough to cause the free movement of the control rod to be jeopardized.

4.2.3.1.7.1. First Mode of Failure

The first mode of failure is evaluated by the addition of all the stresses resulting from the maximum loads for the faulted condition. This results in the maximum theoretical stress value for that condition. Making a linear supposition of all calculated stresses and comparing this value to the allowable limit defined by the ASME Boiler and Pressure Vessel Code yields a factor of safety of approximately 3. For faulted condition, the factor of safety is approximately 4.2.

4.2.3.1.7.2 Second Mode of Failure

Evaluation of the second mode of failure is based on clearance reduction between the guide tube and the control
•←|

•→1
rod. The minimum allowable clearance is about 0.1 in. This assumes maximum ovality and minimum diameter of the guide tube and the maximum control rod dimension. The analysis showed that if the approximate 6,000 psi for the faulted condition were entirely the result of differential pressure, the clearance between the control rod and the guide tube would reduce by a value of approximately 0.01 in. This gives a design margin of 10 between the theoretically calculated maximum displacement and the minimum allowable clearance.

4.2.3.1.8 Analysis of Guide Tube Design

Two types of instability were considered in the analysis of guide tube design. The first was the classic instability associated with vertically loaded columns. The second was the diametral collapse when a circular tube experiences external to internal differential pressure.

The limiting axially applied load is approximately 77,500 lb resulting in a material compressive stress of 17,450 psi (code allowable stress). Comparing the actual load to the yield stress level gives a design margin greater than 20 to 1. From these values it can be concluded that the guide tube is not an unstable column.

When a circular tube experiences external to internal differential pressure, two modes of failure are possible depending on whether the tube is "long" or "short." In the analysis here, the guide tube is taken to be an infinitely long tube with maximum allowable ovality and minimum wall thickness. The conditions will result in the lowest critical pressure calculation for the guide tube (i.e., if the tube "short," the critical pressure calculation would give a higher number). The critical pressure is approximately 140 psi. However, if the maximum allowable stress is reached at a pressure lower than the critical pressure, then that pressure is limiting. This is the case for a BWR guide tube. The allowable stress of 17,450 psi will be reached at approximately 93 psi. Comparing the maximum possible pressure differential for a steam line break to the limiting pressure of 93 psi gives a design margin greater than 3 to 1. Therefore, the guide tube is not unstable with respect to differential pressure.

4.2.3.1.9 Evaluation of Control Rod Velocity Limiter

The control rod velocity limiter limits the free fall velocity of the control rod to a value that cannot result in nuclear system process barrier damage.
•←1

•→1
4.2.4 Testing, Inspection and Surveillance Plans

Fuel assembly testing, inspection and surveillance plans except for control rods and online fuel system monitoring are documented in Subsection 2.3 of Reference 1. Control rod testing, inspection and surveillance are discussed in Subsection 4.2.4.1. Online fuel system monitoring is discussed in Subsection 4.2.4.2.

4.2.4.1 Reactor Control Rods

Inspections and tests are conducted at various points during the manufacture of control rod assemblies to assure that design requirements are being met. All B_4C lots are analyzed and certified by the supplier. Among the items tested are:

1. Chemical composition
2. Boron weight percent
3. Boron isotopic content
4. Particle size distribution.

Following a receipt of the B_4C and review of material certificates, additional samples from each lot are tested including those previously listed. Control is maintained on the B_4C powder through the remaining steps prior to loading into the absorber rod tubes.

Certified test results are obtained on other control rod components.

•→10
The absorber rod tubing is subjected to extensive testing by the tubing supplier, including 100 percent ultrasonic examination. Metallographic examinations are conducted on several tubes randomly selected from each lot to verify cleanliness and absence of conditions resulting from improper fabrication, cleaning, or heat treatment. Other checks are made on the subassemblies and final control rod assembly, including inspection of weld joints and B_4C loading.
10←• •←1

•→8
4.2.4.2 Online Fuel System Monitoring

River Bend Station has two independent radiation detection systems that are directly capable of sensing fission product releases from failed fuel rods. The main steamline radiation (MSLR) monitors are used to detect high radiation levels resulting from gross fuel failure. At River Bend Station, two redundant MSLR monitors will be used, each of which provides a signal to trip mechanical vacuum pumps and isolate the reactor water sample valves independent of operator action. Because the MSLR monitors are located relatively close to the reactor core, they are capable of sensing gross fission product releases relatively quickly (that is, in a few seconds), and the off-gas system radiation (OGSR) monitors are capable of detecting low-level emissions of noble gases, which could indicate the occurrence of minor fuel damage, in 2 to 3 minutes, the time required for the activity to travel from core to the detectors. The OGSR monitors are set to sound alarms that would initiate operator action (see Chapter 11 for details).
•←8

References 4.2

1. General Electric Standard Applications for Reactor Fuel, NEDE-24011-P-A, latest approved revision.

2. K. W. Brayman and K. W. Cook, Evaluation of Control Blade Lifetime with Potential Loss of B_4C, NEDO-24226, December 1979; and Supplement 1 (Proprietary), March 1981.

3. G. A. Potts, Urania-Gadolinia Nuclear Fuel Physical and Irradiation Characteristics and Material Properties, NEDE-20943 (Proprietary), NEDO-20943 (Nonproprietary), January 1977.

4. General Electric Fuel Bundle Designs, NEDE-31152P, latest approved revision.

5. DELETED

6. DELETED

7. DELETED

8. DELETED

•→1
4.3 NUCLEAR DESIGN

The nuclear core design bases and licensing requirements are independent of enrichment.

•→3
4.3.1 Design Bases

The design bases are those that are required for the plant to operate, meeting all safety requirements. Safety design bases fall into two categories: (1) the reactivity basis, which prevents an uncontrolled positive reactivity excursion, and (2) the overpower bases, which prevent the core from operating beyond the fuel integrity limits.

4.3.1.1 Reactivity Basis

The nuclear design shall meet the following basis: The core shall be capable of being made subcritical at any time or at any core condition with the highest worth control rod fully withdrawn.

4.3.1.2 Overpower Bases

•→12
The Technical Specification limits on Minimum Critical Power Ratio (MCPR), Linear Heat Generation Rate (LHGR) and the Maximum Average Planar Linear Heat Generation Rate (MAPLHGR) are determined such that the fuel will not exceed required licensing limits during abnormal operational occurrences or accidents.

1←• 3←• 12←•

• ~~3~~ • ~~1~~ 3←•

4.3.2 Description

The BWR core design utilizes a light-water moderated reactor, fueled with slightly enriched uranium-dioxide. The use of water as a moderator produces a neutron energy spectrum in which fissions are caused principally by thermal neutrons. At normal operating conditions, the moderator boils, producing a spatially variable distribution of steam voids in the core. The BWR design provides a system for which reactivity changes are inversely proportional to the steam void content in the moderator. This void feedback effect is one of the inherent safety features of the BWR system. Any system input which increases reactor power, either in a local or gross sense, produces additional steam voids which reduce reactivity and thereby reduce the power.

4.3.2.1 Nuclear Design Description

• ~~12~~5 • ~~12~~0 • ~~8~~ • ~~6~~ • ~~4~~ • ~~3~~

The reference core loading pattern is the basis for all fuel licensing. The bundle and lattice designations for reload fuel enrichments are given in Section 2 of Reference 4 for GE fuel. Uranium-dioxide and gadolinia distributions for each bundle enrichment and typical lattice nuclear characteristics are given in Reference 23. The typical lattice nuclear characteristic and steady-state core characteristics are also discussed in Section 3 of Reference 1. The reference core loading pattern for the current cycle is described in Appendix 15B.

4←• 6←• 8←• 10←•

4.3.2.2 Power Distribution

• ~~3~~ • ~~1~~

The core power distribution is a function of fuel bundle design, core loading, control rod pattern, core exposure distribution, and core coolant flow rate. Core power distribution can be characterized by maximum peaking for a bundle, node, or fuel rod. Thermal performance parameters limit maximum peakings and thus are used to prevent unacceptable core power distributions. The core power distribution is discussed in Section 3.2.2 of Reference 1 for GE methods.

1←• 3←• 15←•

• →1

4.3.2.2.1 Power Distribution Calculations

A full range of calculated power distributions along with the resultant exposure shapes and the corresponding control rod patterns are shown in Appendix 4A for a typical BWR 6.

4.3.2.2.2 Power Distribution Measurements

• →15 • →10

The techniques for a measurement of the power distribution within the reactor core are discussed in Reference 1 for GE methods.

10←•

4.3.2.2.3 Power Distribution Accuracy

The accuracy of the calculated power distributions is discussed in Subsection 3.2.2 of Reference 1 for GE methods.

15←•

4.3.2.2.4 Power Distribution Anomalies

• →12 • →10 • →6

Stringent inspection procedures are utilized to ensure the correct arrangement of the core following fuel loading. A fuel loading error (a mislocated or a misoriented fuel bundle in the core) would be a very improbable event, but calculations have been performed to determine the effects of such events on CPR. The results are presented in Chapter 15.

6←• 10←• 12←• • →15 • →3

The inherent design characteristics of the BWR are well suited to limit gross power tilting. The stabilizing nature of the large moderator void coefficient effectively reduces perturbations in the power distribution. In addition, the in-core instrumentation system, together with the ancillary core monitoring system, provides the operator with prompt information on power distribution so that he can readily use control rods or other means to limit the undesirable effects of power tilting. Because of these design characteristics, it is not necessary to allocate a specific margin in the peaking factor to account for power tilt. If, for some reason, the power distribution could not be maintained within normal limits using control rods, then the operating power limits would have to be reduced.

1←• 3←• 15←•

•→1
4.3.2.3 Reactivity Coefficients
•→15
Reactivity coefficients are discussed in Section 3.2 of Reference 1 for GE methods.
15←•
4.3.2.4 Control Requirements

The nuclear design in conjunction with the reactivity control system provides an inherently stable system for BWRs.

The control rod system is designed to provide adequate control of the maximum excess reactivity anticipated during the cycle operation. Since fuel reactivity is a maximum and control is a minimum at ambient temperature, the shutdown capability is evaluated assuming a cold, xenon-free core. The safety design basis requires that the core, in its maximum reactivity condition, be subcritical with the control rod of the highest worth fully withdrawn and all others fully inserted.

4.3.2.4.1 Shutdown Reactivity
•→15 •→3
To assure that the safety design basis for shutdown is satisfied, an additional design margin is adopted: k-effective is calculated to be less than or equal to the Plant Technical Specification value with the control rod of highest worth fully withdrawn. This is also discussed in Section 3.2.4.1 of Reference 1.
3←• 15←• •→10
The cold shutdown margin for the reference core loading pattern can be calculated from the $k_{effective}$ with the highest worth (strongest) control rod fully withdrawn, which is provided in Appendix 4B.

4.3.2.4.2 Reactivity Variations
•→15 •→8 •→6 •→4 •→3
The excess reactivity designed into the core is controlled by the control rod system supplemented by gadolinia-urania fuel rods. Enrichment distributions for these rods are given in Reference 23.
3←• 4←• 6←• 8←• 10←• 15←•
Control rods are used during the cycle partly to compensate for burnup and partly to flatten the power distribution.

Reactivity balances are not used in describing BWR behavior because of the strong interdependence of the individual constituents of reactivity. Therefore, the design process does not produce components of a reactivity balance at the conditions of interest. Instead, it gives the k_{eff}
1←•

•→13 •→1
representing all effects combined. Further, any listing of components of a reactivity balance is quite ambiguous unless the sequence of the changes is clearly defined. Typical Cycle k_{eff} values are provided in Appendix 4A.
13←•

4.3.2.5 Control Rod Patterns and Reactivity Worths

A detailed core simulation study for a typical BWR 6 is provided in Appendix 4A showing that the BWR core meets design performance criteria. Typical BWR control rod positions are utilized in the study. The rod patterns described represent only one feasible sequence which results in power distributions well within design limits. Actual operating reactor rod patterns are based upon the measured distributions in the plant and together with the rod worth minimizing systems, limit the amount and rate of reactivity insertion in the event of a control rod drop accident in such a way that the peak fuel pellet enthalpy is less than the 280 cal/gm design limit. Rod worth minimizing systems also assure that the 170 cal/gm fuel enthalpy limit is not exceeded for any cold rod withdrawal error event.

For BWR plants, control rod patterns are not uniquely specified in advance; rather, during normal operation the control rod patterns are selected based on the measured core power distributions, within the constraints imposed by the systems indicated in the following sections.

Typical control rod patterns are calculated during the design phase to ensure that all safety and performance criteria are satisfied. Control rod patterns and the associated power distributions for a typical BWR are presented in Appendix 4A. These control rod patterns are calculated with the BWR core simulator[3]. The ability of this model to predict control rod worth can be inferred from the detailed reactivity data presented in Reference 6. The comparisons of calculated and measured reactivity for the cold condition in both an in-sequence critical, where roughly 25 percent of the control rods are withdrawn, and the stuck rod measurement, where only one or two rods are withdrawn, show the ability of the model to predict rod worth. The data presented in Table 7 of Reference 6 show that no significant bias exists between these two configurations; therefore, it is concluded that the worth of the rods is accurately predicted for the cold condition. Fig. 44 of Reference 6 shows the calculated critical reactivity for a variety of BWR cores and over a wide range of exposures. Since this represents a large variation of
1←•

•→12 •→1
the number of control rods inserted, and since no significant bias is observed, it is concluded that rod worths for the hot operating condition are accurately predicted. Verification of the advanced nodal codes is presented in Reference 1.
•→15
Control rod patterns for the current cycle are calculated with the GE core simulator code described in Reference 1. Data referenced in Reference 1 demonstrate the ability of this model to accurately predict control rod worth at hot and cold conditions.
15←•
4.3.2.5.1 Rod Control and Information System

Control rod patterns and associated control rod reactivity worths are regulated by the rod control and information system (RCIS). This system utilizes redundant inputs to provide rod pattern control over the complete range of reactor operations. The control rod worths are limited to such an extent that the rod drop accident and the power range rod withdrawal error (RWE) become unimportant. The RCIS provides for stable control of core reactivity in both the single rod or rod gang mode of operation. Note: Ganged mode is not fully installed or tested at RBS and is therefore not used. The bank position (BP) mode of RCIS provides protection from a rod drop accident from startup to about 20 percent of rated power. The rod withdrawal limiter provides protection from the RWE for all conditions above 20-percent power. Each of these modes is described in the following sections.
12←•
4.3.2.5.2 Bank Position Mode
•→15
The BP mode restricts control rod patterns to prescribed withdrawal sequences from the all-rods-inserted startup condition until about 10 percent of rated power. This mode minimizes control rod worths to the extent that they are not an important concern in the operation of a BWR. The consequences of a rod drop accident or a RWE in this range are significantly less severe than that required to violate fuel safety limits. This system is described in detail in Reference 8. Above 10 percent of rated power, control rod worths are very small due to the formation of voids in the moderator. Therefore, restrictions on control rod patterns are not required to minimize control rod worths.
15←•
4.3.2.5.3 Rod Withdrawal Limited Mode
•→12
Above the low power setpoint the RCIS relies on the rod withdrawal limited mode to provide regulation of control rod withdrawals in order to prevent the occurrence of an RWE. This mode limits the withdrawal of a single control rod to a predetermined increment depending on the power level. The system senses the location of the rod or rods and automatically blocks withdrawal when the preset increment is reached. The preset limit is determined by generic analyses such that the
1←• 12←•

•→13 •→1
ΔMCPR and ΔLHGR are less than the limiting transient. Withdrawal limits above the low power set point are described in Chapter 15.4. Withdrawal limits below the low power set point are enforced by the rod pattern controller.
13←•
4.3.2.5.4 Control Rod Operation
•→10
The control rods can be operated either individually or in a gang composed of up to four rods (Gang mode is not fully installed or tested at RBS and is therefore not used). The purpose of the ganged rods is to reduce the time required for plant startup or recovery from a scram. The RCIS provides regulation of control rod operation regardless of whether rods are being moved in single or ganged mode. The assignment of control rods to RCIS groups is shown on Fig. 4.3-19 and 4.3-20 for the A pattern and Fig. 4.3-21 and 4.3-22 for the B pattern. Also shown on these figures is the division of the groups into gangs of one to four rods which can be moved simultaneously.
10←•
4.3.2.5.5 Scram Reactivity
•→12 •→10 •→6
The scram reactivity for each Anticipated Operational Occurrence analyzed on a cycle by cycle bases is presented in Appendix 15B.
6←• 10←• 12←•
4.3.2.6 Criticality of Reactor During Refueling
•→3
The core is subcritical at all times.
3←•
4.3.2.7 Stability

4.3.2.7.1 Xenon Transients

Boiling water reactors do not have instability problems due to xenon. This has been demonstrated by operating BWRs for which xenon instabilities have never been observed (such instabilities would readily be detected by the LPRMs), by special tests which have been conducted on operating BWRs in an attempt to force the reactor into xenon instability, and by calculations. All of these indicators have proven that xenon transients are highly damped in a BWR due to the large negative power coefficient.

Analysis and experiments conducted in this area are reported in Reference 5.
1←•

•→1
4.3.2.7.2 Thermal Hydraulic Stability

This subject is covered in Subsection 4.4.4.6.

4.3.2.8 Vessel Irradiations

•→4
The vessel fluence was calculated using the two-dimensional discrete ordinates transport code described in Section 4.1.4.5. The discrete ordinates code was used in a distributed source mode with cylindrical geometry. The geometry described seven regions with the core modeled as two homogenized regions. The coolant water region between the core and the shroud was described containing saturated water at 550°F and 1,050 psi. Subcooled water at 530°F and 1040 psia was used for the coolant between the shroud and the vessel. The material compositions for the stainless steel in the shroud and the carbon steel in the vessel contain the mixtures by weight as specified in the ASME material specifications for ASME SA240, 304L, and ASME SA533, Grade B. In the region between the shroud and the vessel, the presence of the jet pumps was ignored. A diagram showing the regions and dimensions modeled is shown in Fig. 4.3-23.

The distributed source, which can be separated in space and energy, was obtained from the core power shape and the neutron spectra. The integral over position and energy is normalized to the total number of neutrons in the core region. The core region is defined as a 1-cm thick disc with no transverse leakage. The power in this core region is set equal to the maximum power in the axial direction. The optimum axial power distribution is shown in Figure 4.3-13.

•→14
Dosimetry located on the inside surface of the vessel was removed after the first fuel cycle and tested to determine the flux at that location. The lead factor relating the dosimeter location to the peak location was used to calculate the peak vessel inside surface flux. Assuming an 80% capacity factor, or 32 effective full power years (EFPY) in 40 years of operation, the fluence for this operating period was estimated. The measured dosimeter flux, peak flux and fluence calculated considering power uprate beginning at 10.43 EFPY are shown in Table 4.3-5. The calculated neutron flux leaving the cylindrical core is listed in Table 4.3-6.

1←• 4←• 14←•
The increase in rated core power to 3091 MWt, implemented after 12.85 EFPY of operation, has a negligible effect on the 32 EFPY fluence. Further effects of this rated power increase are discussed in Sections 5.3.1 and 5.3.2.

In conjunction with the removal of dosimetry at the end of cycle 9, additional fluence calculations were performed as described in Reference 18. This analysis was performed consistent with the requirements of Regulatory Guide 1.190 employing a methodology that was reviewed and approved by the NRC in Reference 19. The analysis uses the two dimensional discrete ordinates code, DORT (Reference 20) and the BUGLE-96 (Reference 21) cross-sections to

Perform transport calculations of the neutron source from the core region through the reactor vessel. Separate transport calculations were performed for each cycle (1-12) using time integrated neutron source terms. The fluence was projected to 32 EFPY based on a representative fuel cycle (cycle 11) which contained edge bundles which operated at relatively high power. The reactor power, fission fractions and other fuel parameters used to determine the source term were developed using the CASMO-4/Simluate-3 (Reference 22) reactor analysis code system.

This methodology has been qualified by comparisons to controlled experiments and reactor dosimetry. Additionally, an analytic uncertainty analysis has been performed which demonstrated compliance with he 20% acceptance criteria described in Regulatory Guide 1.190. RBS specific benchmarks were performed based on dosimetry removed at the end of cycle 1 and 9. The average calculated-to-measure (C/M) activity ratios for cycle 1 and 9 were 1.04 and 0.94 respectively. These results are consistent with other benchmarks reported in Reference 18 and Regulatory Guide 1.190 requirements. The analysis is based on absolute fluence results and is not biased by the dosimetry results.

The updated dosimetry flux, peak vessel fluence and lead factors determined based on this analysis are summarized in Table 4.3-7. The updated lead factors are evaluated in the BWRVIP ISP to determine dosimetry evaluation schedules. The updated vessel fluence results are evaluated in Section 5.3.1.6.2.

• →15 • →

4.3.3 Analytical Methods

The analytical methods and nuclear data used to determine the nuclear characteristics are provided in Section 3.0 of Reference 1 for GE methods. Qualification of these models is also described.

1←• 15←•

References - 4.3

1. "General Electric Standard Application for Reactor Fuel," NEDE-24011-P-A, latest approved revision.

2. Deleted

3. J. A. Woolley, "3D BWR Core Simulator," NEDO-20953, May 1976.

4. "G.E. Fuel Bundle Designs," NEDE-31152P, latest approved revision.

5. R. L. Crowther, "Xenon Considerations in Design of Boiling Water Reactors," June 1968 (APED-5640).

6. G. R. Parkos, "BWR Simulator Methods Verification," NEDO-20946A, January 1977.

7. Letter, R. E. Engel (GE) to T. A. Ippolito (NRC), "Change to General Electric Methods for Analysis of Mislocated Bundle Accident," November 14, 1980.

8. C. J. Paone, "Banked Position Withdrawal Sequence," NEDO-21231, January 1977.

12. DELETED

13. DELETED

14. DELETED

15. DELETED

16. DELETED

17. DELETED

18. MPM-904779, "Neutron Transport Analysis for River Bend Station," November 2004.
19. TAC No. MB6687, "Nine Mile Point Nuclear Station, Unit No. 1 – Issuance of Amendment RE: Pressure-Temperature Limit Curves and Tables," October 27, 2003.
20. "TORT-DORT-PC, Two and Three Dimensional Discrete Ordinates Transport," Version 2.7.3, CCC-543, RCISS Computer Code Collection.
21. "BUGLE-96, Coupled 47 Neutron, 20 Gamma Ray Group Cross Section Library Derived from ENDF/B-VI for LWR Shielding and Pressure Vessel Dosimetry Applications," DLC-185, RSICC Data Library Collection.
22. "Casmo-4/Simulate-3, Studsvik's Advanced Three-Dimensional Two Group Reactor Analysis Code.
23. 003N9292, Revision 0, "Fuel Bundle Information Report for River Bend Station – Unit 1 Reload 19 Cycle 20," Global Nuclear Fuel – Americas, LLC, November 2016. (Entergy Report # ECH-NE-16-00038, Revision 0).

•→1
4.4 THERMAL-HYDRAULIC DESIGN

4.4.1 Design Bases

4.4.1.1 Safety Design Bases

•→3
Thermal-hydraulic design of the core shall establish the thermal-hydraulic safety limits for use in evaluating the safety margin relating the consequences of fuel cladding failure to public safety.

4.4.1.2 Requirements for Steady-State Conditions

•→13
For purposes of maintaining adequate fuel performance margin during normal steady-state operation, the MCPR must not be less than the required MCPR operating limit, the APLHGR must be maintained below the required APLHGR limit (MAPLHGR), and the LHGR must be maintained below the required MLHGR. The steady-state MCPR, MAPLHGR and MLHGR limits are determined by analysis of the most severe moderate frequency anticipated operational occurrences (A00s) to accommodate uncertainties and provide reasonable assurance that no fuel damage results during moderate frequency A00s at any time in life.

•→15 •→8 •→4
The design steady-state operating limit MCPR values as well as MAPLHGR values are referenced in Appendix 15B.

4←• 15←•
4.4.1.3 Requirements for Anticipated Operational Occurrences (A00s)

•→15
The MCPR, MAPLHGR and MLHGR limits are established such that no safety limit is expected to be exceeded during the most severe moderate frequency (A00s) event as defined in the United States supplement of Reference 1 for GE methods.

15←•
4.4.1.4 Summary of Design Bases

In summary, the steady-state operating limits have been established to assure that the design bases are satisfied for the most severe moderate frequency (A00s). Demonstration that the steady-state MCPR, MAPLHGR and MLHGR limits are not exceeded is sufficient to conclude that the design bases are satisfied.

13←•
4.4.2 Description of Thermal-Hydraulic Design of the Reactor Core

1←• 3←• 8←•

•→1
4.4.2.1 Summary Comparison
•→10
An evaluation of plant performance from a thermal and hydraulic standpoint is provided in Subsection 4.4.4.

Thermal-hydraulic design characteristics are provided in Table 4.4-1.
10←•
4.4.2.2 Critical Power Ratio
•→15 •→6 •→3
A general description of the critical power ratio is provided in Section 3 of Reference 1. The models used to calculate this ratio for the operating cycle are described in Reference 1. The reactor core simulator, reactor system transient and critical power correlation methodologies are described in Reference 1.

4.4.2.3 Linear Heat Generation Rate / Average Planar Linear Heat Generation Rate (LHGR / APLHGR)
•→8
Models used to calculate the LHGR/APLHGR limit with GE methods are given in Section 2 of Reference 1 as pertaining to the fuel mechanical design limits, and in the United States supplement of Reference 1 as pertaining to 10CFR Appendix K limits.

3←• 6←• 8←• 15←•
4.4.2.4 Void Fraction Distribution

The void fraction is calculated for each reload. This value is calculated within the transient code for pressurization events and is not reported separately but is reflected in the figures of void reactivity given for these events as presented in Chapter 15.

4.4.2.5 Core Cooling Flow Distribution and Orificing Pattern
•→15
Hydraulic models, including core coolant flow distribution and bypass, are included in Section 4.0 of Reference 1 for GE methods and References 3.

4.4.2.6 Core Pressure Drop and Hydraulic Loads

Models for pressure drop across the core are given in Section 4.0 of Reference 1 for GE methods.

4.4.2.7 Correlation and Physical Data

Physical data in support of the pressure drop and thermal-hydraulic loads are referenced in Section 4.0 of Reference 1 for GE methods.
1←• 15←•

•→1
4.4.2.8 Thermal Effects of Operational Transients

The evaluation of the core's capability to withstand the thermal effects resulting from anticipated operational transients is covered in Chapter 15.
1←•

THIS PAGE LEFT INTENTIONALLY BLANK

•→1
4.4.2.9 Uncertainties in Estimates
•→15 •→3
Uncertainties in thermal-hydraulic parameters are considered in the statistical analysis which is performed to establish the fuel cladding integrity safety limit documented in Reference 1. The fuel cladding integrity safety limit methodology is documented in Reference 1.
3←•
4.4.2.9.1 Fuel Related Uncertainties

The methodology uses the GEXL17 critical power correlation, additive constants and associated uncertainties reported in Reference 17 for GNF2 fuel.

Power distribution uncertainties are provided in Reference 15, which also contains the allowable equipment out of service and calibration interval.

4.4.2.9.2 System-Related Uncertainties

System related uncertainties are plant specific parameters which include feedwater flow rate, feedwater temperature, core pressure and total core flow rate. The uncertainties used are documented in Reference 16 and are applicable to River Bend.
15←•
4.4.2.10 Flux Tilt Considerations

For flux tilt considerations, refer to Subsection 4.3.2.2.4.

4.4.3 Description of the Thermal-Hydraulic Design of the Reactor Coolant System

4.4.3.1 Plant Configuration Data

The RCS is described in Section 5.4 and shown in isometric perspective in Fig. 5.4-1. The piping sizes, fittings, and valves are listed in Table 5.4-1.

4.4.3.1.1 Reactor Coolant System Thermal-Hydraulic Data

The steady-state distribution of temperature, pressure, and flow rate for each flowpath in the RCS is shown in Fig. 5.1-1.

4.4.3.1.2 Reactor Coolant System Geometric Data

Volumes of regions and components within the reactor vessel are shown in Fig. 5.1-2.

Table 4.4-11 provides the flow path length, height, liquid level, minimum elevations, and minimum flow areas for each major flow path volume within the reactor vessel and recirculation loops of the RCS.

Table 4.4-12 provides the lengths and sizes of all safety injection lines to the RCS. Further geometric data for the ECCS, including a listing of valves and pipe fittings and minimum cross-sectional flow areas, is provided in Table 4.4-13.

4.4.3.2 Operating Restrictions on Pumps

Expected recirculation pump performance curves are shown in Fig. 5.4-3. These curves are valid for all conditions with a normal operating range varying from approximately 20 to 115 percent of rated pump flow.

The pump characteristics, including considerations of net positive suction head (NPSH) requirements, are the same for the conditions of two-pump and one-pump operation as described in Section 5.4.1. Section 4.4.3.3 gives the operating limits imposed on the recirculation pumps by cavitation, pump loads, bearing design flow starvation, and pump speed.
1←•

THIS PAGE LEFT INTENTIONALLY BLANK

•→1
4.4.3.3 Power-Flow Operating Map

4.4.3.3.1 Limits for Normal Operation

•→10
A BWR must operate with certain restrictions because of pump NPSH, overall plant control characteristics, core thermal power limits, etc. The updated power-flow map including MELLL and ICF for the power range of operation is shown in Fig. 4.4-5. The nuclear system equipment, nuclear instrumentation, and the RPS, in conjunction with operating procedures, maintain operations within the area of this map for normal operating conditions. The boundaries on this map are as follows:

10←•

1. Natural Circulation Line, A: The operating state of the reactor moves along this line for the normal control rod withdrawal sequence in the absence of recirculation pump operation.

•→14 •→10

2. Maximum Extended Load Line: This line represents the extended operating region bounded by the rod line which passes through the 100% power/83.4% core flow point (approximately 115% rod line), the rated power line and the rated load line. The operating state for the reactor follows this rod line (or similar ones) during recirculation flow changes with a fixed control rod pattern; however, rated power may not be exceeded. The MELLL is based on a constant xenon concentration at rated power and flow.

14←•

3. Cavitation Protection Lines: This line results from the recirculation pump, flow control valve, and jet pump NPSH requirements.

•→8

4. Maximum Core Flow Line: This line represents the maximum core flow allowed (107 percent) during normal reactor operation.

8←•

Other performance characteristics shown on the power-flow operating map are:

1. Constant Rod Lines: These lines show the change in power associated with flow changes, while maintaining constant control rod position.

•→8

2. Constant Position Lines (A and B) for Flow Control Valves: These lines show the change in flow associated with power changes while maintaining flow-control valves at constant position.

8←•

4.4.3.3.2 Regions of the Power Flow Map

10←• 1←•

•→10 •→1

Region I — This region defines the system operational capability with the recirculation pumps and motors being driven by the low frequency motor-generator set at 25 percent speed. Flow is controlled by the flow control valve and power changes, during normal startup and shutdown, will be in this region. The normal operating procedure is to start up with FCV wide open at 25 percent speed.

10←•

Region II — This region shows the area where 25 percent pump speed and 100 percent pump speed operating regimes overlap. The switching sequence from the low frequency motor-generator set to 100 percent speed will be done in this region.

•→7

Region III — This is the low power area of the operating map where cavitation can be expected in the recirculation pumps, jet pumps, or flow control valves.

Operation within this region is precluded by system interlocks which trip the main motor from the 100 percent speed power source to the 25 percent speed power source (unless the trip occurs for one loop only, in which case the affected loop's motor trips off). A separate interlock is provided for each recirculation pump loop.

7←•

Region IV — This represents the normal operating zone of the map where power changes can be made, by either control rod movement or core flow changes, through use of the flow control valve.

•→12

4.4.3.3.2.1 Stability Regions of the Power Flow Map

Monitored Region — The area of the core power and flow operating domain where the reactor may be susceptible to reactor instabilities under conditions exceeding the licensing basis of the reactor system.

Restricted Region — The area of the core power and flow operating domain where the reactor is susceptible to reactor instabilities in the absence of restrictions on core void distributions.

Exclusion Region — The area of the core power and flow operating domain where the reactor is susceptible to reactor instabilities.

12←•1←•

•→1

4.4.3.3.3 Design Features for Power-Flow Control

The following limits and design features are employed to maintain power-flow conditions to the required values shown in Fig. 4.4-5.

•→10 •→7

1. Minimum Power Limits at Intermediate and High Core Flows To prevent cavitation in the recirculation pumps, jet pumps, and flow control valves, each recirculation pump loop is provided with an interlock to trip off the 100 percent speed power source if the difference between the dome steam temperature (obtained through measurement of the dome pressure) and recirculation pump inlet temperature is less than a preset value (typically 6 to 11°F). If the trip signal occurs simultaneously in both loops, the interlock trips the 100 percent speed power source and closes the 25 percent speed power source for both loops. This differential temperature is measured using high accuracy resistance temperature detectors (RTDs) with a sensing error of less than 0.2°F at the two standard deviation (2s) confidence level and pressure transmitters. This action is initiated electronically through a 15-minute time delay. The 15 minute time delay is to allow the interlock to be bypassed if the differential temperature signal is false, while still protecting the recirculation system from the allowed 3 hours of accumulative cavitation (Reference 2). The interlock is active while in both the automatic and manual operation modes.

10←• 7←• •→8•→14

2. Minimum Power Limit at Low Core Flow During low power, low loop flow operations, the temperature differential interlock may not provide sufficient cavitation protection to the flow control valves. Therefore, the system is provided with an interlock to trip off the 100 percent speed power source and close the 25 percent speed power source if the feedwater flow falls below a preset level of approximately 24 percent of rated. The feedwater flow rate is measured by existing process control instruments. The speed change action is electronically initiated. This interlock is active during both automatic and manual modes of operation.

8←•14←•

3. Pump Bearing Limit For pumps as large as the recirculation pumps, practical limits of pump bearing design require that minimum pump flow be limited to 20 percent of rated. To assure this minimum flow, the system is designed so that the minimum flow control valve position will allow this rate of flow.

1←•

•→1

4. Valve Position To prevent structural or cavitation damage to the recirculation pump due to pump suction flow starvation, the system is provided with an interlock to prevent starting the pumps, or to trip the pumps if the suction or discharge block valves are at less than 90 percent open position. This circuit is activated by a position limit switch and is active before the pump is started, during manual operation mode, and during automatic operation mode.

The principal modes of normal operation with valve flow control-low frequency motor generator (LFMG) set are summarized as follows: the recirculation pumps are started on the 100 percent speed power source in order to unseat the pump bearings. Suction and discharge block valves are full open and the flow control valve is in the minimum position. When the pump is near full speed, the main power source is tripped and the pump allowed to coast down to approximately 25 percent speed where the LFMG set will power the pump and motor. The flow control valve is then opened to the maximum position at which point reactor heatup and pressurization can commence. When operating pressure has been established, reactor power can be increased. This power-flow increase will follow a line within Region I of the flow control map shown in Fig. 4.4-5.

•→14

When reactor power is greater than approximately 24 percent of rated, the low feedwater flow interlock is cleared and the main recirculation pumps can be switched to the 100 percent speed power source. The flow control valve is closed to the minimum position before the speed change to prevent large increases in core power and a potential flux scram. This operation occurs within Region II of the operating map. The system is then brought to the desired power-flow level within the normal operating area of the map (Region IV) by opening the flow control valves and withdrawing control rods.

14←•

Control rod withdrawal with constant flow control valve position will result in power/flow changes along lines of constant c_v (constant position). Flow control valve movement with constant control rod position will result in power/flow changes along, or nearly parallel to, the rated flow control line.

4.4.3.4 Temperature-Power Operating Map (PWR)

Not applicable.

4.4.3.5 Load-Following Characteristics

Large negative operating reactivity coefficients inherent in the BWR provide the following important advantages:

1←•

•→1

1. Good load-following with well damped behavior and little undershoot or overshoot in the heat transfer response

2. Load-following with recirculation flow control

3. Strong damping of spatial power disturbances.

4.4.3.6 Thermal and Hydraulic Characteristics Summary Table

The thermal-hydraulic characteristics are provided in Table 4.4-1 for the core and tables of Section 5.4 for other portions of the reactor coolant system.

4.4.4 Evaluation

•→3

The thermal-hydraulic design of the reactor core and reactor coolant system is based upon an objective of no fuel damage during normal operation or during anticipated operational occurrences. This design objective is demonstrated by analysis as described in the following sections.

4.4.4.1 Critical Power

•→15

The critical power is discussed in Subsection 4.3.1 of Reference 1 for GE methods.

4.4.4.2 Core Hydraulics

Core hydraulic models and correlations are discussed in Section 4.2 of Reference 1 for GE methods.

4.4.4.3 Influence of Power Distributions

The influence of power distributions on the thermal-hydraulic design is discussed in Section 4.3.3 of Reference 1 for GE methods.

3←• 15←•

4.4.4.4 Core Thermal Response

The thermal response of the core for accidents and expected transient conditions is discussed in Chapter 15.

4.4.4.5 Analytical Methods

•→3 •→15

The analytical methods, thermodynamic data, and hydrodynamic data used in determining the thermal and hydraulic characteristics of the core are documented in Section 4.0 of Reference 1 and the United States supplement of Reference 1 for GE methods.

1←• 3←• 15←•

•→1
4.4.4.6 Thermal-Hydraulic Stability Analysis
•→15 •→10 •→3
Criteria for stability and models used to analyze stability are documented in Section S.4 of the United States Supplement of Reference 1 for GE methods. Cycle-specific results are given in Appendix 4B.
3←• 10←• 15←•
4.4.5 Testing and Verification

The testing and verification techniques to be used to assure that the planned thermal and hydraulic design characteristics of the core have been provided, and will remain within required limits throughout core lifetime, are discussed in Chapter 14.

4.4.6 Instrumentation Requirements
•→10
The reactor vessel instrumentation monitors the key reactor vessel operating parameters during planned operations. This ensures sufficient control of the parameters. The reactor vessel sensors are discussed in Subsections 7.5, 7.6, and 7.7.
10←•
4.4.6.1 Deleted
•→14
14←•
Reference 4.4
•→6 •→3
1. General Electric Standard Application for Reactor Fuel, NEDE-24011-P-A, latest approved revision.
1←• 3←• 6←•
•→10
2. River Bend Jet Pump Cavitation Model, GE-NE-B3300280-01, May 1996
10←• •→15
3. DELETED
15←•

•→15
4. DELETED

5. DELETED

6. DELETED

7. DELETED

8. DELETED

9. DELETED

10. DELETED

11. DELETED

12. DELETED

13. DELETED
15←•
14. DELETED

15. NEDC-32694P-A, "Power Distribution Uncertainties for Safety Limit MCPR Evaluations," General Electric, August 1999.

16. NEDC-32601P-A, "Methodology and Uncertainties for Safety Limit MCPR Evaluations," General Electric, August 1999.

17. NEDC-33202P-A, Revision 3, "GEXL17 Correlation for GNF2 Fuel", Global Nuclear Fuel - Americas, LLC, April 2009.

4.5 REACTOR MATERIALS

4.5.1 Control Rod System Structural Materials

4.5.1.1 Material Specifications

1. Material List

The following material listing applies to the CRD mechanism supplied for this application. The position indicator and minor nonstructural items are omitted.

1. Cylinder, Tube, and Flange Assembly

Flange	ASME SA 182, Grade F304
Plugs	ASME SA 182, Grade F304
Cylinder	ASTM A269, Grade TP 304
Outer tube	ASTM A269, Grade TP 304
Tube	ASME SA 351, Grade CF-3
Spacer	ASME SA 351, Grade CF-3

2. Piston Tube Assembly

Piston tube	ASME SA 479, Grade XM-19
Nose	ASME SA 479, Grade XM-19
Base	ASME SA 479, Grade XM-19
Ind. tube	ASME SA 312, Type 316
Cap	ASME SA 182, Grade F316

3. Drive Line Assembly

Coupling spud	Inconel X-750
Compression cylinder	ASME SA479, Grade XM-19
Index tube	ASME SA 479 or SA 249, Grade XM-19
Piston head	Armco 17-4 PH
Piston coupling	ASTM A312, Grade TP 304 or ASTM A269, Grade TP 304
Magnet housing	ASTM A269 or A312, Grade TP 304 or ASTM A312, A249, or A213, Grade TP 316L

4. Collet Assembly

Collet piston	ASTM A269 or A312, Grade TP 304
Finger	Inconel X-750
Retainer	ASTM A269, Grade TP 304
Guide cap	ASTM A269, Grade TP 304

5. Miscellaneous Parts

Stop piston	Armco 17-4 PH
O-Ring spacer	ASTM A240, Type 304
Nut	ASME SA 479, Grade XM-19
Barrel	ASTM A269, Grade TP 304; ASTM A312, Grade TP 304; or ASTM A240, Type 304
Collet spring	Inconel X-750
Ring flange	ASME SA 182, Grade F304
Buffer shaft	Armco 17-4 PH
Buffer piston	Armco 17-4 PH
Buffer spring	Inconel X-750
Nut (hex)	Inconel X-750

The austenitic 300 Series stainless steels listed are all in the annealed condition (with the exception of the outer tube in the cylinder, tube, and flange assembly), and their properties are readily available. The outer tube is approximately 1/8 hard, and has a tensile of 90,000/125,000 psi, yield of 50,000/85,000 psi, and minimum elongation of 25 percent. The coupling spud, collet fingers, buffer spring, nut (hex), and collet spring are fabricated from Inconel X-750 in the annealed or equalized condition, and aged 20 hr at 1,300°F to produce a tensile of 165,000 psi minimum, yield of 105,000 psi minimum, and elongation of 20 percent minimum. The piston head, stop piston, buffer shaft, and buffer piston are Armco 17-4 PH in condition H-1100 (aged 4 hr at 1,100°F), with a tensile of 140,000 psi minimum, yield of 115,000 psi minimum, and elongation of 15 percent minimum.

These are widely used materials, whose properties are well known. The parts are readily accessible for inspection and replaceable if necesary.

All materials, except SA 479, Grade XM-19, have been successfully used for the past 10 to 15 yr in similar drive mechanisms. Extensive laboratory tests have demonstrated that ASME SA 479, Grade XM-19 is a suitable material and that it is resistant to stress corrosion in a BWR environment.

2. Special Materials

No cold-worked austenitic stainless steels with a yield strength greater than 90,000 psi are employed in the CRD system. Martensitic Armco 17-4 PH stainless steel (precipitation-hardened stainless steel) is used for the piston head, stop piston, buffer shaft, and buffer piston. This material is aged to the H-1100 condition to produce

resistance to stress corrosion cracking in BWR environments. Armco 17-4 PH (H-1100) has been success-fully used for the past 10 to 15 yr in BWR drive mechanisms.

4.5.1.2 Austenitic Stainless Steel Components

1. Processes, Inspections, and Tests

Proper solution annealing of 300 Series stainless steel used in the CRD is verified by testing in accordance with ASTM-A262, Recommended Practices for Detecting Susceptibility to Intergranular Attack in Stainless Steels.

Two special processes are employed which subject selected 300 Series stainless steel components to temperatures in the sensitization range:

1. Cylinder and spacer (cylinder, tube, and flange assembly) and retainer (collet assembly) are hard surfaced with Colmonoy 6.

2. Collet piston and guide cap (collet assembly) are nitrided to provide a wear-resistant surface.

Colmonoy hard surfacing is applied by the flame spray process. Parts are preheated to 550-800°F and then sprayed with Colmonoy. The sprayed coating is fused at about 2,000°F, using an oxyacetylene torch followed by air cooling.

Nitriding is accomplished using a proprietary process called New Malcomizing. Components are exposed to a temperature of about 1,080°F for approximately 20 hr during the nitriding cycle.

Colmonoy hard-surfaced components have performed successfully for the past 10 to 15 yr in drive mechanisms. Nitrided components have been used in CRDs since 1967. It is normal practice to remove some CRDs at each refueling outage. At this time, both the Colmonoy hard-surfaced parts and nitrided surfaces are accessible for visual examination. In addition, dye penetrant examinations have been performed on nitrided surfaces of the longest service drives. This inspection program is adequate to detect any incipient defects before they can become serious enough to cause operating problems.

Welding of austenitic stainless steel parts is performed in accordance with Section IX (Welding and Brazing Qualification) and Section II, Part C (Welding Rod Electrode and Filler Metals) of the ASME Boiler and Pressure Vessel

Code. Welded austenitic stainless steel assemblies require solution annealing to minimize the possibility of sensitizing. However, welded assemblies are dispensed from this requirement when there is documentation that welds are not subjected to sustained loads and assemblies have been free of service failure. Other reasons, in line with Regulatory Guide 1.44, for dispensing with the solution annealing are that assemblies are exposed to reactor coolant during normal operation service, which is below 200°F, or assemblies are of material of low carbon content, less than 0.025 percent. These controls are employed to comply with the intent of Regulatory Guide 1.44 as indicated in Section 1.8.

2. Control of Delta Ferrite Content

The delta ferrite content for weld materials used in welding austenitic stainless steel assemblies is verified on undiluted weld deposits for each heat or lot of filler metal and electrodes. The minimum delta ferrite content is defined for weld materials as 8.0 FN (Ferrite Number). This ferrite content is considered adequate to prevent any microfissuring (hot cracking) in austenitic stainless steel welds. The application of Regulatory Guide 1.31 is discussed in Section 1.8.

4.5.1.3 Other Materials

These are discussed in Section 4.5.1.1, item 2.

4.5.1.4 Protection of Materials During Fabrication, Shipping, and Storage

All the CRD parts listed in Section 4.5.1.1 are fabricated under a process specification which limits contaminants in cutting, grinding, and tapping coolants and lubricants. It also restricts all other processing materials (marking inks, tape, etc) to those which are completely removable by the applied cleaning process. All contaminants are then required to be removed by the appropriate cleaning process prior to any of the following:

1. Any processing which increases part temperature above 200°F.

2. Assembly which results in decrease of accessibility for cleaning.

3. Release of parts for shipment.

The specification for packaging and shipping the CRD provides the following:

The drive is rinsed in hot, deionized water and dried in preparation for shipment. The ends of the drive are then covered with a vapor-tight barrier with dessicant. Packaging is designed to protect the drive and prevent damage to the vapor barrier. The planned storage period considered in the design of the container and packaging is 2 yr. This packaging has been qualified and in use for a number of years. Periodic audits have indicated satisfactory protection.

The degree of surface cleanliness obtained by these procedures meets the requirements of Regulatory Guide 1.37.

Site or warehouse storage specifications require inside heated storage comparable to level B of ANSI N 45.2.2. However, exception has been taken to heated storage, so that unheated storage is allowed so long as the temperature does not fall below 40°F.

Semiannual examination of the humidity indicators of 10 percent of the units during inside heated warehouse storage is required to verify that the units are dry and in satisfactory condition. This inspection shall be performed with a GE-engineering designated representative present. Position indicator probes are not subject to this inspection.

4.5.2 Reactor Internal Materials

4.5.2.1 Material Specifications

Materials used for the core support structure include:

Shroud support	Nickel chrome-iron-alloy, ASME SB166 or SB168
Shroud, core plate, and top guide	ASME SA240, SA182, SA479, SA312, SA249, or SA213, (all Type 304L)
Peripheral fuel supports	SA312 Type 304, and 304L
Core plate and top guide hardware:	
Core plate studs	ASTM A479, TP 304 or or ASTM A193, Grade B8A

Core plate nuts	ASTM A479, TP 304 or ASTM A194, Grade 8A
Core plate wedges	ASME SA 479, TP 304
Top guide studs/ nuts	ASME SA 479, TP XM-19
Top guide sleeves	ASME SA 182, Grade F304L or F316L; ASME SA 213, TP 304L or 316L; ASME SA 249, TP 304L, 316, or 316L; or ASME SA 479, TP 304, 304L, 316L, or XM-19
Control rod drive housing	ASME SA 312, Type 304; ASME SA 182, Type 304; and ASME SB 167, Type Inconel 600
Control rod guide tube	ASME SA 351, Type CF8; ASME SA 358, SA 312, SA 249 (Type 304)
Orificed fuel support	ASME SA 351, Type CF8

Materials employed in other reactor internal structures include:

1. Steam Separator and Steam Dryer

All materials are Type 304 or 304L stainless steel.

Plate, sheet and strip	ASTM A240, Type 304 or 304L
Forgings	ASTM Al82, Grade F304 or 304L
Bars	ASTM A276, Type 304
Pipe	ASTM A312, Grade TP 304
Tube	ASTM A269, Grade TP 304
Castings	ASTM A351, Grade CF8

2. Jet Pump Assemblies

The components in the jet pump assemblies are a riser, inlet mixer, diffuser, and riser brace. Materials used for these components are to the following specifications:

Castings	ASTM A351, Grade CF8 and ASME SA 351, Grade CF3
Bars	ASTM A276, Type 304; ASTM A479, Type 316L; and ASTM A637, Grade 688
Bolts	ASTM A193, Grade B8 or B8M, ASME SA479 Type 316L
Sheet and plate	ASTM A240, Type 304, and ASME SA 240, Type 304L, 316L
Tubing	ASTM A269, Grade TP 304
Pipe	ASTM A358, Type 304, 316L and ASME SA312, Grade TP 304, 316L
Forged or rolled parts	ASME SA182, Grade F304, F316L, ASTM B166, and ASTM A637 Grade 688

Materials in the jet pump assemblies which are not austenitic stainless steel include:

a. The inlet mixer adaptor casting, the wedge casting, bracket casting adjusting screw casting, and the diffuser collar casting are hard surfaced with Stellite 6 for slip fit joints.

b. The diffuser is a bimetallic component made by welding a stainless steel forged ring to a forged Inconel 600 ring, made to Specification ASTM B166.

c. The inlet-mixer contains a pin, insert, and beam made of Inconel X750 to Specification ASTM A637, Grade 688.

The probability of occurrence of intergranular stress corrosion cracking of the jet pump beams has been significantly reduced for River Bend Station. This has been accomplished by decreasing the specified preload from 30 kips to 25 kips, and by having lower peak operational stresses than facilities which have previously experienced this problem. The beams are designed to be replaceable if required by the inservice inspection program.

All core support structures are fabricated from ASME-specified materials and designed in accordance with requirements of ASME Code, Section III, Subsection NG. Other reactor internals are noncoded and are fabricated from ASTM or ASME specification materials. Material requirements in the ASTM specifications are identical to requirements in corresponding ASME material specifications.

4.5.2.2 Controls on Welding

Core support structures are fabricated in accordance with requirements of ASME Code Section III, Subsection NG. Other internals are not required to meet ASME Code requirements. Requirements of ASME Boiler and Pressure Vessel Code, Section IX are followed in fabrication of core support structures and other internals.

4.5.2.3 Nondestructive Examination of Wrought Seamless Tubular Products

Wrought seamless tubular products for CRD guide tubes, CRD housings, and peripheral fuel supports were supplied in accordance with ASME Section III, Class CS, which requires examination of the tubular products by radiographic and/or ultrasonic methods according to paragraph NG-2550.

Wrought seamless tubular products for other internals were supplied in accordance with the applicable ASTM or ASME material specifications. These specifications require a hydrostatic test on each length of tubing.

4.5.2.4 Fabrication and Processing of Austenitic Stainless Steel - Regulatory Guide Conformance

Cold-worked stainless steels are not used in the reactor internals.

Regulatory Guide 1.31

All austenitic stainless steel weld filler materials were supplied with a minimum of 5 percent delta ferrite. This amount of ferrite is considered adequate to prevent

microfissuring in austenitic stainless steel welds. An extensive test program performed by GE, with the concurrence of the regulatory staff, has demonstrated that controlling weld filler metal ferrite at 5 percent minimum produces production welds which meet the requirements of Regulatory Guide 1.31. A total of 338 production welds in five BWR plants were measured and all welds met the intent of Regulatory Guide 1.31.

Regulatory Guide 1.34

Electroslag welding is not employed for any reactor internals.

Regulatory Guide 1.36

For external applications, all nonmetallic insulation meets the requirements of Regulatory Guide 1.36.

Regulatory Guide 1.37

Exposure to contaminant was avoided by carefully controlling all cleaning and processing materials which contact stainless steel during manufacture and construction. Any inadvertent surface contamination was removed to avoid potental detrimental effects.

Special care was exercised to ensure removal of surface contaminants prior to any heating operation. Water quality for rinsing, flushing, and testing was controlled and monitored.

The degree of cleanliness obtained by these procedures meets the require-ments of Regulatory Guide 1.37.

Regulatory Guide 1.44

All wrought austenitic stainless steel was purchased in the solution heat-treated condition. Heating above 800°F was prohibited (except for welding) unless the stainless steel was subsequently solution annealed. For 304 steel with carbon content in excess of 0.035 percent carbon, purchase specifications restricted the maximum weld heat input to 110,000 joules per in, and the weld interpass temperature to 350°F maximum. Welding was performed in accordance with Section IX of the ASME Boiler and Pressure Vessel Code. These controls were employed to avoid severe sensitization and comply with the intent of Regulatory Guide 1.44.

Regulatory Guide 1.71

There are few restrictive welds involved in the fabrication of items described in this section. Mockup welding was performed on the welds with most difficult access. Mockups were examined with radiography or by sectioning.

4.5.2.5 Other Materials

Hardenable martensitic stainless steels and precipitation-hardening stainless steels are not used in the reactor internals.

Materials, other than 300 Series stainless steel, employed in vessel internals are:

SA 479, Type XM-19 stainless steel
SB 166, 167, and 168 Nickel-Chrome-Iron (Inconel 600)
SA 637, Grade 688 Inconel X-750

Inconel 600 tubing plate and sheet are used in the annealed condition. Bar may be in the annealed or cold-drawn condition.

Inconel X-750 components are fabricated in the annealed or equalized condition and aged 20 hr at 1,300°F.

Stellite 6 hard surfacing is applied to austenitic stainless steel castings using the gas tungsten arc welding or plasma arc surfacing processes.

Colmonoy 5 hard surfacing is applied to austenitic stainless steel castings using the oxyacetylene metal-spray process.

All materials, except SA 479, Grade XM-19, have been successfully used for the past 10 to 15 yr in BWR applications. Extensive laboratory tests have demonstrated that XM-19 is a suitable material and that it is resistant to stress corrosion in a BWR environment.

4.5.3 Control Rod Drive Housing Supports

All CRD housing support subassemblies are fabricated of ASTM-A-36 structural steel, except for the following items:

	Material
Grid	ASTM-A-441
Disc springs	Schnorr, Type BS-125-71-8
Hex bolts and nuts	ASTM-A-307
6 x 4 x 3/8 tubes	ASTM-A-500, Grade B

For further CRD housing support information, refer to Section 4.6.1.2.

4.6 FUNCTIONAL DESIGN OF REACTIVITY CONTROL SYSTEMS

•→10
The reactivity control systems consist of control rods and CRDs, supplementary reactivity control for the initial core (Section 4.1.3.3) and the standby liquid control system (Section 9.3.5).
10←•

4.6.1 Information for the Control Rod Drive System

4.6.1.1 Control Rod Drive System Design

4.6.1.1.1 Design Bases

4.6.1.1.1.1 Safety Design Bases

The CRD mechanical system shall meet the following safety design bases:

1. The design shall provide for a sufficiently rapid control rod insertion so that no fuel damage results from any abnormal operating transient.

2. The design shall include positioning devices, each of which individually supports and positions a control rod.

3. Each positioning device shall:

   a. Prevent its control rod from initiating withdrawal as a result of a single malfunction.

   b. Be individually operated so that a failure in one positioning device does not affect the operation of any other positioning device.

   c. Be individually energized when rapid control rod insertion (scram) is signaled so that failure of power sources external to the positioning device does not prevent other positioning devices' control rods from being inserted.

4.6.1.1.1.2 Power Generation Design Basis

The CRD system drive design shall provide for positioning the control rods to control power generation in the core.

4.6.1.1.2 Description

•→1

The CRD system controls gross changes in core reactivity by incrementally positioning neutron absorbing control rods within the reactor core in response to manual control signals. It is also required to quickly shut down the reactor (scram) in emergency situations by rapidly inserting all control rods into the core in response to a manual or automatic signal from the RPS or Alternate Rod Insertion (ARI) logic. The CRD system consists of locking piston CRD mechanisms, and the CRD hydraulic system (including power supply and regulation, hydraulic control units, interconnecting piping, instrumentation and electrical controls).

1←•

4.6.1.1.2.1 Control Rod Drive Mechanisms

The CRD mechanism (drive) used for positioning the control rod in the reactor core is a double-acting, mechanically latched, hydraulic cylinder using water as its operating fluid. (Fig. 4.6-1 through 4.6-4.) The individual drives are mounted on the bottom head of the RPV. The drives do not interfere with refueling and are operative even when the head is removed from the reactor vessel.

The drives are also readily accessible for inspection and servicing. The bottom location makes maximum utilization of the water in the reactor as a neutron shield and gives the least possible neutron exposure to the drive components. Using water from the condensate treatment system, and/or condensate storage tanks as the operating fluid eliminates the need for special hydraulic fluid. Drives are able to utilize simple piston seals whose leakage does not contaminate the reactor water but provides cooling for the drive mechanisms and their seals.

The drives are capable of inserting or withdrawing a control rod at a slow, controlled rate, as well as providing rapid insertion when required. A mechanism on the drive locks the control rod at 6-in increments of stroke over the length of the core.

A coupling spud at the top end of the drive index tube (piston rod) engages and locks into a mating socket at the base of the control rod. The weight of the control rod is sufficient to engage and lock this coupling. Once locked, the drive and rod form an integral unit that must be manually unlocked by specific procedures before the components can be separated.

The drive holds its control rod in distinct latch positions until the hydraulic system actuates movement to a new

position. Withdrawal of each rod is limited by the seating of the rod in its guide tube. Withdrawal beyond this position to the overtravel limit can be accomplished only if the rod and drive are uncoupled. Withdrawal to the overtravel limit is annunciated by an alarm.

•→14

The individual rod indicators, grouped in one control panel display, correspond to relative rod locations in the core. The display module is divided into two sections. There is a display section and a rod select section;

•→10 10←• ←•14

4.6.1.1.2.2 Drive Components

Fig. 4.6-2 illustrates the operating principle of a drive. Fig. 4.6-3 and 4.6-4 illustrate the drive in more detail. The main components of the drive and their functions are described below.

4.6.1.1.2.2.1 Drive Piston

The drive piston is mounted at the lower end of the index tube. The function of the index tube is similar to that of a piston rod in a conventional hydraulic cylinder. The drive piston and index tube make up the main moving assembly in the drive. The drive piston operates between positive end stops, with a hydraulic cushion provided at the upper end only. The piston has both inside and outside seal rings and operates in an annular space between an inner cylinder (fixed piston tube) and an outer cylinder (drive cylinder). Because the type of inner seal used is effective in only one direction, the lower sets of seal rings are mounted with one set sealing in each direction.

A pair of nonmetallic bushings prevents metal-to-metal contact between the piston assembly and the inner cylinder surface. The outer piston rings are segmented, step-cut seals with expander springs holding the segments against the cylinder wall. A pair of split bushings on the outside of the piston prevents piston contact with the cylinder wall. The effective piston area for downtravel (withdrawal) is approximately 1.2 sq in versus 4.1 sq in for uptravel

(insertion). This difference in driving area tends to balance the control rod weight and assures a higher force for insertion than for withdrawal.

4.6.1.1.2.2.2 Index Tube

The index tube is a long hollow shaft made of nitrided stainless steel. Circumferential locking grooves, spaced every 6 in along the outer surface, transmit the weight of the control rod to the collet assembly.

4.6.1.1.2.2.3 Collet Assembly

The collet assembly serves as the index tube locking mechanism. It is located in the upper part of the drive unit. This assembly prevents the index tube from accidentally moving downward. The assembly consists of the collet fingers, a return spring, a guide cap, a collet housing (part of the cylinder, tube, and flange), and the collet piston.

Locking is accomplished by fingers mounted on the collet piston at the top of the drive cylinder. In the locked or latched position the fingers engage a locking groove in the index tube.

The collet piston is normally held in the latched position by a force of approximately 150 lb supplied by a spring. Metal piston rings are used to seal the collet piston from reactor vessel pressure. The collet assembly will not unlatch until the collet fingers are unloaded by a short, automatically sequenced, drive-in signal. A pressure approximately 180 psi above reactor vessel pressure must then be applied to the collet piston to overcome spring force, slide the collet up against the conical surface in the guide cap, and spread the fingers out so they do not engage a locking groove.

A guide cap is fixed in the upper end of the drive assembly. This member provides the unlocking cam surface for the collet fingers and serves as the upper bushing for the index tube.

If reactor water is used during a scram to supplement accumulator pressure, it is drawn through a filter on the guide cap.

4.6.1.1.2.2.4 Piston Tube

The piston tube is an inner cylinder, or column, extending upward inside the drive piston and index tube. The piston

tube is fixed to the bottom flange of the drive and remains stationary. Water is brought to the upper side of the drive piston through this tube. A buffer shaft, at the upper end of the piston tube, supports the stop piston and buffer components.

4.6.1.1.2.2.5 Stop Piston

•→15
A stationary piston called the stop piston is mounted on the upper end of the piston tube. This piston provides the seal between reactor vessel pressure and the space above the drive piston. It also functions as a positive end stop at the upper limit of control rod travel. Piston rings and bushings, similar to those used on the drive piston, are mounted on the upper portion of the stop piston. The lower portion of the stop piston forms a thin-walled cylinder containing the buffer piston, its metal seal ring, and the buffer piston return spring. As the drive piston reaches the upper end of the scram stroke, it strikes the buffer piston. A series of orifices or a tapered flow surface in the buffer shaft provides a progressive water shutoff to cushion the buffer piston as it is driven to its limit of travel. The high pressures generated in the buffer are confined to the cylinder portion of the stop piston, and are not applied to the stop piston and drive piston seals.
15←•
The center tube of the drive mechanism forms a well to contain the position indicator probe. The probe is an aluminum extrusion attached to a cast aluminum housing. Mounted on the extrusion are hermetically sealed, magnetically operated, reed switches. The entire probe assembly is protected by a thin-walled stainless steel tube. The switches are actuated by a ring magnet located at the bottom of the drive piston.

The drive piston, piston tube, and indicator tube are all of nonmagnetic stainless steel, allowing the individual switches to be operated by the magnet as the piston passes. Two switches are located at each position corresponding to an index tube groove, thus allowing redundant indication at each latching point. Two additional switches are located at each midpoint between latching points to indicate the intermediate positions during drive motion. Thus, indication is provided for each 3 in of travel. Duplicate switches are provided for the full-in and full-out positions. Redundant overtravel switches are located at a position below the normal full-out position. Because the limit of downtravel is normally provided by the control rod itself as it reaches the backseat position, the drive can pass this position and actuate the overtravel switches only if it is uncoupled from its control rod. A convenient means

is thus provided to verify that the drive and control rod are coupled after installation of a drive or at any time during plant operation.

4.6.1.1.2.2.6 Flange and Cylinder Assembly

A flange and cylinder assembly is made up of a heavy flange welded to the drive cylinder. A sealing surface on the upper face of this flange forms the seal to the drive housing flange. The seals contain reactor pressure and the two hydraulic control pressures. Teflon coated, stainless steel rings are used for these seals. The drive flange contains the integral ball, or two-way, check (ball-shuttle) valve. This valve directs either the reactor vessel pressure or the driving pressure, whichever is higher, to the underside of the drive piston. Reactor vessel pressure is admitted to this valve from the annular space between the drive and drive housing through passages in the flange.

Water used to operate the collet piston passes between the outer tube and the cylinder tube. The inside of the cylinder tube is honed to provide the surface required for the drive piston seals.

Both the cylinder tube and outer tube are welded to the drive flange. The upper ends of these tubes have a sliding fit to allow for differential expansion.

The upper end of the index tube is threaded to receive a coupling spud. The coupling (Fig. 4.6-1) accommodates a small amount of angular misalignment between the drive and the control rod. Six spring fingers allow the coupling spud to enter the mating socket on the control rod. A plug then enters the spud and prevents uncoupling.

4.6.1.1.2.2.7 Lock Plug

Two means of uncoupling are provided. With the reactor vessel head removed, the lock plug can be raised against the spring force of approximately 50 lb by a rod extending up through the center of the control rod to an unlocking handle located above the control rod velocity limiter. The control rod, with the lock plug raised, can then be lifted from the drive.

If it is desired to uncouple a drive without removing the RPV head for access, the lock plug can also be pushed up from below. In this case, the piston tube assembly is pushed up against the uncoupling rod assembly, which raises the lock plug and allows the coupling spud to disengage the socket as the drive piston and index tube are driven down.

The control rod is heavy enough to force the spud fingers to enter the socket and push the lock plug up, allowing the spud to enter the socket completely and the plug to snap back into place. Therefore, the drive can be coupled to the control rod using only the weight of the control rod.

4.6.1.1.2.3 Materials of Construction

Factors that determine the choice of construction materials are discussed in the following sections.

4.6.1.1.2.3.1 Index Tube

The index tube must withstand the locking and unlocking action of the collet fingers. A compatible bearing combination must be provided that is able to withstand moderate misalignment forces. Large tensile and column loads are applied during scram. The reactor environment limits the choice of materials suitable for corrosion resistance. To meet these varied requirements, the index tube is made from annealed, single-phase, nitrogen-strengthened, austenitic stainless steel. The wear and bearing requirements are provided by Malcomizing the complete tube. To obtain suitable corrosion resistance, a carefully controlled process of surface preparation is employed.

4.6.1.1.2.3.2 Coupling Spud

The coupling spud is made of Inconel X-750 that is aged for maximum physical strength and the required corrosion resistance. Because misalignment tends to cause chafing in the semispherical contact area, the part is protected by a thin chromium plating (electrolized). This plating also prevents galling of the threads attaching the coupling spud to the index tube.

4.6.1.1.2.3.3 Collet Fingers

Inconel X-750 is used for the collet fingers, which must function as leaf springs when cammed open to the unlocked position. Colmonoy 6 hard facing provides a long wearing surface, adequate for design life, to the area contacting the index tube and unlocking cam surface of the guide cap.

4.6.1.1.2.3.4 Seals and Bushings

Graphitar is selected for seals and bushings on the drive piston and stop piston. The material is inert and has a low friction coefficient when water-lubricated. Because some loss of Graphitar strength is experienced at higher

•→14
temperatures, the drive is supplied with cooling water to limit the amount of time that temperature is above 250°F. The Graphitar is relatively soft, which is advantageous when an occasional particle of foreign matter reaches a seal. The resulting scratches in the seal reduce sealing efficiency until worn smooth, but the drive design can tolerate considerable water leakage past the seals into the reactor vessel.
14←•

4.6.1.1.2.3.5 Summary

All drive components exposed to reactor vessel water are made of austenitic stainless steel except the following:

1. Seals and bushings on the drive piston and stop piston are Graphitar.

2. All springs and members requiring spring action (collet fingers, coupling spud, and spring washers) are made of Inconel X-750.

3. The ball check valve is a Haynes Stellite cobalt-base alloy.

4. Elastomeric O-ring seals are ethylene propylene.

5. Metal piston rings are Haynes 25 alloy.

6. Certain wear surfaces are hard-faced with Colmonoy 6.

7. Nitriding by a proprietary new Malcomizing process and chromium plating are used in certain areas where resistance to abrasion is necessary.

8. The drive piston head, stop piston, buffer shaft and buffer piston are made of Armco 17-4 PH.

9. Certain fasteners and locking devices are made of Inconel X-750 or 600.

Pressure-containing portions of the drives are designed and fabricated in accordance with requirements of Section III of the ASME Boiler and Pressure Vessel Code.

4.6.1.1.2.4 Control Rod Drive Hydraulic System

The CRD hydraulic system (Fig. 4.6-5a through 4.6-5d) supplies and controls the pressure and flow to and from the drives through hydraulic control units (HCU). The water discharged from the drives during a scram flows through the HCUs to the scram discharge volume. The water discharged

from a drive during a normal control rod positioning operation flows through the HCU and the exhaust header, and is returned to the reactor vessel via the HCUs of nonmoving drives. There are as many HCUs as the number of CRDs.

4.6.1.1.2.4.1 Hydraulic Requirements

•→10
The CRD hydraulic system design is shown on Fig. 4.6-5. The hydraulic requirements, identified by the function they perform, are as follows:
10←•

1. An accumulator hydraulic charging pressure of approximately 1,750 to 2,000 psig is required. Flow to the accumulators is required only during scram reset or system startup.

•→14

2. Drive pressure of 250 psi minimum above reactor vessel pressure is required. A flow rate of approximately 4 gpm to insert each control rod and 2 gpm to withdraw each control rod is required. These values will increase as the CRD seal characteristic change with time.

3. Cooling water to the drives is required at approximately 10 psi above reactor vessel pressure and at a flow rate of approximately 0.34 gpm per drive unit. The cooling water differential pressure will decrease as the CRD seal characteristics change with time.

14←•

4. The scram discharge volume is sized to receive, and contain, all the water discharged by the drives during a scram; a minimum volume of 3.34 gal per drive is required (excluding the instrument volume).

4.6.1.1.2.4.2 System Description

The CRD hydraulic system provides the required functions with the pumps, filters, valves, instrumentation, and piping shown on Fig. 4.6-5 and described in the following sections.

Duplicate components are included, where necessary, to assure continuous system operation if an inservice component requires maintenance.

4.6.1.1.2.4.2.1 Supply Pump

One supply pump pressurizes the system with water from the condensate treatment system and/or condensate storage tanks. One spare pump is provided for standby. A discharge check valve prevents backflow through the nonoperating pump. A portion of the pump discharge flow is diverted through a minimum flow bypass line to the condensate storage tank. This flow is controlled by an orifice and is sufficient to

prevent pump damage if the pump discharge is inadvertently closed.
•→8
Condensate water is processed by two filters in the system. The pump suction filter is a disposable element type with a 25-micron absolute rating. A 250-micron strainer in the filter bypass line protects the pump when the filters are being serviced. The drive water filter, down stream of the pump, is a cleanable element type with a filtration rating ranging from 50-micron absolute to 15-micron absolute. A differential pressure indicator and main control room alarm monitor the filter element as it collects foreign materials.
8←•
4.6.1.1.2.4.2.2 Accumulator Charging Pressure

Accumulator charging pressure is established by precharging the nitrogen accumulator to a precisely controlled pressure at known temperature. During scram, the scram inlet (and outlet) valves open and permit the stored energy in the accumulators to discharge into the drives. The resulting pressure decrease in the charging water header allows the CRD supply pump to run out (i.e., flow rate to increase substantially) into the CRDs via the charging water header. The flow element upstream of the accumulator charging header senses high flow and provides a signal to the manual auto-flow control station which in turn closes the system flow control valve. This action maintains increased flow through the charging water header, while avoiding prolonged pump operation at run-out conditions.
•→14
Pressure in the charging header is monitored in the main control room with a pressure indicator and low pressure alarm.
←•14
During normal operation the flow control valve maintains a constant system flow rate. This flow is used for drive flow and drive cooling.

4.6.1.1.2.4.2.3 Drive Water Pressure
•→14
Drive water pressure required in the drive header is maintained by the drive/cooling pressure control valve, which is manually adjusted from the main control room. A flow rate approximately equal to the sum of the flow rate required to insert 4 control rods normally passes from the drive water pressure stage through eight solenoid-operated stabilizing valves (arranged in parallel) into the cooling water header. The flow through two stabilizing valves equals the drive insert flow for one drive; that of one stabilizing valve equals the drive withdrawal flow for one drive. When operating a drive(s), the required flow is
14←•

diverted to the drives by closing the appropriate stabilizing valves, at the same time opening the drive directional control and exhaust solenoid valves. Thus, flow through the drive/cooling pressure control valve is always constant.

Flow indicators in the drive water header and in the line downstream from the stabilizing valves allow the flow rate through the stabilizing valves to be adjusted when necessary. Differential pressure between the reactor vessel and the drive pressure stage is indicated in the main control room.

4.6.1.1.2.4.2.4 Cooling Water Header

•→14
The cooling water header is located downstream from the drive/cooling pressure valve. Two parallel path equalizing valves connect the cooling water header and the exhaust water header and a stainless steel flow stabilizer loop is routed to the cooling water header. The drive/cooling pressure control valve is manually adjusted from the main control room to produce the required drive/cooling water pressure balance.
←•14
The RBS CRD return line nozzle on the reactor vessel has been capped to address NUREG-0619, BWR Feedwater Nozzle and Control Rod Drive Return Line Nozzle Cracking.

•→16
The flow through the flow control valve is virtually constant. Therefore, once adjusted, the drive/cooling pressure control valve will maintain the correct drive pressure and cooling water pressure, independent of reactor vessel pressure. Changes in setting of the pressure control valve are required only to adjust for changes in the cooling requirements of the drives, as the drive seal characteristics change with time. A flow indicator in the main control room monitors cooling water flow. A differential pressure indicator in the main control room indicates the difference between reactor vessel pressure and drive cooling water pressure. Although the drives can function without cooling water, seal life is shortened by long term exposure to reactor temperatures. The temperature of each drive is indicated and recorded, and excessive temperatures are annunciated in the main control room.
←•16

4.6.1.1.2.4.2.5 Scram Discharge Volume

The scram discharge system complies with the criteria enumerated in the Generic Safety Evaluation Report - BWR Scram Discharge System, as indicated in the LRG-II position 1-ASB.

The scram discharge volume consists of header piping which connects to each HCU and drains into an instrument volume. The header piping is sized to receive and contain all the water discharged by the drives during a scram, independent of the instrument volume. A minimum scram discharge volume of 3.34 gal per drive is provided. This minimum scram discharge volume is based on conservative assumptions of the performance of the scram system. In the event of a coolant leak into the SDV, an automatic scram occurs before the required SDV availability is threatened.

During normal plant operation the scram discharge volume is empty and vented to atmosphere through its open vent and drain valve. When a scram occurs, upon a signal from the safety circuit these vent and drain valves are closed to conserve reactor water. Lights in the main control room indicate the position of these valves.

No single active failure in the scram system design can prevent a reactor scram. The SDV and associated vent and drain piping is classified as important to safety and required to meet the ASME Section III Class II and Seismic Category I requirements. Partial or full loss of service functions does not adversely affect the scram system function or result in a full reactor scram. The power-operated vent and drain valves close under loss of air and/or electric power. Valve position indication is provided in the main control room.

There is no reduction in the pipe size of the header piping going from the HCUs to and including the scram discharge instrument volume (SDIV). All SDV piping is required to be continuously sloped from its high point to its low point. The SDIV is directly connected to the scram discharge volume at the low point of the scram discharge header piping. This hydraulic coupling permits operability of the scram level instrumentation prior to loss of system function. The scram level instrumentation is redundant and diverse to assure no single failure or common mode failure prevents a reactor scram.

Redundant SDV vent and drain valves are provided. The redundant SDV valve configuration assures that no single active failure can result in an uncontrolled loss of reactor coolant. An additional solenoid operated pilot valve controls the redundant vent and drain valve. The vent and drain system is therefore sufficiently redundant to avoid a failure to isolate the SDV due to solenoid failure. The vent and drain valve opening and closing sequences are controlled to minimize excessive hydro-dynamic forces.

During a scram, the scram discharge volume partly fills with water discharged from above the drive pistons. After scram is completed, the CRD seal leakage from the reactor continues to flow into the scram discharge volume until the discharge volume pressure equals the reactor vessel pressure. A check valve in each HCU prevents reverse flow from the scram discharge header volume to the drive. When the initial scram signal is cleared from the RPS, the scram discharge volume signal is overridden with a keylock override switch, and the scram discharge volume is drained and returned to atmospheric pressure.

A dedicated vent line with a nonsubmerged discharge to the atmosphere is provided as part of the scram discharge system to assure proper drainage in preparation for scram reset. Additional vent capability is provided by the vent line vacuum breakers, which are required to have a differential pressure no greater than 5 in of water.

The SDV vent and drain lines are dedicated lines that discharge into the reactor building equipment and drain system. Vacuum breakers on the SDV vent line and shut-off valves on the SDV vent and drain lines preclude water from siphoning back into the SDIV from the reactor building equipment and drain system.

•→14
Remote manual switches in the pilot valve solenoid circuits allow the discharge volume vent and drain valves to be tested without disturbing the RPS.

←•14
Diverse, and redundant level sensing instrumentation on the scram discharge instrument volume (SDIV) is provided for the automatic scram function. SDIV water level is measured by utilization of both float sensing and pressure sensing devices. Instrument taps are located to protect the level sensing instrumentation from the flow dynamics in the scram discharge system. Each SDIV has a redundant instrument loop. A one-out-of-two twice logic is employed for the automatic scram function. This instrumentation arrangement assures the automatic scram function on high SDIV water level in the event of a single active or passive failure. Instrumentation is also provided to aid the operator in the detection of water accumulation in the instrumented volume(s) prior to scram initiation.

The SDIV scram level instrumentation arrangement and trip logic allows instrument adjustment or surveillance without bypassing the scram function or directly causing a scram.

Each level instrument can be individually isolated without bypassing the scram function. Technical Specifications will ensure that the scram function is not bypassed during repair, replacement, adjustment or surveillance of any system component.

Eight liquid-level trip units activated by six transmitters connected to the instrument volume monitor the volume for abnormal water level. They are set at three different levels. At the lowest level, either of two trip units activates an alarm annunciator to indicate that the volume is not completely empty during post-scram draining or to indicate that the volume starts to fill through leakage accumulation at other times during reactor operation. At the second level, two trip units produce a rod withdrawal block to prevent further withdrawal of any control rod when leakage accumulates to half the capacity of the instrument volume. The remaining four trip units are interconnected with the trip channels of the RPS and will initiate a reactor scram should water accumulation fill the instrument volume. A non-indicating float type level switch in each channel provides redundancy and diversity to each RPS trip unit.

Supervisory instrumentation and alarms provided include accumulator trouble, scram valve air supply low pressure, and scram discharge volume not drained alarms. These instruments provide operator surveillance of scram system readiness.

Minimizing the exposure of operating personnel to radiation is a consideration in equipment design and location.

4.6.1.1.2.4.3 Hydraulic Control Units

•→10

Each HCU furnishes pressurized water, on signal, to a drive unit. The drive then positions its control rod as required. Operation of the electrical system that supply scram and normal control rod positioning signals to the HCU is described in Sections 7.2.1.1 and 7.7.1.1.

The basic components in each HCU are manual, pneumatic, and electrical valves, and accumulator, related piping, electrical connections, filters, and instrumentation (Figure 4.6-5 and 4.6-7). The components and their functions are described in the following sections.

10←•

4.6.1.1.2.4.3.1 Insert Drive Valve

The insert drive valve is solenoid-operated and opens on an insert signal. The valve supplies drive water to the bottom side of the main drive piston.

4.6.1.1.2.4.3.2 Insert Exhaust Valve

The insert exhaust solenoid valve also opens on an insert signal. The valve discharges water from above the drive piston to the exhaust water header.

4.6.1.1.2.4.3.3 Withdraw Drive Valve

The withdraw drive valve is solenoid-operated and opens on a withdraw signal. The valve supplies drive water to the top of the drive piston.

4.6.1.1.2.4.3.4 Withdraw Exhaust Valve

The solenoid-operated withdraw exhaust valve opens on a withdraw signal and discharges water from below the main drive piston to the exhaust header. It also serves as the settle valve, which opens, following any normal drive movement (insert or withdraw), to allow the control rod and its drive to settle back into the nearest latch postion.

4.6.1.1.2.4.3.5 Speed Control Units

The insert drive valve and withdraw exhaust valve have a speed control unit. The speed control unit regulates the control rod insertion and withdrawal rates during normal operation. The manually adjustable flow control unit is used to regulate the water flow to and from the volume beneath the main drive piston. A correctly adjusted unit does not require readjustment except to compensate for changes in drive seal leakage.

4.6.1.1.2.4.3.6 Scram Pilot Valve Assembly

The scram pilot valve assembly is operated from the RPS. The scram pilot valve assembly, with two solenoids, controls both the scram inlet valve and the scram exhaust valve. The scram pilot valve assembly is solenoid-operated and is normally energized. On loss of electrical signal to the solenoids, such as the loss of external ac power, the inlet port closes and the exhaust port opens. The pilot valve assembly (Fig. 4.6-5) is designed so that the trip system signal must be removed from both solenoids before air pressure can be discharged from the scram valve operators.

This prevents inadvertent scram of a single drive in the event of a failure of one of the pilot valve solenoids.

4.6.1.1.2.4.3.7 Scram Inlet Valve

The scram inlet valve opens to supply pressurized water to the bottom of the drive piston. This quick opening globe valve is operated by an internal spring and system pressure. It is closed by air pressure applied to the top of its diaphragm operator. A position indicator switch on this valve energizes a light in the main control room as soon as the valve starts to open.

4.6.1.1.2.4.3.8 Scram Exhaust Valve

The scram exhaust valve opens slightly before the scram inlet valve, exhausting water from above the drive piston. The exhaust valve opens faster than the inlet valve because of the higher air pressure spring setting in the valve operator.

4.6.1.1.2.4.3.9 Scram Accumulator

The scram accumulator stores sufficient energy to fully insert a control rod at any vessel pressure. The accumulator is a hydraulic cylinder with a free-floating piston. The piston separates the water on top from the nitrogen below. A check valve in the accumulator charging line prevents loss of water pressure in the event supply pressure is lost.

During normal plant operation, the accumulator piston is seated at the bottom of its cylinder. Loss of nitrogen decreases the nitrogen pressure, which actuates a pressure switch and sounds an alarm in the main control room.

To ensure that the accumulator is always able to produce a scram, it is continuously monitored for water leakage. A float type level switch actuates an alarm if water leaks past the piston barrier and collects in the accumulator instrumentation block.

4.6.1.1.2.5 Control Rod Drive System Operation

The CRD system performs rod insertion, rod withdrawal, and scram. These operational functions are described in the following sections.

4.6.1.1.2.5.1 Rod Insertion

Rod insertion is initiated by a signal from the operator to the insert valve solenoids. This signal causes both insert valves to open. The insert drive valve applies reactor pressure plus approximately 90 psi to the bottom of the drive piston. The insert exhaust valve allows water from above the drive piston to discharge to the exhaust header.

•→14
As is illustrated in Fig. 4.6-3, the locking mechanism is a ratchet-type device and does not interfere with rod insertion. The speed at which the drive moves is determined by the flow through the insert speed control valve, which is set for a control rod shim speed (nonscram operation) of approximately 3 in/sec. During normal insertion, the pressure on the downstream side of the speed control valve is 90 to 100 psi above reactor vessel pressure. However, if the drive slows for any reason, the flow through and pressure drop the insert speed control valve will decrease. The full differential pressure (260 psi) will then be available to cause continued insertion. With 260-psi differential pressure acting on the drive piston, the piston exerts an upward force of 1,066 lb.

14←•
4.6.1.1.2.5.2 Rod Withdrawal

Rod withdrawal is, by design, more involved than insertion. The collet finger (latch) must be raised to reach the unlocked position (Fig. 4.6-3). The notches in the index tube and the collet fingers are shaped so that the downward force on the index tube holds the collet fingers in place. The index tube must be lifted before the collet fingers can be released. This is done by opening the drive insert valves (in the manner described in the preceding section) for approximately 1 sec. The withdraw valves are then opened, applying driving pressure above the drive piston and opening the area below the piston to the exhaust header. Pressure is simultaneously applied to the collet piston. As the piston raises, the collet fingers are cammed outward, away from the index tube, by the guide cap.

The pressure required to release the latch is set and maintained at a level high enough to overcome the force of the latch return spring plus the force of reactor pressure opposing movement of the collet piston. When this occurs, the index tube is unlatched and free to move in the withdraw direction. Water displaced by the drive piston flows out through the withdraw speed control valve, which is set to give the control rod a shim speed of 3 in/sec. The entire valving sequence is automatically controlled and is initiated by a single operation of the rod withdraw switch.

4.6.1.1.2.5.3 Scram

During a scram the scram pilot valve assembly and scram valves are operated as previously described. With the scram valves open, accumulator pressure is admitted under the drive piston, and the area over the drive piston is vented to the scram discharge volume.

The large differential pressure (approximately 1,750 psi, initially, and always several hundred psi, depending on reactor vessel pressure) produces a large upward force on the index tube and control rod. This force gives the rod a high initial acceleration and provides a large margin of force to overcome friction. After the initial acceleration is achieved, the drive continues at a diminishing velocity. This characteristic provides a high initial rod insertion rate. As the drive piston nears the top of its stroke, the piston reaches the buffer and the driveline is brought to a stop at the full-in position.

•→14
Prior to a scram signal the accumulator in the HCU has 1,750 to 2,000 psig on the water side and approximately 1,750 psig on the nitrogen side. As the inlet scram valve opens, the full water side pressure is available at the CRD acting on a 4.1 sq in area. As CRD motion begins, this pressure drops to the gas side pressure less line losses between the accumulator and the CRD. When the drive reaches the full-in position, the accumulator completely discharges with a resulting gas side pressure of approximately 1,200 psig.
14←•
The CRD accumulators are necessary to scram the control rods within the required time. Each drive, however, has an internal ballcheck valve which allows reactor pressure to be admitted under the drive piston. If the reactor is above 600 psi this valve ensures rod insertion in the event the accumulator is not charged or the inlet scram valve fails to open. The insertion time, however, will be slower than the scram time with a properly functioning scram system.

The CRD system, with accumulators, provides the following scram performances at full power operation, in terms of average elapsed time after the opening of the RPS trip actuator (scram signal) for the drives to attain the scram strokes listed:

Percent of full stroke	1	10	40	75
Stroke, in	1.4	14.4	57.6	108
Time, sec	0.138	0.317	0.874	1.620

4.6.1.1.2.6 Instrumentation

The instrumentation for both the control rods and CRDs is defined by that given for the RCIS. The objective of the RCIS is to provide the operator with the means to make changes in nuclear reactivity so that reactor power level and power distribution can be controlled. The system allows the operator to manipulate control rods.

The design bases and further discussion are covered in Chapter 7.

4.6.1.2 Control Rod Drive Housing Supports

4.6.1.2.1 Safety Objective

The CRD housing supports prevent any significant nuclear transient in the event a drive housing breaks or separates from the bottom of the reactor vessel.

4.6.1.2.2 Safety Design Bases

The CRD housing supports shall meet the following safety design bases:

1. Following a postulated CRD housing failure, control rod downward motion shall be limited so that any resulting nuclear transient could not be sufficient to cause fuel damage.

2. The clearance between the CRD housings and the supports shall be sufficient to prevent vertical contact stresses caused by thermal expansion during plant operation.

4.6.1.2.3 Description

The CRD housing supports are shown in Fig. 4.6-8. Horizontal beams are installed immediately below the bottom head of the reactor vessel, between the rows of CRD housings. The beams are welded to brackets which are welded to the steel form liner of the drive room in the reactor support pedestal.

Hanger rods, approximately 10 ft long and 1 3/4 inches in diameter, are supported from the beams on stacks of disc springs. These springs compress approximately 2 in under the design load.

The support bars are bolted between the bottom ends of the hanger rods. The spring pivots at the top, and the beveled,

loose fitting ends on the support bars prevent substantial bending moment in the hanger rods if the support bars are overloaded.

Individual grids rest on the support bars between adjacent beams. Because a single piece grid would be difficult to handle in the limited work space and because it is necessary that CRDs, position indicators, and incore instrumentation components be accessible for inspection and maintenance, each grid is designed for inplace assembly or disassembly. Each grid assembly is made from two grid plates, a clamp, and a bolt. The top part of the clamp guides the grid to its correct position directly below the CRD housing that it would support in the postulated accident.

When the support bars and grids are installed, a gap of approximately 1 in at room temperature (approximately 70°F) is provided between the grid and the bottom contact surface of the CRD flange. During system heatup, this gap is reduced by a net downward expansion of the housings with respect to the supports. In the hot operating condition, the gap is approximately 3/4 in.

In the postulated CRD housing failure, the CRD housing supports are loaded when the lower contact surface of the CRD flange contacts the grid. The resulting load is then carried by two grid plates, two support bars, four hanger rods, their disc springs, and two adjacent beams.

The American Institute of Steel Construction (AISC) Manual of Steel Construction, "Specification for the Design, Fabrication and Erection of Structural Steel for Buildings," was used in designing the CRD housing support system. However, to provide a structure that absorbs as much energy as practical without yielding, the allowable tension and bending stresses used were 90 percent of yield and the shear stress used was 60 percent of yield. These design stresses are 1.5 times the AISC allowable stresses (60 and 40 percent of yield, respectively).

•→14
For purposes of mechanical design, the postulated failure resulting in the highest forces is an instantaneous circumferential separation of the CRD housing from the reactor vessel, with the reactor at an operating pressure of 1100 psig (at the bottom of the vessel) acting on the area of the separated housing. The weight of the separated housing, CRD, and blade, plus the pressure of 1100 psig acting on the area of the separated housing, gives a force of approximately 32,500 lb. This force is used to calculate the impact force, conservatively assuming that the housing travels through a 1-in gap before it contacts the supports.
14←•

•→16
The impact force (109,000 lb) is then treated as a static load in design. The CRD housing supports are designed as Seismic Category I equipment in accordance with Section 3.2. Loading conditions and examples of stress analysis results and limits are shown in Table 3.9A-2. Safety evaluation is discussed in Section 4.6.2.3.3.
←•16

4.6.2 Evaluations of the CRDs

4.6.2.1 Failure Modes and Effects Analysis

The evaluation of failure of the control rod drive system (CRDS) is covered under Nuclear Safety Operational Analysis (NSOA) in Appendix 15A, Section 15A.6.5.3.

4.6.2.2 Protection from Common Mode Failures

The evaluation of failure of the CRDS is covered under Nuclear Safety Operational Analysis (NSOA) in Appendix 15A, Section 15A.6.5.3.

4.6.2.3 Safety Evaluation

Safety evaluation of the control rods, CRDs, and CRD housing supports is described in the following sections. Further description of control rods is contained in Section 4.2.

4.6.2.3.1 Control Rods

4.6.2.3.1.1 Materials Adequacy Throughout Design Lifetime

The adequacy of the materials throughout the design life was evaluated in the mechanical design of the control rods. The primary materials, B-C powder and 304 austenitic stainless steel, have been found suitable in meeting the demands of the BWR environment.

4.6.2.3.1.2 Dimensional and Tolerance Analysis

Layout studies are done to assure that, given the worst combination of part tolerance ranges at assembly, no interference exists which will restrict the passage of control rods. In addition, preoperational verification is made on each control blade system to show that the acceptable levels of operational performance are met.

4.6.2.3.1.3 Thermal Analysis of the Tendency to Warp

The various parts of the control rod assembly remain at approximately the same temperature during reactor operation, negating the problem of distortion or warpage. What little

differential thermal growth could exist is allowed for in the mechanical design. A minimum axial gap is maintained between absorber rod tubes and the control rod frame assembly for the purpose. In addition, to further this end, dissimilar metals are avoided.

4.6.2.3.1.4 Forces for Expulsion

•→10
An analysis has been performed which evaluates the maximum pressure forces which could tend to eject a control rod from the core. The results of this analysis are given in Section 4.6.2.3.2.2. In summary, if the collet were to remain open, which is unlikely, calculations indicate that the steady-state control rod withdrawal velocity would be 2 ft/sec for a pressure-under line break, the limiting case for rod withdrawal.
10←•

4.6.2.3.1.5 Functional Failure of Critical Components

The consequences of a functional failure of critical components have been evaluated and the results are covered in Section 4.6.2.3.2.2.

4.6.2.3.1.6 Precluding Excessive Rates of Reactivity Addition

In order to preclude excessive rates of reactivity addition, analysis has been performed both on the velocity limiter device and the effect of probable control rod failures (Section 4.6.2.3.2.2).

4.6.2.3.1.7 Effect of Fuel Rod Failure on Control Rod Channel Clearances

The CRD mechanical design ensures a sufficiently rapid insertion of control rods to preclude the occurrence of fuel rod failures which could hinder reactor shutdown by causing significant distortions in channel clearances.

4.6.2.3.1.8 Mechanical Damage

•→10
In addition to the analysis performed on the CRD (Sections 4.6.2.3.2.2 and 4.6.2.3.2.3), and the control rod blade, analyses were performed on the control rod guide tube (Sections 4.2.3.1.7 and 4.2.3.1.8).
10←•

4.6.2.3.1.9 Evaluation of Control Rod Velocity Limiter

The control rod velocity limiter limits the free fall velocity of the control rod to a value that cannot result in nuclear system process barrier damage. This velocity is evaluated by the rod drop accident analysis in Chapter 15.

4.6.2.3.2 Control Rod Drives

4.6.2.3.2.1 Evaluation of Scram Time

•→10

The rod scram function of the CRD system provides the negative reactivity insertion required by safety design basis No. 1 in Section 4.6.1.1.1.1. The scram time shown in the description (Section 4.6.1.1.2.5.3) is adequate as shown by the transient analyses of Chapter 15.

10←•

4.6.2.3.2.2 Analysis of Malfunction Relating to Rod Withdrawal

There are no known single malfunctions that cause the unplanned withdrawal of even a single control rod. However, if multiple malfunctions are postulated, studies show that an unplanned rod withdrawal can occur at withdrawal speeds that vary with the combination of malfunctions postulated. In all cases the subsequent withdrawal speeds are less than those assumed in the rod drop accident analysis as discussed in Chapter 15. Therefore, the physical and radiological consequences of such rod withdrawals are less than those analyzed in the rod drop accident.

•→14

The calculated values shown in the following postulated malfunction events may increase slightly (up to approximately 5% to 10%) when operating at a power uprate reactor pressure condition.

14←•

4.6.2.3.2.2.1 Drive Housing Fails at Attachment Weld

The bottom head of the reactor vessel has a penetration for each CRD location. A drive housing is raised into position inside each penetration and fastened by welding. The drive is raised into the drive housing and bolted to a flange at the bottom of the housing.

The CRD housing material at the vessel penetration is seamless, Type Inconel 600 tubing with a minimum tensile strength of 80,000 psi, and Type 304 stainless steel pipe below the vessel with a minimum strength of 75,000 psi. The basic failure considered here is a complete circumferential crack through the housing wall at an elevation just below the J-weld.

Static loads on the housing wall include the weight of the drive and the control rod, the weight of the housing below the J-weld, and the reactor pressure acting on the 6-in diameter cross-sectional area of the housing and the drive.

Dynamic loading results from the reaction force during drive operation.

If the housing were to fail as described, the following sequence of events is foreseen. The housing would separate from the vessel. The CRD and housing would be blown downward against the support structure by reactor pressure acting on the cross-sectional area of the housing and the drive. The downward motion of the drive and associated parts would be determined by the gap between the bottom of the drive and the support structure and by the deflection of the support structure under load. In the current design, maximum deflection is approximately 3 in. If the collet were to remain latched, no further control rod ejection would occur[1], the housing would not drop far enough to clear the vessel penetration, and reactor water would leak at a rate of approximately 180 gpm through the 0.03-in diametral clearance between the housing and the vessel penetration.

If the basic housing failure were to occur while the control rod is being withdrawn (this is a small fraction of the total drive operating time) and if the collet were to stay unlatched, the following sequence of events is foreseen. The housing would separate from the vessel and the drive and housing would be blown downward against the CRD housing support. Calculations indicate that the steady-state rod withdrawal velocity would be 0.3 ft/sec. During withdrawal, pressure under the collet piston would be approximately 250 psi greater than the pressure over it. Therefore, the collet would be held in the unlatched position until driving pressure was removed from the pressure-over port.

4.6.2.3.2.2.2 Rupture of Hydraulic Line(s) to Drive Housing Flange

There are three types of possible rupture of hydraulic lines to the drive housing flange: 1) pressure-under (insert) line break, 2) pressure-over (withdrawn) line break, and 3) coincident breakage of both these lines.

4.6.2.3.2.2.2.1 Pressure-Under (Insert) Line Break

For the case of a pressure-under (insert) line break, a partial or complete circumferential opening is postulated at or near the point where the line enters the housing flange. Failure is more likely to occur after another basic failure wherein the drive housing or housing flange separates from the reactor vessel. Failure of the housing, however, does not necessarily lead directly to failure of the hydraulic lines.

If the pressure-under (insert) line were to fail and if the collet were latched, no control rod withdrawal would occur. There would be no pressure differential across the collet piston and, therefore, no tendency to unlatch the collet. Consequently, the associated control rod could not be withdrawn, but if reactor pressure is greater than 600 psig, it will insert on a scram signal.

The ball check valve is designed to seal off a broken pressure-under line by using reactor pressure to shift the check ball to its upper seat. If the ball check valve were prevented from seating, reactor water would leak to the containment. Because of the broken line, cooling water could not be supplied to the drive involved. Loss of cooling water would cause no immediate damage to the drive. However, prolonged exposure of the drive to temperatures at or near reactor temperature could lead to deterioration of material in the seals. High temperature would be indicated to the operator by the thermocouple in the position indicator probe. A second indication would be high cooling water flow.

If the basic line failure were to occur while the control rod is being withdrawn the hydraulic force would not be sufficient to hold the collet open, and spring force normally would cause the collet to latch and stop rod withdrawal. However, if the collet were to remain open, calculations indicate that the steady-state control rod withdrawal velocity would be 2 ft/sec.

4.6.2.3.2.2.2.2 Pressure-Over (Withdrawn) Line Break

The case of the pressure-over (withdrawn) line breakage considers the complete breakage of the line at or near the point where it enters the housing flange. If the line were to break, pressure over the drive piston would drop from reactor pressure to atmospheric pressure. Any significant reactor pressure (approximately 600 psig or greater) would act on the bottom of the drive piston and fully insert the drive. Insertion would occur regardless of the operational mode at the time of the failure. After full insertion, reactor water would leak past the stop piston seals. This leakage would exhaust to the containment through the broken pressure-over line. The leakage rate at 1,000 psi reactor pressure is estimated to be 1 to 3 gpm, however with the graphitar seals of the stop piston removed, the leakage rate could be as high as 10 gpm, based on experimental measurements. If the reactor were hot, drive temperature would increase. This situation would be indicated to the reactor operator by the drift alarm, by the fully inserted drive, by a high drive temperature annunciated in the main

control room, by sump water level change detected by the high-sensitivity drywell-sump leak detection system, and by operation of the drywell sump pump.

4.6.2.3.2.2.2.3 Simultaneous Breakage of the Pressure-Over (Withdrawn) and Pressure-Under (Insert) Lines

For the simultaneous breakage of the pressure-over (withdrawn) and pressure-under (insert) lines, pressures above and below the drive piston would drop to zero, and the ball check valve would close the broken pressure-under line. Reactor water would flow from the annulus outside the drive, through the vessel ports, and to the space below the drive piston. As in the case of pressure-over line breakage, the drive would then insert (at reactor pressure approximately 600 psig or greater) at a speed dependent on reactor pressure. Full insertion would occur regardless of the operational mode at the time of failure. Reactor water would leak past the drive seals and out the broken pressure-over line to the containment, as described above. Drive temperature would increase. Indication in the main control room would include the drift alarm, the fully inserted drive, the high drive temperature annunciated in the main control room, and operation of the drywell sump pump.

4.6.2.3.2.2.3 All Drive Flange Bolts Fail in Tension

Each CRD is bolted to a flange at the bottom of a drive housing. The flange is welded to the drive housing. Bolts are made of AISI-4140 steel with a minimum tensile strength of 125,000 psi. Each bolt has an allowable load capacity of 15,200 lb. Capacity of the eight bolts is 121,600 lb. As a result of the reactor design pressure of 1,250 psig, the major load on all eight bolts is 30,400 lb.

If a progressive or simultaneous failure of all bolts were to occur, the drive would separate from the housing. The control rod and the drive would be blown downward against the support structure. Impact velocity and support structure loading would be slightly less than that for drive housing failure, because reactor pressure would act on the drive cross-sectional area only and the housing would remain attached to the reactor vessel. The drive would be isolated from the cooling water supply. Reactor water would flow downward past the velocity limiter piston, through the large drive filter, and into the annular space between the thermal sleeve and the drive. For worst-case leakage calculations, the large filter is assumed to be deformed or swept out of the way so it would offer no significant flow restriction. At a point near the top of the annulus, where pressure would

have dropped to 350 psi, the water would flash to steam and cause choke-flow conditions. Steam would flow down the annulus and out the space between the housing and the drive flanges to the drywell. Steam formation would limit the leakage rate to approximately 840 gpm.

If the collet were latched, control rod ejection would be limited to the distance the drive can drop before coming to rest on the support structure. There would be no tendency for the collet to unlatch, because pressure below the collet piston would drop to zero. Pressure forces, in fact, exert 1,435 lb to hold the collet in the latched position.

If the bolts failed during control rod withdrawal, pressure below the collet piston would drop to zero. The collet, with 1,650 lb return force, would latch and stop rod withdrawal.

4.6.2.3.2.2.4 Weld Joining Flange to Housing Fails in Tension

The failure considered is a crack in or near the weld that joins the flange to the housing. This crack extends through the wall and completely around the housing. The flange material is forged, Type 304 stainless steel, with a minimum tensile strength of 75,000 psi. The housing material is seamless, Type 304 stainless steel pipe, with a minimum tensile strength of 75,000 psi. The conventional, full penetration weld of Type 308 stainless steel has a minimum tensile strength approximately the same as that for the parent metal. The design pressure and temperature are 1,250 psig and 575°F. Reactor pressure acting on the cross-sectional area of the drive; the weight of the control rod, drive, and flange; and the dynamic reaction force during drive operation result in a maximum tensile stress at the weld of approximately 5,100 psi.

If the basic flange-to-housing joint failure occurred, the flange and the attached drive would be blown downward against the support structure. The support structure loading would be slightly less than that for drive housing failure, because reactor pressure would act only on the drive cross-sectional area. Lack of differential pressure across the collet piston would cause the collet to remain latched and limit control rod motion to approximately 3 in. Downward drive movement would be small; therefore, most of the drive would remain inside the housing. The pressure-under and pressure-over lines are flexible enough to with- stand the small displacement and remain attached to the flange. Reactor water would follow the same leakage path described above for the flange-bolt failure, except that

exit to the drywell would be through the gap between the lower end of the housing and the top of the flange. Water would flash to steam in the annulus surrounding the drive. The leakage rate would be approximately 840 gpm.

If the basic failure were to occur during control rod withdrawal (a small fraction of the total operating time) and if the collet were held unlatched, the flange would separate from the housing. The drive and flange would be blown downward against the support structure. The calculated steady-state rod withdrawal velocity would be 0.13 ft/sec. Because pressure-under and pressure-over lines remain intact, driving water pressure would continue to the drive, and the normal exhaust line restriction would exist. The pressure below the velocity limiter piston would drop below normal as a result of leakage from the gap between the housing and the flange. This differential pressure across the velocity limiter piston would result in a net downward force of approximately 70 lb. Leakage out of the housing would greatly reduce the pressure in the annulus surrounding the drive. Thus, the net downward force on the drive piston would be less than normal. The overall effect of these events would be to reduce rod withdrawal to approximately one-half of normal speed. With a 560-psi differential across the collet piston, the collet would remain unlatched; however, it should relatch as soon as the drive signal is removed.

4.6.2.3.2.2.5 Housing Wall Ruptures

This failure is a vertical split in the drive housing wall just below the bottom head of the reactor vessel. The flow area of the hole is considered equivalent to the annular area between the drive and the thermal sleeve. Thus, flow through this annular area, rather than flow through the hole in the housing, would govern leakage flow. The CRD housing is made of Inconel 600 seamless tubing (at the penetration to the vessel), with a minimum tensile strength of 80,000 psi, and of Type 304 stainless steel seamless pipe below the vessel with a minimum tensile strength of 75,000 psi. The maximum hoop stress of 9,000 psi results primarily from the reactor design pressure (1,250 psig) acting on the inside of the housing.

If such a rupture were to occur, reactor water would flash to steam and leak through the hole in the housing to the drywell at approximately 1,030 gpm. Choke-flow conditions would exist, as described previously for the flange-bolt failure. However, leakage flow would be greater because flow resistance would be less, that is, the leaking water and steam would not have to flow down the length of the

housing to reach the drywell. A critical pressure of 350 psi causes the water to flash to steam.

There would be no pressure differential acting across the collet piston to unlatch the collet; but the drive would insert as a result of loss of pressure in the drive housing causing a pressure drop in the space above the drive piston.

If this failure occurred during control rod withdrawal, drive withdrawal would stop, but the collet would remain unlatched. The drive would be stopped by a reduction of the net downward force action on the drive line. The net force reduction would occur when the leakage flow of 1,030 gpm reduces the pressure in the annulus outside the drive to approximately 540 psig, thereby reducing the pressure acting on top of the drive piston to the same value. A pressure differential of approximately 710 psi would exist across the collet piston and hold the collet unlatched as long as the operator held the withdraw signal.

4.6.2.3.2.2.6 Flange Plug Blows Out

To connect the vessel ports with the bottom of the ball check valve, a hole of 3/4-in diameter is drilled in the drive flange. The outer end of this hole is sealed with a plug of 0.812-in diameter and 0.25-in thickness. A full-penetration, Type 308 stainless steel weld holds the plug in place. The postulated failure is a full circumferential crack in this weld and subsequent blowout of the plug.

If the weld were to fail, the plug were to blow out, and the collet remained latched, there would be no control rod motion. There would be no pressure differential acting across the collet piston to unlatch the collet. Reactor water would leak past the velocity limiter piston, down the annulus between the drive and the thermal sleeve, through the vessel ports and drilled passage, and out the open plug hole to the drywell at approximately 320 gpm. Leakage calculations assume only liquid flows from the flange. Actually, hot reactor water would flash to steam, and choke-flow conditions would exist. Thus, the expected leakage rate would be lower than the calculated value. Drive temperature would increase and initiate an alarm in the main control room.

If this failure were to occur during control rod withdrawal and if the collet were to stay unlatched, calculations indicate that control rod withdrawal speed would be approximately 0.24 ft/sec. Leakage from the open plug hole in the flange would cause reactor water to flow downward past the velocity limiter piston. A small differential

pressure across the piston would result in an insignificant driving force of approximately 10 lb, tending to increase withdraw velocity.

A pressure differential of 295 psi across the collet piston would hold the collet unlatched as long as the driving signal was maintained.

Flow resistance of the exhaust path from the drive would be normal because the ball check valve would be seated at the lower end of its travel by pressure under the drive piston.

4.6.2.3.2.2.7 Ball Check Valve Plug Blows Out

As a means of access for machining the ball check valve cavity, a 1.25-in diameter hole has been drilled in the flange forging. This hole is sealed with a plug of 1.31-in diameter and 0.38-in thickness. A full-penetration weld, utilizing Type 308 stainless steel filler, holds the plug in place. The failure postulated is a circumferential crack in this weld leading to a blowout of the plug.

If the plug were to blow out while the drive was latched, there would be no control rod motion. No pressure differential would exist across the collet piston to unlatch the collet. As in the previous failure, reactor water would flow past the velocity limiter, down the annulus between the drive and thermal sleeve, through the vessel ports and drilled passage, through the ball check valve cage and out the open plug hole to the drywell. The leakage calculations indicate the flow rate would be 350 gpm. This calculation assumes liquid flow, but flashing of the hot reactor water to steam would reduce this rate to a lower value. Drive temperature would rapidly increase and initiate an alarm in the main control room.

•→10
If the plug failure were to occur during control rod withdrawal (it would not be possible to unlatch the drive after such a failure), the collet would relatch at the first locking groove. If the collet were to stick, calculations indicate the control rod withdrawal speed would be 11.8 ft/sec. There would be a large retarding force exerted by the velocity limiter due to a 35 psi pressure differential across the velocity limiter piston. This event requires multiple failures and is therefore beyond the design basis. The Control Rod Drop Analysis (CRDA) assumes a control rod withdrawal speed of 3.11 ft/sec and this speed is bounding for all single failure events.
10←•

4.6.2.3.2.2.8 Drive/Cooling Water Pressure Control Valve Closure (Reactor Pressure, 0 psig)

The pressure to move a drive is generated by the pressure drop of practically the full system flow through the drive/cooling water pressure control valve. This valve is

either a motor-operated valve or a standby manual valve; either one is adjusted to a fixed opening. The normal pressure drop across this valve develops a pressure 260 psi in excess of reactor pressure.

If the flow through the drive/cooling water pressure control valve were to be stopped, as by a valve closure or flow blockage, the drive pressure would increase to the shutoff pressure of the supply pump. The occurrence of this condition during withdrawal of a drive at zero vessel pressure will result in a drive pressure increase from 260 psig to no more than 2,000 psig. Calculations indicate that the drive would accelerate from 3 in/sec to approximately 7 in/sec. A pressure differential of 1,970 psi across the collet piston would hold the collet unlatched. Flow would be upward, past the velocity limiter piston, but retarding force would be negligible. Rod movement would stop as soon as the driving signal was removed.

4.6.2.3.2.2.9 Ball Check Valve Fails to Close Passage to Vessel Ports

Should the ball check valve sealing the passage to the vessel ports be dislodged and prevented from reseating following the insert portion of a drive withdrawal sequence, water below the drive piston would return to the reactor through the vessel ports and the annulus between the drive and the housing rather than through the speed control valve. Because the flow resistance of this return path would be lower than normal, the calculated withdrawal speed would be 2 ft/sec. During withdrawal, differential pressure across the collet piston would be approximately 40 psi. Therefore, the collet would tend to latch and would have to stick open before continuous withdrawal at 2 ft/sec could occur. Water would flow upward past the velocity limiter piston, generating a small retarding force of approximately 120 lb.

4.6.2.3.2.2.10 Hydraulic Control Unit Valve Failures

Various failures of the valves in the HCU can be postulated, but none could produce differential pressures approaching those described in the preceding sections and none alone could produce a high velocity withdrawal. Leakage through either one or both of the scram valves produces a pressure that tends to insert the control rod rather than to withdraw it. If the pressure in the scram discharge volume should exceed reactor pressure following a scram, a check valve in the line to the scram discharge header prevents this pressure from operating the drive mechanisms.

4.6.2.3.2.2.11 Collet Fingers Fail to Latch

The failure is presumed to occur when the drive withdraw signal is removed. If the collet fails to latch, the drive continues to with- draw at a fraction of the normal speed. This assumption is made because there is no known means for the collet fingers to become unlocked without some initiating signal. Because the collet fingers will not cam open under a load, accidental application of a down signal does not unlock them. (The drive must be given a short insert signal to unload the fingers and cam them open before the collet can be driven to the unlock position.) If the drive withdrawal valve fails to close following a rod withdrawal, the collet would remain open and the drive continue to move at a reduced speed.

4.6.2.3.2.2.12 Withdrawal Speed Control Valve Failure

Normal withdrawal speed is determined by differential pressures in the drive and is set for a nominal value of 3 in/sec. Withdrawal speed is maintained by the pressure regulating system and is independent of reactor vessel pressure. Tests have shown that accidental opening of the speed control valve to the full-open position produces a velocity of approximately 5 in/sec.

The CRD system prevents unplanned rod withdrawal and it has been shown above that only multiple failures in a drive unit and in its control unit could cause an unplanned rod withdrawal.

4.6.2.3.2.3 Scram Reliability

High scram reliability is the result of a number of features of the CRD system. For example:

1. An individual accumulator is provided for each CRD with sufficient stored energy to scram at any reactor pressure. The reactor vessel itself, at pressures above 600 psi, will supply the necessary force to insert a drive if its accumulator is unavailable.

2. Each drive mechanism has its own scram valves and a dual solenoid scram pilot valve; therefore, only one drive can be affected if a scram valve fails to open. Both pilot valve solenoids must be deenergized to initiate a scram.

3. The RPS and the HCUs are designed so that the scram signal and mode of operation override all others.

4. The collet assembly and index tube are designed so they will not restrain or prevent control rod insertion during scram.

5. The scram discharge volume is monitored for accumulated water and the reactor will scram before the volume is reduced to a point that could interfere with a scram.

•→1

6. The Alternate Rod Insertion (ARI) system is designed such that in the event an RPS scram signal is not received, an independate means is available to automatically vent the scram air header.

1←•

4.6.2.3.2.4 Control Rod Support and Operation

As described in the preceding sections, each control rod is independently supported and controlled as required by safety design bases.

4.6.2.3.3 Control Rod Drive Housing Supports

Downward travel of the CRD housing and its control rod following the postulated housing failure equals the sum of these distances: 1) the compression of the disc springs under dynamic loading, and 2) the initial gap between the grid and the bottom contact surface of the CRD flange. If the reactor were cold and pressurized, the downward motion of the control rod would be limited to the spring compression (approximately 2 in) plus a gap of approximately 1 in. If the reactor were hot and pressurized, the gap would be approximately 3/4 in and the spring compression would be slightly less than in the cold condition. In either case, the control rod movement following a housing failure is substantially limited below one drive "notch" movement (6 in). Sudden withdrawal of any control rod through a distance of one drive notch at any position in the core does not produce a transient sufficient to damage any radioactive material barrier.

The CRD housing supports are in place during power operation and when the nuclear system is pressurized. If a control rod is ejected during shutdown, the reactor remains subcritical because it is designed to remain subcritical with any one control rod fully withdrawn at any time.

•→10

At plant operating temperature, a gap of approximately 3/4 in exists between the CRD housing and the supports. At lower temperatures the gap is greater. Because the supports do not contact any of the CRD housing except during the postulated accident condition, vertical contact stresses are prevented. Inspection and testing of CRD housing supports is discussed in Section 4.6.3.2.

10←•

4.6.3 Testing and Verification of the CRDs

4.6.3.1 Control Rod Drives

4.6.3.1.1 Testing and Inspection

4.6.3.1.1.1 Development Tests

The initial development drive (prototype of the standard locking piston design) testing included more than 5,000 scrams and approximately 100,000 latching cycles. One prototype was exposed to simulated operating conditions for 5,000 hr. These tests demonstrated the following:

1. The drive easily withstands the forces, pressures, and temperatures imposed.

2. Wear, abrasion, and corrosion of the nitrided stainless parts are negligible. Mechanical performance of the nitrided surface is superior to that of materials used in earlier operating reactors.

3. The basic scram speed of the drive has a satisfactory margin above minimum plant requirements at any reactor vessel pressure.

4. Usable seal lifetimes in excess of 1,000 scram cycles can be expected.

4.6.3.1.1.2 Factory Quality Control Tests

Quality control of welding, heat treatment, dimensional tolerances, material verification, and similar factors is maintained throughout the manufacturing process to assure reliable performance of the mechanical reactivity control components. Some of the quality control tests performed on the control rods, CRD mechanisms, and HCUs are listed below:

1. CRD mechanism tests:

   a. Pressure welds on the drives are hydrostatically tested in accordance with ASME codes.

   b. Electrical components are checked for electrical continuity and resistance to ground.

   c. Drive parts that cannot be visually inspected for dirt are flushed with filtered water at

high velocity. No significant foreign material is permitted in effluent water.

d. Seals are tested for leakage to demonstrate correct seal operation.

e. Each drive is tested for shim motion, latching, and control rod position indication.

f. Each drive is subjected to cold scram tests at various reactor pressures to verify correct scram performance.

2. HCU tests:

a. Hydraulic systems are hydrostatically tested in accordance with the applicable code.

b. Eectrical components and systems are tested for electrical continuity and resistance to ground.

c. Correct operation of the accumulator pressure and level switches is verified.

d. The unit's ability to perform its part of a scram is demonstrated.

e. Correct operation and adjustment of the insert and withdrawal valves is demonstrated.

4.6.3.1.1.3 Operational Tests

After installation, all rods and drive mechanisms can be tested through their full strokes for operability.

During normal operation, each time a control rod is withdrawn a notch, the operator can observe the incore monitor indications to verify that the control rod is following the drive mechanism. All control rods that are partially withdrawn from the core can be tested for rod-following by inserting or withdrawing the rod one notch and returning it to its original position, while the operator observes the incore monitor indications.

To make a positive test of control rod to CRD coupling integrity, the operator can withdraw a control rod to the end of its travel and then attempt to withdraw the drive to the overtravel position. Failure of the drive to overtravel demonstrates rod-to-drive coupling integrity.

Hydraulic supply subsystem pressures can be observed from instrumentation in the main control room. Scram accumulator pressures can be observed on the nitrogen pressure gages.

4.6.3.1.1.4 Acceptance Tests

Criteria for acceptance of the individual CRD mechanisms and the associated control and protection systems will be incorporated in specifications and test procedures covering three distinct phases: 1) preinstallation, 2) after installation prior to startup, and 3) during startup testing.

The preinstallation specification will define criteria and acceptable ranges of such characteristics as seal leakage, friction, and scram performance under fixed test conditions which must be met before the component can be shipped.

The after installation, prestartup tests (Chapter 14) include normal and scram motion and are primarily intended to verify that piping, valves, electrical components, and instrumentation are properly installed. The test specifications will include criteria and acceptable ranges for drive speed, timer settings, scram valve response times, and control pressures. These tests are intended more to document system condition than system performance.

As fuel is placed in the reactor, the startup test procedure (Chapter 14) will be followed. The tests in this procedure are intended to demonstrate that the initial operational characteristics meet the limits of the specifications over the range of primary coolant temperatures and pressures from ambient to operating. The detailed specifications and procedures have not as yet been prepared but will follow the general pattern established for such specifications and procedures in BWRs presently under construction and in operation.

4.6.3.1.1.5 Surveillance Tests

The surveillance requirements for the CRD system are described in the Technical Specifications and the Technical Requirements Manual.
•→14

14←•

4.6.3.1.1.6 Functional Tests

•→16
The functional testing program of the CRDs consists of the 5 yr maintenance life and the 1.5 times design life test programs as described in Section 3.9.4.4B.
←•16

There are a number of failures that can be postulated on the CRD but it would be very difficult to test all possible failures. A partial test program with postulated accident conditions and imposed single failures is available.

The following tests with imposed single failures have been performed to evaluate the performance of the CRDs under these conditions.

1. Simulated ruptured scram line test
2. Stuck ball check valve in CRD flange
3. HCU drive down inlet flow control valve (V122) failure
4. HCU drive down outlet flow control valve (V120) failure
5. CRD scram performance with Vl20 malfunction
6. HCU drive up outlet control valve (V121) failure
7. HCU drive up inlet control valve (V123) failure
8. Cooling water check valve (V138) leakage
9. CRD flange check valve leakage
10. CRD stabilization circuit failure
11. HCU filter restriction
12. Air trapped in CRD hydraulic system
13. CRD collet drop test
14. Control rod qualification velocity limiter drop test

•→10
Additional postulated CRD failures are discussed in Sections 4.6.2.3.2.2.1 through 4.6.2.3.2.2.12.
10←•

•→10
4.6.3.1.1.7 HCU Charging Water Riser Inspection Program

During and following a scram the ball check valve V115 which is located immediately upstream of the connection of the charging water line to the accumulator tends to chatter as charging water enters through it into the scram insert line. This gives rise to acoustic coupling among all 145 valves V115. The design did not predict the magnitude and duration of this fluid forcing function. Fluid dynamic analysis can not reliably quantify the phenomenon due to its chaotic nature. Recordings of the vibratory response of the piping in 1991 showed that the stress amplitudes near the junction of the charging water riser to the accumulator riser coupling can be large enough to lead the fatigue cracking at the fillet welds of the short pipe segment between valve V115 and the coupling.

The first crack observed was a circumferential through-wall crack at the toe of the fillet weld at the junction of charging water line and accumulator riser coupling in February 1991, after 5 1/2 years of operation. Other, smaller cracks were found at this occasion and in several subsequent scrams from power in 1991 and 1992, none of them through-wall. All indications were reworked, and the J-clamp which acts as lateral restraint of the riser, but also restricts the pipe from sliding vertically, was tightened to its specified value.

Liquid penetrant (PT) and visual inspections did not detect any more indications after September 1992, including a PT inspection in June 1997. The absence of further cracking may be due to a combination of factors, among them the replacement of some welds with better welds, and the tightening of the J-clamps.

The charging water riser experiences large loads only during a scram, and testing has shown that only a full core scram from power produces the large stress amplitudes that contribute to fatigue. Analysis of scram recordings permitted the conclusion that a crack of visually detectable size would require several more scrams before it could grow through-wall and could begin to leak, that a leak would tend to develop only after all the rods are inserted, and that even a leaking pipe would not break in one scram.

This permitted to put a compensatory inspection program in place which will ensure that the plant is not started up with a known crack indication in any of the 145 charging water risers and that therefore the plant can scram without producing a leak in these lines.

The monitoring program was initiated in 1991 after discovery of the first cracks. All CRD HCU charging water risers are inspected for leakage and cracks after every plant shutdown from power. If a crack is detected, the associated control rod is to be driven in, the HCU is isolated, and the pipe is reworked.
10←•

4.6.3.2 Control Rod Drive Housing Supports

CRD housing supports are removed for inspection and maintenance of the CRDs. When the support structure is reinstalled, it is inspected for correct assembly with

particular attention to maintaining the correct gap between the CRD flange lower contact surface and the grid.

4.6.4 Information for Combined Performance of Reactivity Control Systems

4.6.4.1 Vulnerability to Common Mode Failures

The system is located such that it is protected from common mode failures of moderate and high energy piping and fire. Sections 3.5, 3.6, and 9.5.1 discuss protection of essential systems against missiles, pipe ruptures, and fire.

4.6.4.2 Accidents Taking Credit for Multiple Reactivity Control Systems

There are no postulated accidents evaluated in Chapter 15 that take credit for two or more reactivity control systems preventing or mitigating each accident.

4.6.5 Evaluation of Combined Performance

As indicated in Section 4.6.4.2, credit is not taken for multiple reactivity control systems for any postulated accidents in Chapter 15.

Reference - 4.6

1. Benecki, J. E. Impact Testing on Collet Assembly for Control Rod Drive Mechanism 7RD B144A, General Electric Company, Atomic Power Equipment Department, APED-5555, November 1967.

APPENDIX 4A

CORE SIMULATION STUDIES FOR BWR 6

APPENDIX 4A

CORE SIMULATION STUDIES FOR BWR 6

TABLE OF CONTENTS

APPENDIX 4A

LIST OF FIGURES

APPENDIX 4A

LIST OF FIGURES (Cont)

LIST OF FIGURES (Cont)

LIST OF FIGURES (Cont)

APPENDIX 4A

CORE SIMULATION STUDIES FOR BWR 6

4A.1 INTRODUCTION

The purpose of this appendix is to present the results of detailed core simulation studies performed to demonstrate that the BWR 6 core, utilizing the improved fuel design, meets design performance criteria of operating within thermal limits, i.e., MCPR and LHGR, throughout the cycle. The standard BWR analytical methods[1] were used in these evaluations. The analysis is performed in a stepwise manner in which a three-dimensional power distribution is obtained at a specific exposure step for a control rod pattern. The control rod pattern may be reiterated until a satisfactory power shape is obtained and all limits, within specified margins, are met. The resulting three-dimensional power distribution, assuming 100-percent power and flow at equilibrium conditions, is used to expose the core over a specific interval. This process is then repeated at the new exposure step. At intervals of 1,000 MWd/t, the control rod sequences are alternated from the A sequence to the B sequence in order to minimize exposure mismatch between fuel bundles.

It should be noted that the described rod patterns and power distributions are by no means unique for a specific plant or to any given reactor. The GE BWR has sufficient operating flexibility that a variety of rod patterns may give satisfactory power shapes at any given step in the cycle. Thus, the rod patterns described here represent only one feasible sequence which results in power distributions well within design limits. Use of rod patterns in an actual operating reactor is determined by actual operating history, supplier recommendations based on analytical calculations, and, most importantly, by actual observed power distributions as indicated by the instrument and process computer systems. The success of this concept is demonstrated by the many currently operating BWR plants.

4A.2 POWER DISTRIBUTION STRATEGY

4A.2.1 Principle

A basic operating principle used to minimize power peaking throughout an operating cycle has been developed and is applied to BWRs. The principle is described in Reference 2 and is referred to as the Haling principle or the minimum

power peaking principle. The main concept is that "for any given set of EOC conditions, the power peaking factor is maintained at the minimum value when the power shape does not change during the operating cycle."

4A.2.2 Explanation of Principle

Assume that the target constant power shape has been determined and assume further that at some point during an operating cycle a flatter power distribution can be attained. To achieve this lower peaking, the reactivity distribution must be such that in the region of peak power, the reactivity is less than in the target case. Since fuel reactivity is normally a decreasing function of exposure, this lower value of reactivity implies that the exposure in the region of peak power is high, relative to the target case. This could have been achieved only by operating with a power distribution more peaked than the target distribution during some earlier portion of the operating cycle. In short, it is possible to obtain a power peaking factor lower than the constant power shape peak at some time during the cycle only by operating with a peaking factor higher than that of the target shape at some earlier time in the cycle. Therefore, the constant power shape corresponds to the minimum peak-to-average value that can be maintained throughout the cycle.

4A.2.3 Target Power Shape

The desired EOC power distribution is calculated uniquely for each operating cycle using the Haling principle. This shape, if maintained through the cycle, would result in minimum power peaking throughout the cycle and is, therefore, used as the target shape. Operationally, compromises are made because the target power shape cannot be held precisely throughout the cycle.

The calculated target average axial power distribution is shown on Fig. 4A-1B. This was calculated using a three-dimensional BWR simulator code[1].

The desired power distribution is determined by iterating between the EOC exposure and power to determine mutually consistent distributions. Based upon the assumed beginning and EOC conditions, the results of the calculation supply the target power distribution. If the objectives are fully realized, the chosen set of conditions for the EOC will permit operation at full power with all rods withdrawn.

Given the target power shape, a series of additional calculations are performed to devise control rod sequences that will produce this shape throughout the cycle. Many items such as finite control elements (rods), electrical system demands, and other hardware and procedural constraints must be factored into the rod sequence and operating strategy. The basic strategy is to deliberately peak the axial power in the bottom portion of the core early in the cycle more strongly than the target shape dictates. This compensates for the condition late in the cycle in which most of the control rods are fully withdrawn and not available for axial power shaping.

4A.2.4 Operational Implementation

The resulting control rod sequences are utilized throughout the cycle to approach the EOC target power shape as closely as possible, using the core nuclear instrumentation as a check. Since power shaping is the goal, the rod sequences are used as guides in producing the desired power shapes. Using this strategy, operating conditions that require deviations from the desired power shapes can be accommodated later in the cycle by deliberate power-shaping action.

The control rods are divided into two sequences of rods designated A and B. In general, only one sequence of rods is used at any one time. Within each sequence the control rods are divided into "deep" and "shallow" rods. (See Section 4A.4 for definitions.)

The deep rods are used to control the reactivity and radial power shape. The shallow rods are of very little reactivity worth and, therefore, do not appreciably affect the reactivity, but, in combination with the axial gadolinia, provide the axial power flattening.

Since shallow rods tend to retard exposure near the bottom of the core, they are used only when necessary.

In summary, the total strategy involves calculating the target power shape for the cycle, calculating control rod sequences that approximate that shape, and using those rod sequences and incore nuclear instruments as guides to operationally produce the target power shape as closely as possible.

4A.3 RESULTS OF CORE SIMULATION STUDIES

4A.3.1 Description of Model

The model used for the simulation studies was the standard 748 bundle BWR 6 reactor plant with a core average enrichment of 1.9 wt% U-235. The performance of this standard plant is representative of the BWR 6 product line which includes River Bend Station. The following table describes the pertinent characteristics of this plant.

Product line	BWR 6
Rated power, MWt	3,579
Rated flow, Mlbs/hr	104
Core average pressure, psia	1,055
Inlet enthalpy, Btu/lb	527.7
Number of bundles	748
Number of control rods	177
Size of pressure vessel id, in	238
Active core height, in	150
Average core enrichment, wt%	1.9
Lattice type	8x8C
Number of high enrichment bundles	424
Number of medium enrichment bundles	232
Number of natural uranium bundles	92
Number of bundles in central orifice region	656
Number of bundles in peripheral orifice region	92
Circumscribed core diameter, ft	16.16
Average core power density, kW/liter	54.1

The analytical procedures for this study were described in preceding sections. The performance limits which apply to

this study are as follows:

MLHGR, kW/ft	13.4
MCPR	1.23
Gross peaking	2.00
Local peaking	1.13
Overall peaking	2.26

4A.3.2 Cycle Analysis

Near BOC, the steps typically are 0-200, 200-1000 MWd/t, and then in intervals of 1000 MWd/t to EOC. Figures and graphs are included to show the following data at each exposure step:

1. Control rod pattern with associated:

   Maximum core average power and location (AXIAL)
   Maximum radial power and location (RADIAL)
   Maximum gross power and location (GROSS)

   Minimum critical power ratio and location (MCPR)
   Maximum linear heat generation rate and location (MLHGR)

2. Core average axial power distribution

3. Core average axial exposure distribution

4. Bundle radial power map

5. Bundle average exposure map.

The following table itemizes the exposure step and its related figure numbers:

Exposure (GWd/t)	Sequence*	Figure Numbers
9.138	All rods out - Haling EOC	4A-1A through 4A-1D
0.2	A-2	4A-2A through 4A-2E
1.0	B-1	4A-3A through 4A-3E
2.0	A-1	4A-4A through 4A-4E
3.0	B-2	4A-5A through 4A-5E
4.0	A-2	4A-6A through 4A-6E

5.0	B-1	4A-7A through 4A-7E
6.0	A-1	4A-8A through 4A-8E
7.0	B-2	4A-9A through 4A-9E
8.0	A-2	4A-10A through 4A-10E
9.0	B-1	4A-11A through 4A-11E
9.2	All rods out - EOC	4A-12A through 4A-12E

In summary, the detailed data presented demonstrate that this design can be operated throughout the cycle with adequate margins to allow for operating flexibility. The variation of the MLHGR with exposure is presented on Fig. 4A-15. The upper limit of the MLHGR is 13.4 kW/ft, and as the data show, significant margin exists. The variation of the MCPR with exposure is shown on Fig. 4A-14. Similarily, a large margin is indicated with respect to the expected MCPR limit of 1.23. Fig. 4A-16 shows a comparison of the achieved EOC axial exposure distribution and the target Haling distribution. This illustrates that deviations from the Haling target distribution can be tolerated and still meet all design limits, as evidenced by the data presented.

4A.3.3 Uncertainty Analysis

In addition to the nominal design state, the core should be able to meet all performance requirements for off-nominal reactivity conditions. Therefore, in the unlikely event that the reactivity is over or undercalculated, an uncertainty analysis is performed.

Specifically, control rod patterns are determined at near beginning-of-life for Æ0.5 percent k bias to the model critical reactivity and Æ1.0 percent k at the most reactive point in the cycle. These biases are considered to be reasonable limits to the reactivity error which might occur in any such plant. At 200 MWd/t the +0.5 percent k bias is applied, and at 6,000 MWd/t the Æ1.0 percent k bias is applied. A summary is presented on Fig. 4A-17 for near beginning-of-life and on Fig. 4A-18 and 4A-19 for 6,000 MWd/t. Comparison of these figures, with the corresponding nominal cases, indicated that although some modification of

the control rod pattern is necessary, the same performance limits can be attained.

An inherent assumption in this procedure is that the effect of the uncertainty on the exposure distribution is negligible. That is, an exposure shape based on nominal reactivity is used for the uncertainty analysis when, in fact, a different exposure pattern could exist if there were an actual reactivity error. However, if the control rod patterns at the off-nominal conditions are chosen so that a Haling shape is approached at EOC, then the exposure shape at any point in the cycle is roughly independent of the reactivity level. The reactivity uncertainty criteria are not applied at EOC since only the cycle length is affected.

4A.4 GLOSSARY OF TERMS

Axial Power Peaking Factor - The maximum relative axial power density. Also called axial factor and axial peak. Defined as:

$$\text{Max}\left[\frac{1}{ixj}\ \Sigma_{i,j}\ P_{i,j,k}\right] \text{ for all } k$$

where:

ixj = Total number of assemblies in the core

k = The number of nodes per assembly

Integrated Radial Power Peaking Factor - The maximum of the integrated relative power of all channels. Commonly called radial factor or radial peak. Defined as:

$$\text{Max}\left[\frac{1}{k}\ \Sigma_{k}\ P_{i,j,k}\right] \text{ for all } i,j$$

Local Power Peaking Factor - The maximum of the ratio of the power density in a fuel rod to the power density in the fuel bundle based on the unit cell lattice calculation. Also called local factor. Defined as:

$$\text{Max}\left[N\ \frac{P_n}{\Sigma_n P_n}\right] \text{ for all n fuel rods}$$

Gross Power Peaking Factor - The maximum nodal relative power density in the core. Often called gross peaking factor and sometimes called the global power factor. Defined as:

Max $P_{i,j,k}$ for all i,j,k

Overall Power Peaking Factor - The maximum relative power in any fuel rod at any node in the model (product of the gross and local factors).

Relative Power Density - The ratio of the power density at any node in the model to the average power in the model. Designated $P_{i,j,k}$.

Linear Heat Generation Rate (LHGR) - The heat generated in a fuel rod per unit length of the fuel rod. It is expressed in terms of kW/ft and bears a constant relationship with overall power peaking factor.

Minimum Critical Power Ratio (MCPR) - The minimum value of the ratio of the bundle power at start of boiling transition to the calculated bundle power.

Control Rod Notch - A 6-in movement of the control rod. Each control rod has 24 notches.

Control Rod Position - The notches referred to in the analysis are actually positions. Notch position 48 is fully withdrawn (indicated by a blank square on the rod pattern maps), and notch position 0 is fully inserted.

Shallow Control Rod - A control rod inserted a relatively short distance into the core (not more than 3 ft).

Deep Control Rod - A control rod inserted a relatively long distance into the core (at least 8 ft).

Control Rod Pattern - A group of control rods and the respective positions of the control rods. The rods are divided in a checkerboard fashion into sequence A and B rods.

Exposure Step - An exposure calculation covering a fixed interval with a calculated power shape.

Haling Step - An iterative power-exposure step to EOC under the assumption of the same slope for the power and exposure.

Model Critical Reactivity - A value of the model reactivity, i.e., k-effective or eigenvalue, for which the actual core would reasonably be expected to be critical. This is different from unity by any model bias or reactivity allowance such as crud, spacers, instruments, etc.

Shutdown Margin - The reactivity difference between the calculated shutdown reactivity and the model critical reactivity.

References - 4A

1. Woolley, J. A., Three Dimensional BWR Core Simulator, May 1976 (NEDO-20953).

2. Haling, R. K., Operating Strategy for Maintaining an Optimum Power Distribution Throughout Life, Page 205, ANS Topical Meeting, Nuclear Performance of Power Reactor Cores, September 26-27, 1963, San Francisco, California.

C(9/79)

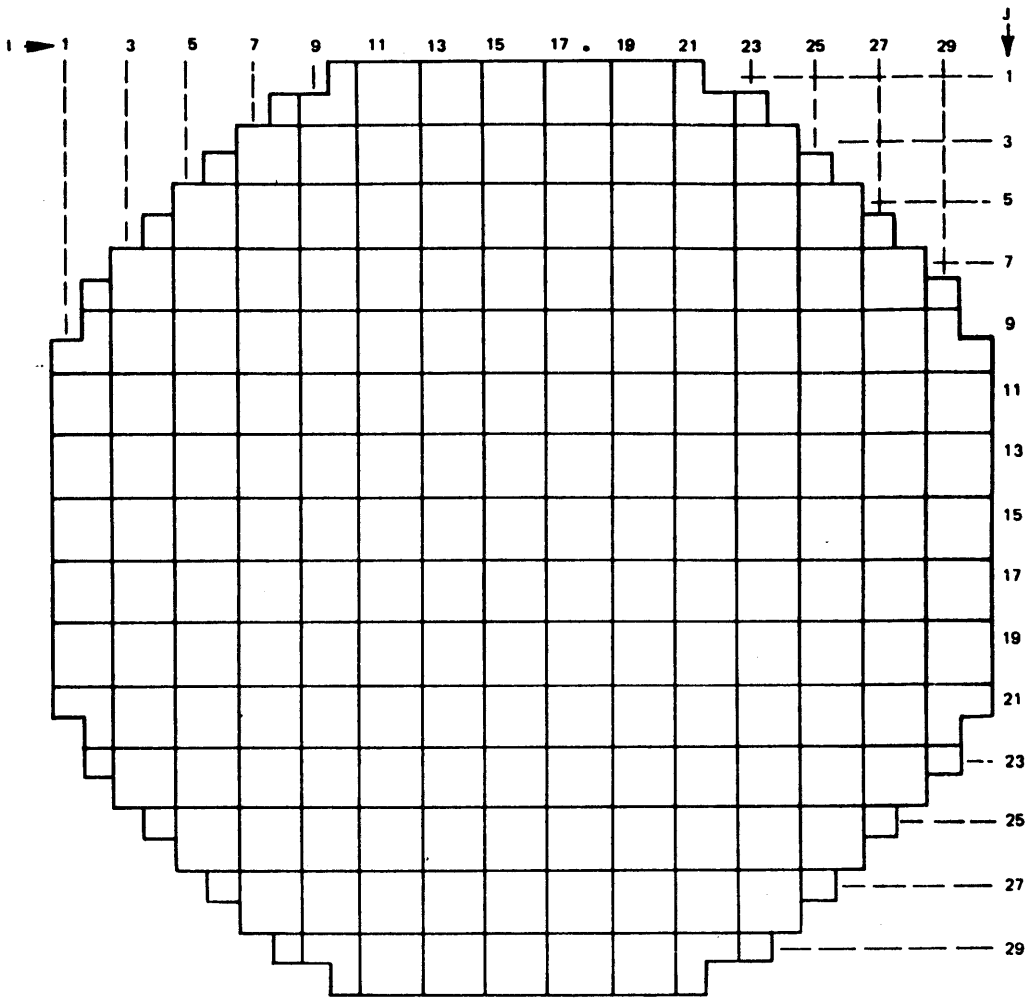

CONTROL ROD PATTERN (NOTCHES WITHDRAWN)

EXPOSURE		9138 MWd/t		
K_{eff}		1.0060		
ROD SEQUENCE		ALL RODS OUT		
POWER DISTRIBUTIONS		LOCATION		
		I	J	K
AXIAL	1.2412	–	–	7
RADIAL	1.2257	11	10	–
GROSS	1.4989	10	6	6
MCPR	1.4804	11	10	–
MLHGR	9.8559	10	6	5

I, J, K CODE COORDINATES
K = 1 = BOTTOM OF CORE
K = 25 = TOP OF CORE

FIGURE 4 A-1A

SUMMARY OF HALING CONDITION

RIVER BEND STATION
UPDATED SAFETY ANALYSIS REPORT

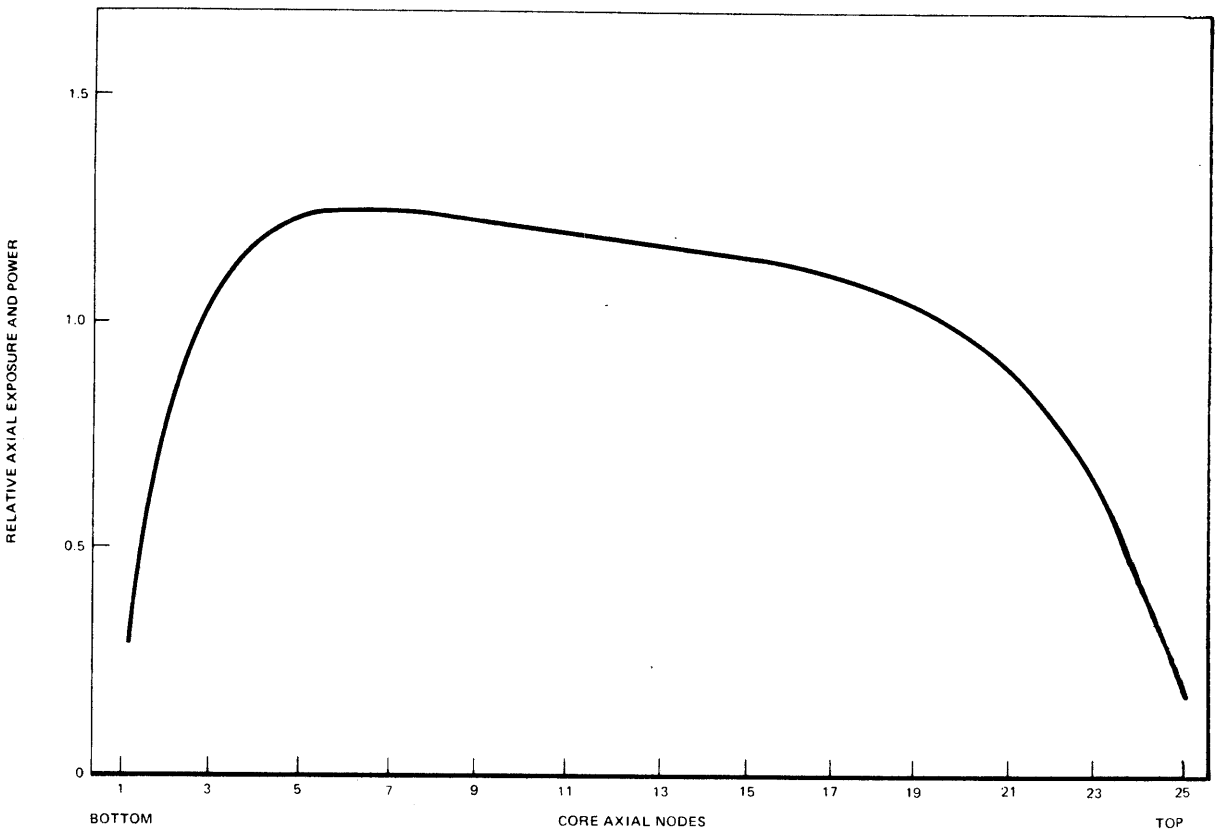

FIGURE 4A-1B

RELATIVE AXIAL POWER AND EXPOSURE AT HALING EXPOSURE (9138 MWd/t)

RIVER BEND STATION
UPDATED SAFETY ANALYSIS REPORT

I →	1	2	3	4	5	6	7	8	9	10	11	12	13	14	15
J															
1										0.2279	0.3018	0.3400	0.3589	0.3678	0.3713
2								0.2752	0.3727	0.4491	0.7340	0.7950	0.8232	0.8361	0.8409
3							0.3540	0.6851	0.8082	0.8896	0.9568	0.9955	1.0148	1.0240	1.0263
4						0.3772	0.7495	0.9002	0.9919	1.0507	1.0895	1.1099	1.1169	1.1214	1.1177
5					0.3828	0.7695	0.9342	1.0376	1.1020	1.1421	1.1629	1.1660	1.1134	1.1586	1.0983
6				0.3772	0.7695	0.9425	1.0531	1.1216	1.1620	1.1889	1.1956	1.1422	1.1860	1.1261	1.1099
7			0.3540	0.7495	0.9342	1.0531	1.1260	1.1649	1.1376	1.2041	1.1579	1.2064	1.1507	1.1893	1.1221
8		0.2752	0.6851	0.9002	1.0376	1.1216	1.1649	1.1379	1.2029	1.1629	1.2167	1.1650	1.2091	1.1451	1.1267
9		0.3727	0.8082	0.9919	1.1020	1.1620	1.1375	1.2029	1.1035	1.2203	1.1720	1.2209	1.1637	1.2016	1.1329
10	0.2279	0.4491	0.8896	1.0507	1.1421	1.1889	1.2041	1.1629	1.2203	1.1740	1.2260	1.1725	1.2162	1.1514	1.1325
11	0.3018	0.7340	0.9568	1.0895	1.1629	1.1956	1.1579	1.2167	1.1720	1.2260	1.1753	1.2234	1.1656	1.2032	1.1344
12	0.3400	0.7950	0.9955	1.1099	1.1660	1.1422	1.2064	1.1650	1.2209	1.1725	1.2234	1.1694	1.2129	1.1481	1.1295
13	0.3589	0.8232	1.0148	1.1169	1.1134	1.1860	1.1507	1.2091	1.1037	1.2162	1.1656	1.2129	1.1559	1.1937	1.1265
14	0.3678	0.8361	1.0240	1.1214	1.1586	1.1260	1.1893	1.1451	1.2016	1.1514	1.2032	1.1481	1.1937	1.1296	1.1159
15	0.3713	0.8409	1.0263	1.1177	1.0983	1.1099	1.1221	1.1267	1.1329	1.1325	1.1344	1.1295	1.1265	1.1159	1.1083

FIGURE 4A-1C

INTEGRATED HALING POWER
PER BUNDLE, 9138 MWd/t

RIVER BEND STATION

UPDATED SAFETY ANALYSIS REPORT

I → / J	1	2	3	4	5	6	7	8	9	10	11	12	13	14	15
1										2078.0	2752.7	3100.2	3272.9	3354.6	3386.3
2								2509.5	3398.9	4095.8	6713.2	7271.2	7528.6	7647.0	7690.5
3							3228.5	6265.8	7392.0	8136.3	8750.6	9104.3	9280.8	9364.7	9386.0
4						3440.2	6854.8	8233.0	9071.7	9609.0	9964.5	10150.9	10214.7	10256.1	10222.0
5					3490.9	7037.2	8543.6	9489.7	10078.2	10445.0	10635.2	10664.1	10166.6	10596.5	10028.7
6				3440.2	7037.2	8620.1	9631.7	10258.2	10627.0	10873.5	10934.7	10429.5	10846.4	10262.4	10134.6
7			3228.5	6854.8	8543.6	9631.7	10297.7	10653.8	10387.4	11012.5	10573.0	11033.5	10507.7	10877.3	10246.7
8		2509.4	6265.8	8233.0	9489.7	10258.2	10653.8	10390.9	11000.9	10619.1	11127.4	10637.7	11057.6	10456.4	10288.0
9		3398.9	7391.9	9071.7	10078.2	10626.9	10387.4	11000.9	10624.0	11160.0	10702.0	11166.3	10626.1	10989.2	10345.1
10	2078.0	4095.8	8134.3	9609.0	10444.9	10873.5	11012.5	10619.1	11160.0	10719.9	11212.4	10706.9	11123.1	10513.4	10341.0
11	2752.7	6713.2	8750.6	9964.5	10635.1	10934.7	10572.9	11127.4	10702.0	11212.4	10732.4	11189.1	10643.1	11004.3	10358.4
12	3100.2	7271.1	9104.3	10150.9	10664.1	10429.5	11033.5	10637.7	11166.3	10706.9	11189.1	10678.0	11092.3	10484.1	10314.3
13	3272.8	7528.6	9280.8	10214.6	10166.6	10846.4	10507.7	11057.6	10626.1	11123.1	10643.1	11092.3	10554.8	10916.9	10286.1
14	3354.5	7647.0	9364.7	10256.1	10596.5	10282.3	10877.3	10456.4	10989.2	10513.4	11004.3	10484.1	10916.9	10315.0	10189.2
15	3386.3	7690.5	9384.0	10222.0	10028.7	10134.5	10246.7	10288.0	10345.1	10341.0	10358.4	10314.3	10286.1	10189.2	10120.5

FIGURE 4A-1D

AVERAGE HALING EXPOSURE
PER BUNDLE (MWd/t)

RIVER BEND STATION
UPDATED SAFETY ANALYSIS REPORT

C(9/79)

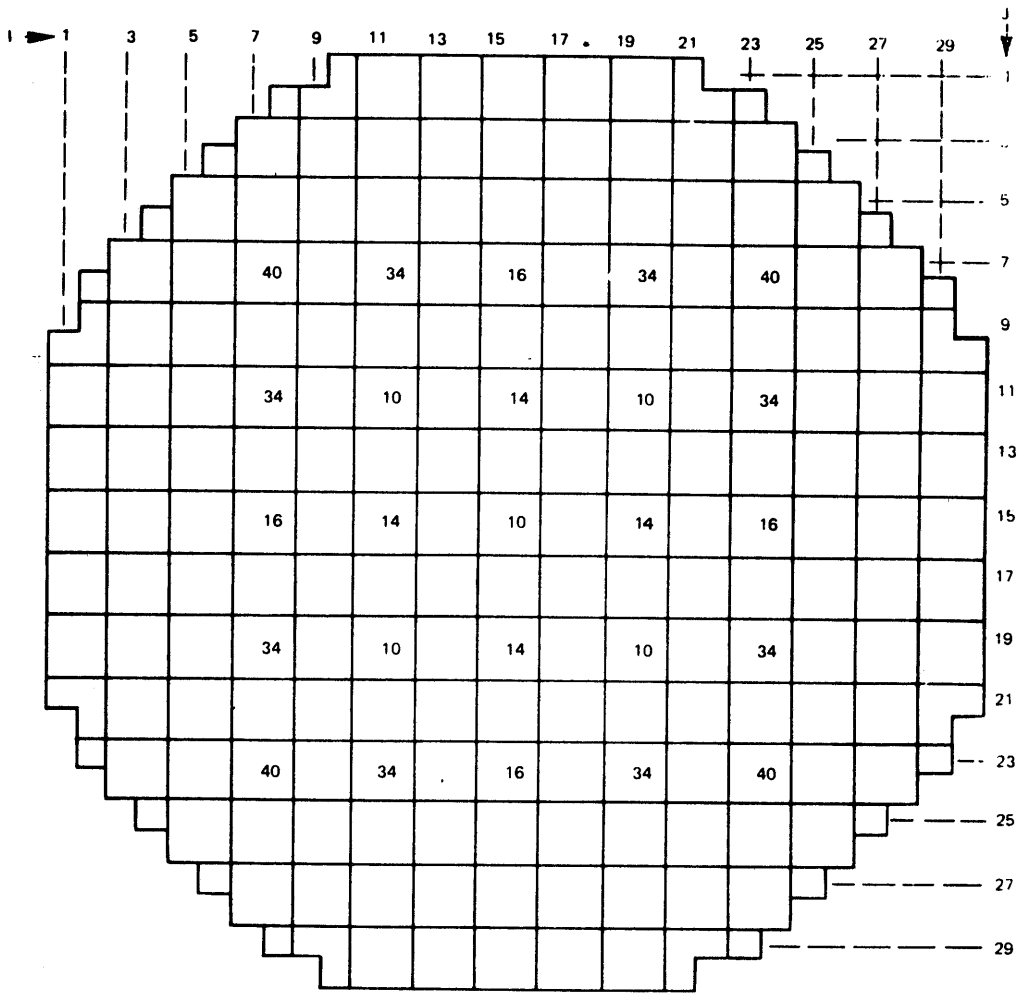

CONTROL ROD PATTERN (NOTCHES WITHDRAWN)

EXPOSURE		2000 MWd/t		
K_{eff}		1.0019		
ROD SEQUENCE		A-2		
POWER DISTRIBUTIONS		LOCATION		
		I	J	K
AXIAL	1.2224	–	–	4
RADIAL	1.3261	9	9	–
GROSS	1.8371	8	11	11
MCPR	1.3175	8	11	–
MLHGR	12.1130	8	11	11

I, J, K CODE COORDINATES
K = 1 = BOTTOM OF CORE
K = 25 = TOP OF CORE

FIGURE 4A-2A

SUMMARY OF 200 MWd/t CONDITION

RIVER BEND STATION
UPDATED SAFETY ANALYSIS REPORT

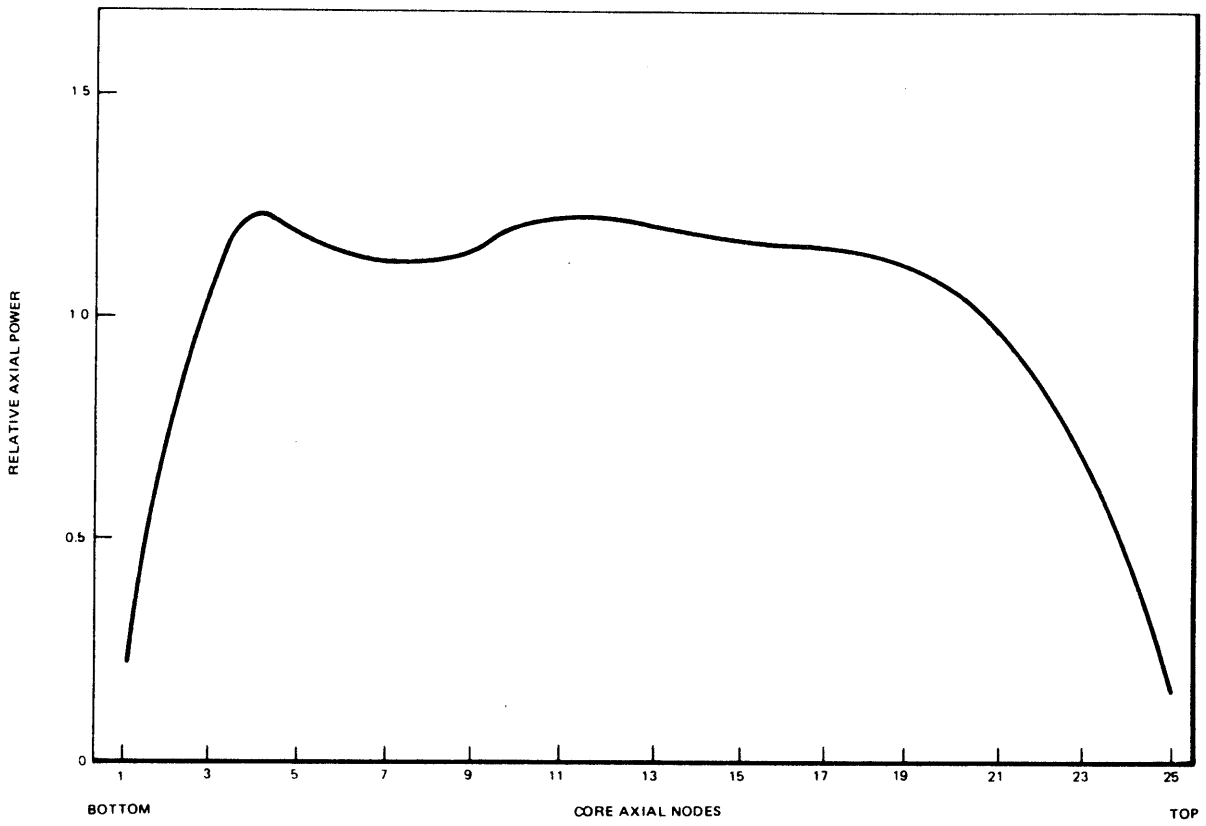

FIGURE 4A-2B

RELATIVE AXIAL POWER AT 200 MWd/t CORE AVERAGE EXPOSURE

RIVER BEND STATION
UPDATED SAFETY ANALYSIS REPORT

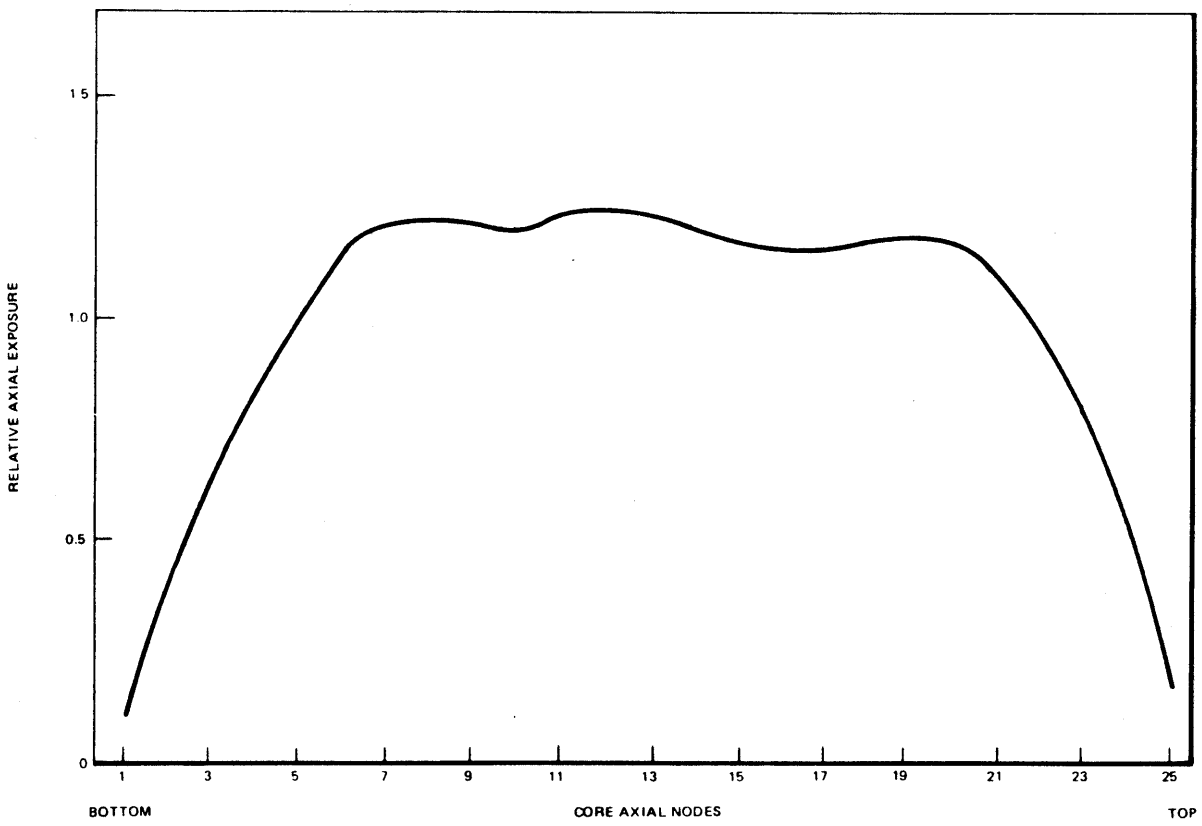

FIGURE 4A-2C

RELATIVE AXIAL EXPOSURE AT 200 MWd/t CORE AVERAGE EXPOSURE

RIVER BEND STATION

UPDATED SAFETY ANALYSIS REPORT

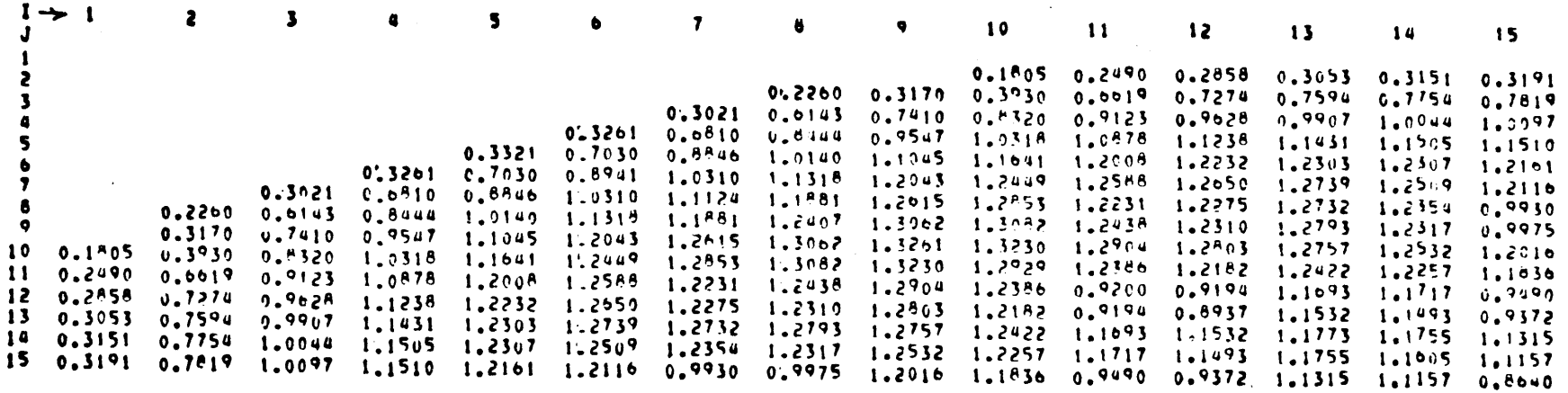

I → / J	1	2	3	4	5	6	7	8	9	10	11	12	13	14	15
1										0.1805	0.2490	0.2858	0.3053	0.3151	0.3191
2								0.2260	0.3170	0.3930	0.6619	0.7274	0.7594	0.7754	0.7819
3							0.3021	0.6143	0.7410	0.8320	0.9123	0.9628	0.9907	1.0044	1.0097
4						0.3261	0.6810	0.8444	0.9547	1.0318	1.0878	1.1238	1.1431	1.1505	1.1510
5					0.3321	0.7030	0.8846	1.0140	1.1045	1.1641	1.2008	1.2232	1.2303	1.2307	1.2161
6				0.3261	0.7030	0.8941	1.0310	1.1318	1.2043	1.2449	1.2588	1.2650	1.2739	1.2509	1.2116
7			0.3021	0.6810	0.8846	1.0310	1.1124	1.1881	1.2615	1.2853	1.2231	1.2275	1.2732	1.2354	0.9930
8		0.2260	0.6143	0.8444	1.0140	1.1318	1.1881	1.2407	1.3062	1.3082	1.2438	1.2310	1.2793	1.2317	0.9975
9		0.3170	0.7410	0.9547	1.1045	1.2043	1.2615	1.3062	1.3261	1.3230	1.2904	1.2803	1.2757	1.2532	1.2016
10	0.1805	0.3930	0.8320	1.0318	1.1641	1.2449	1.2853	1.3082	1.3230	1.2929	1.2386	1.2182	1.2422	1.2257	1.1836
11	0.2490	0.6619	0.9123	1.0878	1.2008	1.2588	1.2231	1.2438	1.2904	1.2386	0.9200	0.9194	1.1693	1.1717	0.9490
12	0.2858	0.7274	0.9628	1.1238	1.2232	1.2650	1.2275	1.2310	1.2803	1.2182	0.9194	0.8937	1.1532	1.1493	0.9372
13	0.3053	0.7594	0.9907	1.1431	1.2303	1.2739	1.2732	1.2793	1.2757	1.2422	1.1693	1.1532	1.1773	1.1755	1.1315
14	0.3151	0.7754	1.0044	1.1505	1.2307	1.2509	1.2354	1.2317	1.2532	1.2257	1.1717	1.1493	1.1755	1.1605	1.1157
15	0.3191	0.7819	1.0097	1.1510	1.2161	1.2116	0.9930	0.9975	1.2016	1.1836	0.9490	0.9372	1.1315	1.1157	0.8640

FIGURE 4A-2D

INTEGRATED POWER PER
BUNDLE, 200 MWd/t

RIVER BEND STATION

UPDATED SAFETY ANALYSIS REPORT

I →	1	2	3	4	5	6	7	8	9	10	11	12	13	14	15
J															
1										37.9	52.0	59.8	64.3	66.5	67.2
2								48.1	66.6	81.7	138.5	152.6	160.7	164.4	165.1
3							69.6	131.4	156.7	173.9	185.3	195.7	206.8	210.2	206.5
4						69.8	146.1	179.3	199.9	213.0	218.2	225.3	235.0	237.5	233.1
5					71.2	150.9	188.3	212.9	224.9	233.5	241.0	245.3	245.0	247.7	246.2
6				69.8	150.9	190.5	217.1	234.7	241.7	244.2	243.8	244.2	248.7	247.3	244.6
7			64.6	146.1	188.3	217.1	229.5	241.5	252.2	248.5	197.8	200.7	245.0	245.1	192.2
8		48.1	131.4	179.3	212.9	234.7	241.5	248.8	259.1	250.6	202.5	199.5	247.0	244.3	192.6
9		66.6	156.7	199.9	224.9	241.7	252.2	259.1	257.0	253.9	246.3	246.7	252.4	252.7	242.4
10	37.9	81.7	173.9	213.0	233.5	244.2	248.5	250.6	253.9	249.0	243.6	241.8	251.1	249.2	240.1
11	52.0	138.5	185.3	218.2	241.0	243.8	197.8	202.5	246.3	243.6	180.4	182.5	238.5	239.6	184.2
12	59.8	152.6	195.7	225.3	245.3	244.2	200.7	199.5	246.7	241.8	182.5	178.5	237.8	236.5	182.7
13	64.3	160.7	206.8	235.0	245.0	248.7	245.0	247.0	252.4	251.1	238.5	237.8	244.4	244.9	234.4
14	66.5	164.4	210.2	237.5	247.7	247.3	245.1	244.3	252.7	249.2	239.6	236.5	244.9	242.3	232.5
15	67.2	165.1	206.5	233.1	246.2	244.6	192.2	192.6	242.4	240.1	184.2	182.7	234.4	232.5	174.6

FIGURE 4A-2E

AVERAGE BUNDLE
EXPOSURE, 200 MWd/t

RIVER BEND STATION
UPDATED SAFETY ANALYSIS REPORT

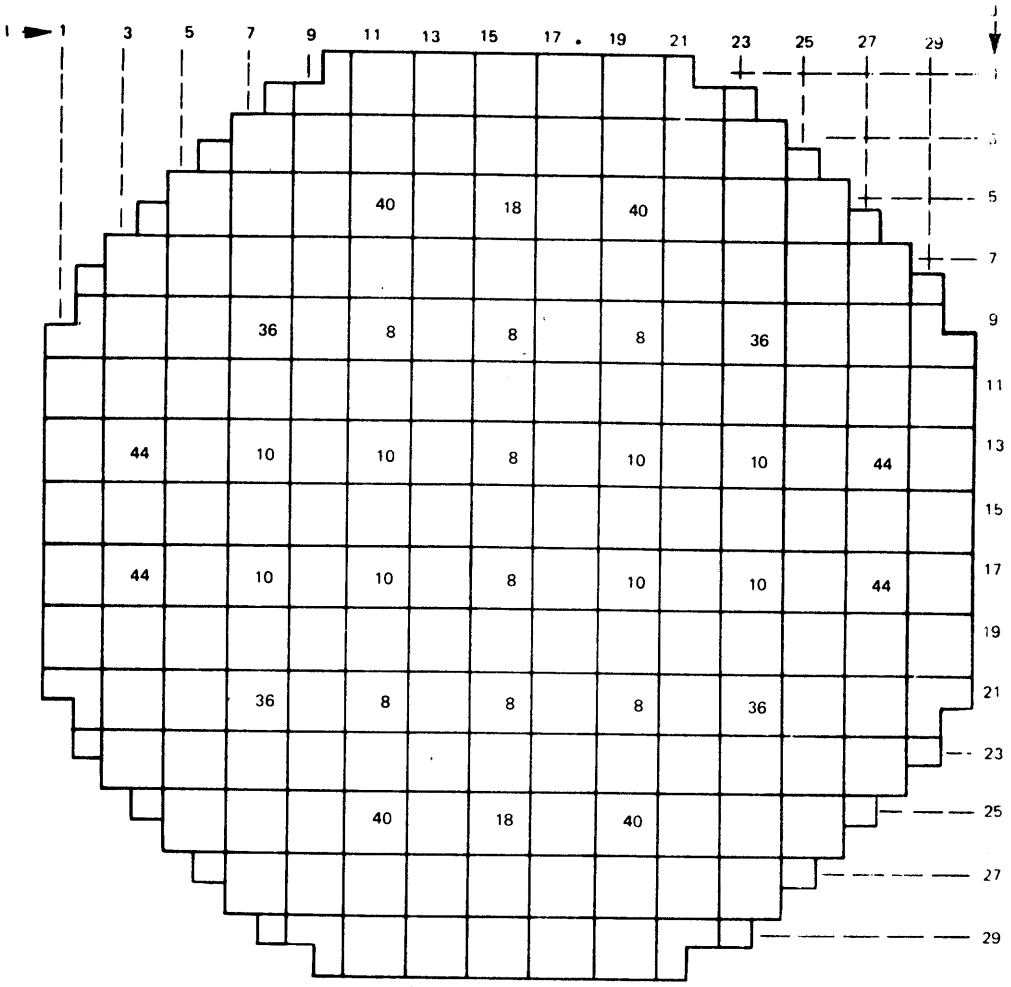

CONTROL ROD PATTERN (NOTCHES WITHDRAWN)

EXPOSURE		1000 MWd/t		
K_{eff}		0.9999		
ROD SEQUENCE		B-1		
POWER DISTRIBUTIONS		LOCATION		
		I	J	K
AXIAL	1.2698		–	4
RADIAL	1.3373	9	8	–
GROSS	1.8523	4	14	4
MCPR	1.3196	8	9	–
MLHGR	12.1232	4	14	4

I, J, K CODE COORDINATES
K = 1 BOTTOM OF CORE
K = 25 TOP OF CORE

FIGURE 4 A-3A

SUMMARY OF 1000 MWd/t CONDITION

RIVER BEND STATION
UPDATED SAFETY ANALYSIS REPORT

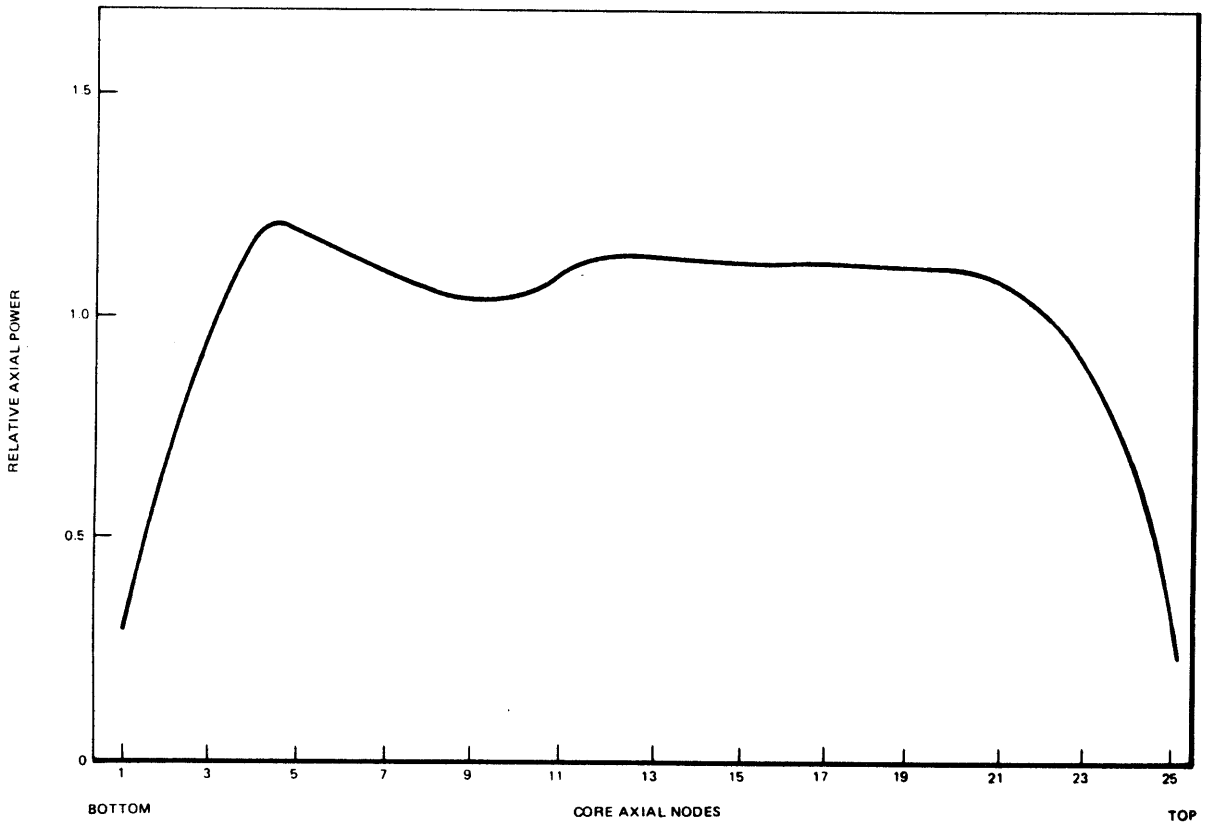

FIGURE 4A-3B

RELATIVE AXIAL POWER AT 1000 MWd/t CORE AVERAGE EXPOSURE

RIVER BEND STATION
UPDATED SAFETY ANALYSIS REPORT

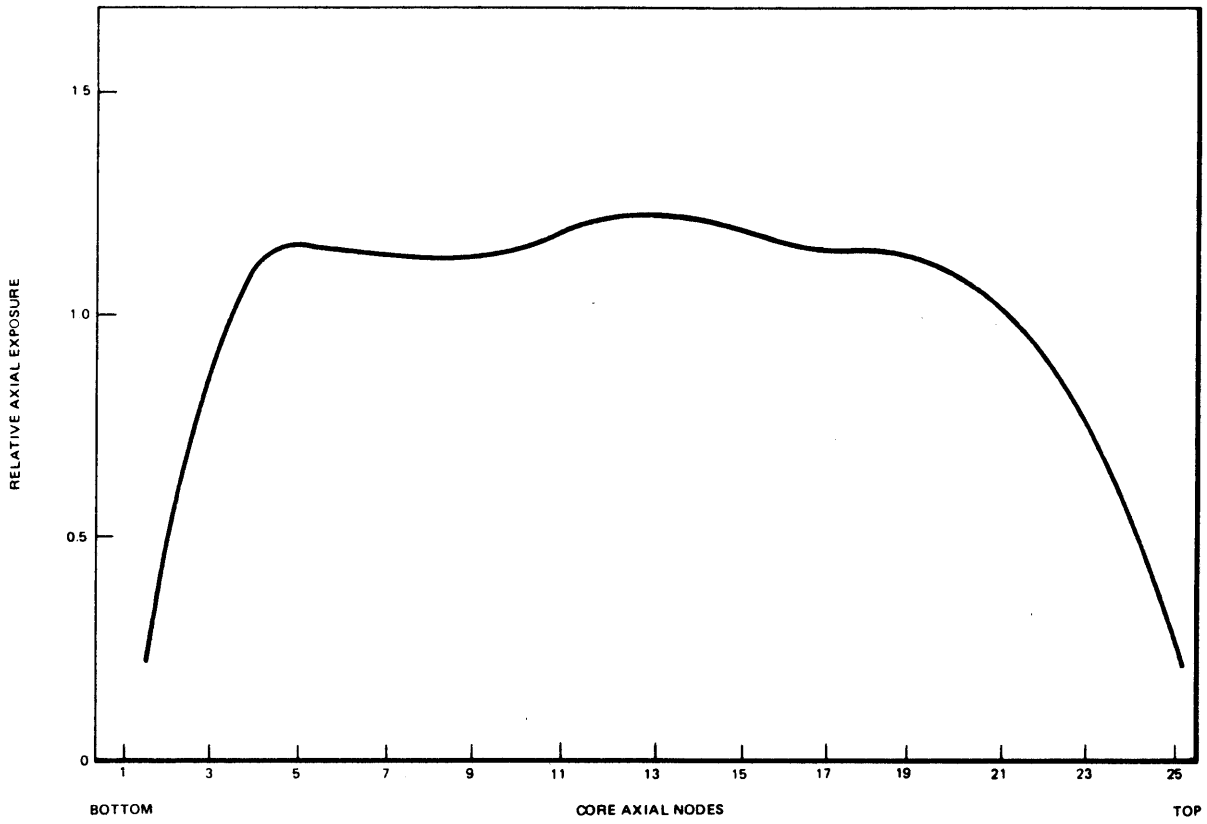

FIGURE 4A-3C

RELATIVE AXIAL EXPOSURE AT 1000 MWd/t CORE AVERAGE EXPOSURE

RIVER BEND STATION
UPDATED SAFETY ANALYSIS REPORT

I → / J	1	2	3	4	5	6	7	8	9	10	11	12	13	14	15
1										0.1957	0.2659	0.3026	0.3204	0.3276	0.3294
2								0.2460	0.3427	0.4206	0.6888	0.7506	0.7777	0.7865	0.7867
3							0.3284	0.6493	0.7780	0.8688	0.9439	0.9880	1.0075	1.0074	0.9960
4						0.3561	0.7229	0.8907	1.0009	1.0726	1.1175	1.1441	1.1528	1.1351	1.0987
5					0.3629	0.7483	0.9379	1.0703	1.1567	1.2051	1.2035	1.2153	1.2317	1.1918	0.9752
6				0.3547	0.7467	0.9490	1.0958	1.1976	1.2609	1.2887	1.2679	1.2044	1.2831	1.2323	1.0128
7			0.3266	0.7195	0.9336	1.0915	1.2024	1.2775	1.3173	1.3286	1.3094	1.3035	1.2968	1.2695	1.2137
8		0.2448	0.6462	0.8856	1.0622	1.1847	1.2610	1.3093	1.3373	1.3145	1.2605	1.2415	1.2651	1.2419	1.1862
9		0.3416	0.7750	0.9958	1.1466	1.2374	1.2964	1.2712	1.3203	1.2657	0.9117	0.9084	1.1667	1.1758	0.8696
10	0.1959	0.4204	0.8675	1.0710	1.2013	1.2710	1.2545	1.2682	1.3150	1.2481	0.9107	0.8813	1.1677	1.1524	0.8575
11	0.2669	0.6898	0.9451	1.1222	1.2325	1.2859	1.2943	1.3060	1.3069	1.2701	1.1887	1.1689	1.1952	1.1672	1.1306
12	0.3047	0.7535	0.9909	1.1494	1.2395	1.2623	1.2412	1.2411	1.2708	1.2445	1.1518	1.1595	1.1914	1.1756	1.1235
13	0.3245	0.7835	1.0076	1.1526	1.2279	1.2159	0.9187	0.9321	1.1977	1.1885	0.9029	0.9034	1.1409	1.1311	0.8446
14	0.3348	0.7998	1.0213	1.1605	1.2314	1.2049	0.9190	0.9079	1.1838	1.1730	0.9091	0.8697	1.1391	1.1226	0.8422
15	0.3394	0.8081	1.0365	1.1761	1.2384	1.2351	1.1832	1.1759	1.2145	1.2073	1.1548	1.1424	1.1736	1.1625	1.1109

FIGURE 4A-3D

INTEGRATED POWER
PER BUNDLE, 1000 MWd/t

RIVER BEND STATION

UPDATED SAFETY ANALYSIS REPORT

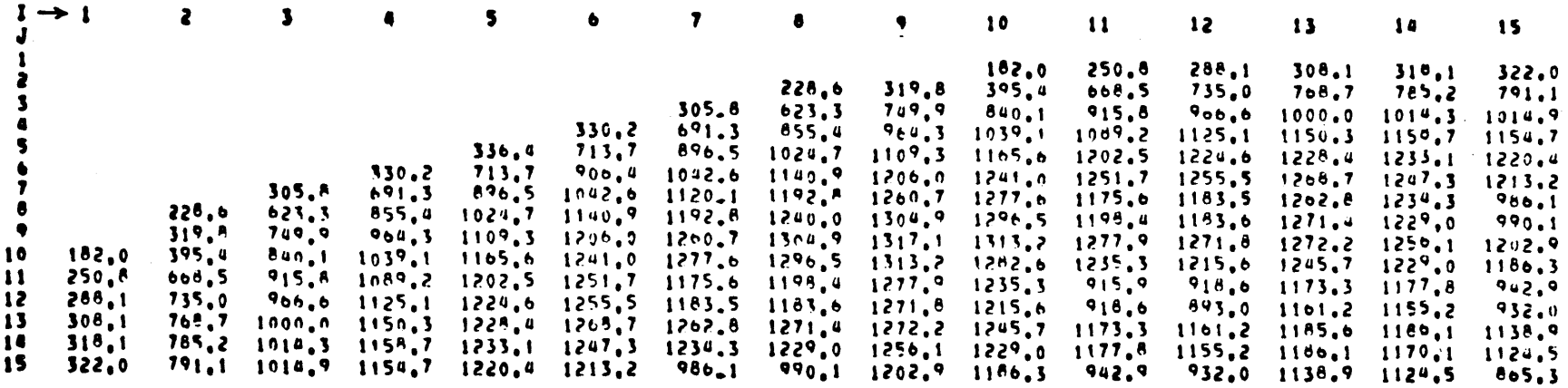

I → / J	1	2	3	4	5	6	7	8	9	10	11	12	13	14	15
1										182.0	250.8	288.1	308.1	318.1	322.0
2								228.6	319.8	395.4	668.5	735.0	768.7	785.2	791.1
3							305.8	623.3	749.9	840.1	915.8	966.6	1000.0	1014.3	1014.9
4						330.2	691.3	855.4	964.3	1039.1	1089.2	1125.1	1150.3	1150.7	1154.7
5					336.4	713.7	896.5	1024.7	1109.3	1165.6	1202.5	1224.6	1228.4	1235.1	1220.4
6				330.2	713.7	906.4	1042.6	1140.9	1206.0	1241.0	1251.7	1255.5	1268.7	1247.3	1213.2
7			305.8	691.3	896.5	1042.6	1120.1	1192.8	1260.7	1277.6	1175.6	1183.5	1202.8	1234.3	986.1
8		228.6	623.3	855.4	1024.7	1140.9	1192.8	1240.0	1304.9	1296.5	1198.4	1183.6	1271.4	1229.0	990.1
9		319.8	749.9	964.3	1109.3	1206.0	1260.7	1304.9	1317.1	1313.2	1277.9	1271.8	1272.2	1256.1	1202.9
10	182.0	395.4	840.1	1039.1	1165.6	1241.0	1277.6	1296.5	1313.2	1282.6	1235.3	1215.6	1245.7	1229.0	1186.3
11	250.8	668.5	915.8	1089.2	1202.5	1251.7	1175.6	1198.4	1277.9	1235.3	915.9	918.6	1173.3	1177.8	942.9
12	288.1	735.0	966.6	1125.1	1224.6	1255.5	1183.5	1183.6	1271.8	1215.6	918.6	893.0	1161.2	1155.2	932.0
13	308.1	768.7	1000.0	1150.3	1228.4	1268.7	1202.8	1271.4	1272.2	1245.7	1173.3	1161.2	1185.6	1180.1	1138.9
14	318.1	785.2	1014.3	1158.7	1233.1	1247.3	1234.3	1229.0	1256.1	1229.0	1177.8	1155.2	1186.1	1170.1	1124.5
15	322.0	791.1	1014.9	1154.7	1220.4	1213.2	986.1	990.1	1202.9	1186.3	942.9	932.0	1138.9	1124.5	865.3

FIGURE 4A-3E

AVERAGE BUNDLE EXPOSURE,
1000 MWd/t

RIVER BEND STATION
UPDATED SAFETY ANALYSIS REPORT

C(9/79)

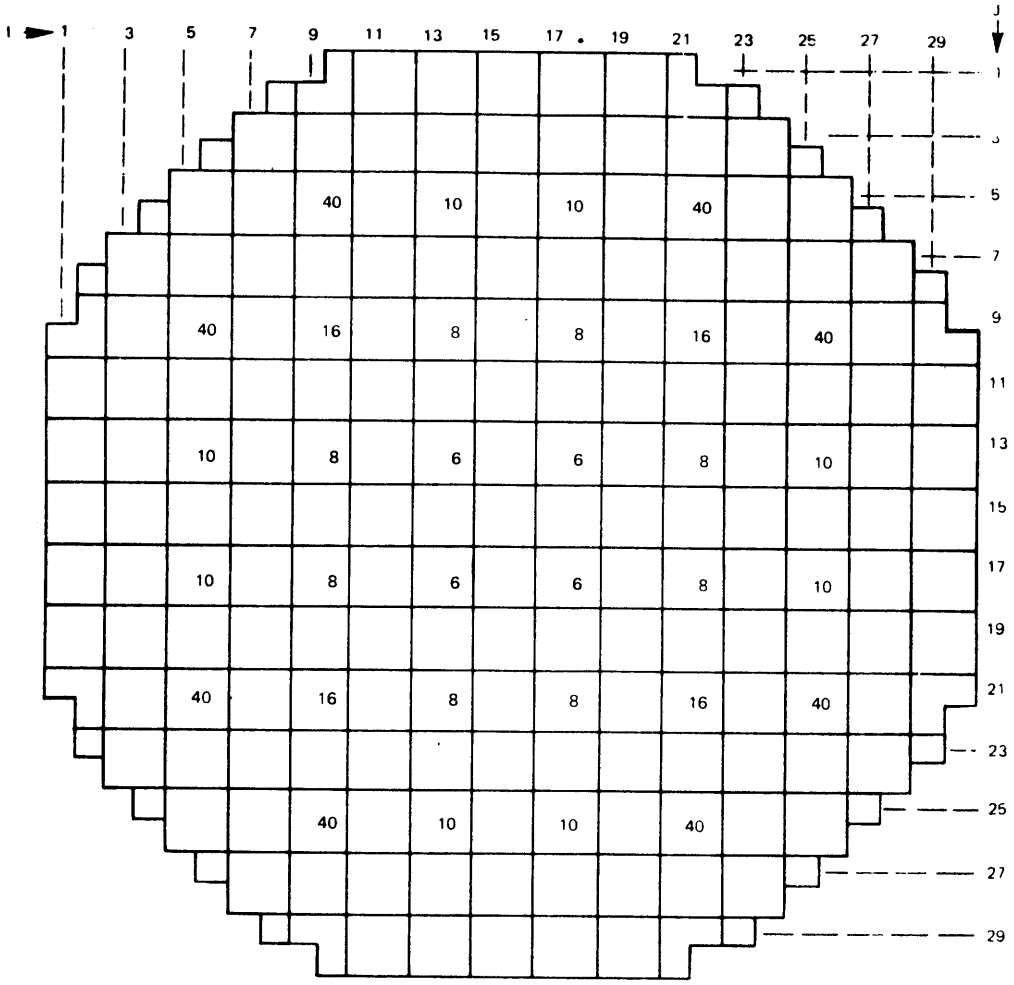

CONTROL ROD PATTERN (NOTCHES WITHDRAWN)

EXPOSURE	2000 MWd/t			
K_{eff}	0.9983			
ROD SEQUENCE	A-1			
POWER DISTRIBUTIONS		LOCATION		
		I	J	K
AXIAL	1.2079	–	–	4
RADIAL	1.3467	10	7	–
GROSS	1.8695	9	10	18
MCPR	1.3293	10	7	–
MLHGR	12.1064	10	9	18

I, J, K CODE COORDINATES
K = 1 - BOTTOM OF CORE
K = 25 - TOP OF CORE

FIGURE 4 A-4A

SUMMARY OF 2000 MWd/t CONDITION

RIVER BEND STATION
UPDATED SAFETY ANALYSIS REPORT

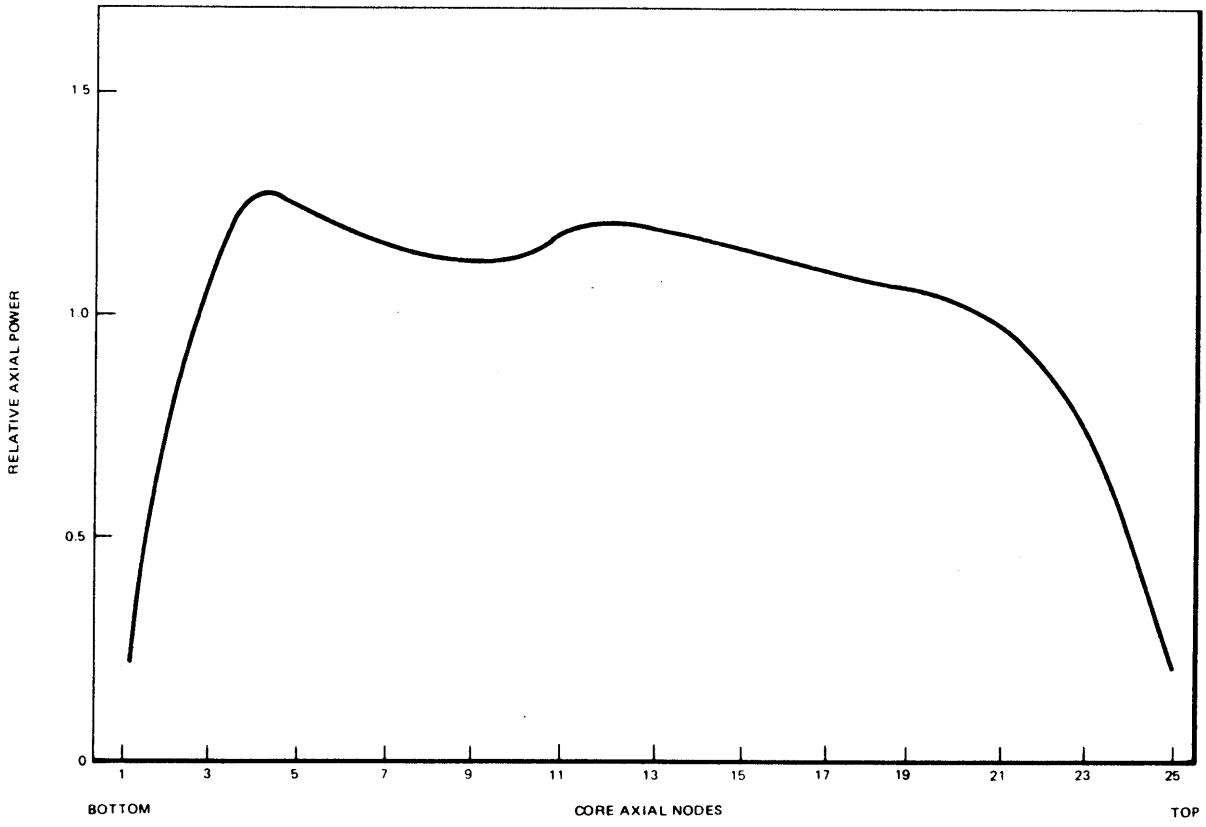

FIGURE 4A-4B

RELATIVE AXIAL POWER AT 2000 MWd/t CORE AVERAGE EXPOSURE

RIVER BEND STATION

UPDATED SAFETY ANALYSIS REPORT

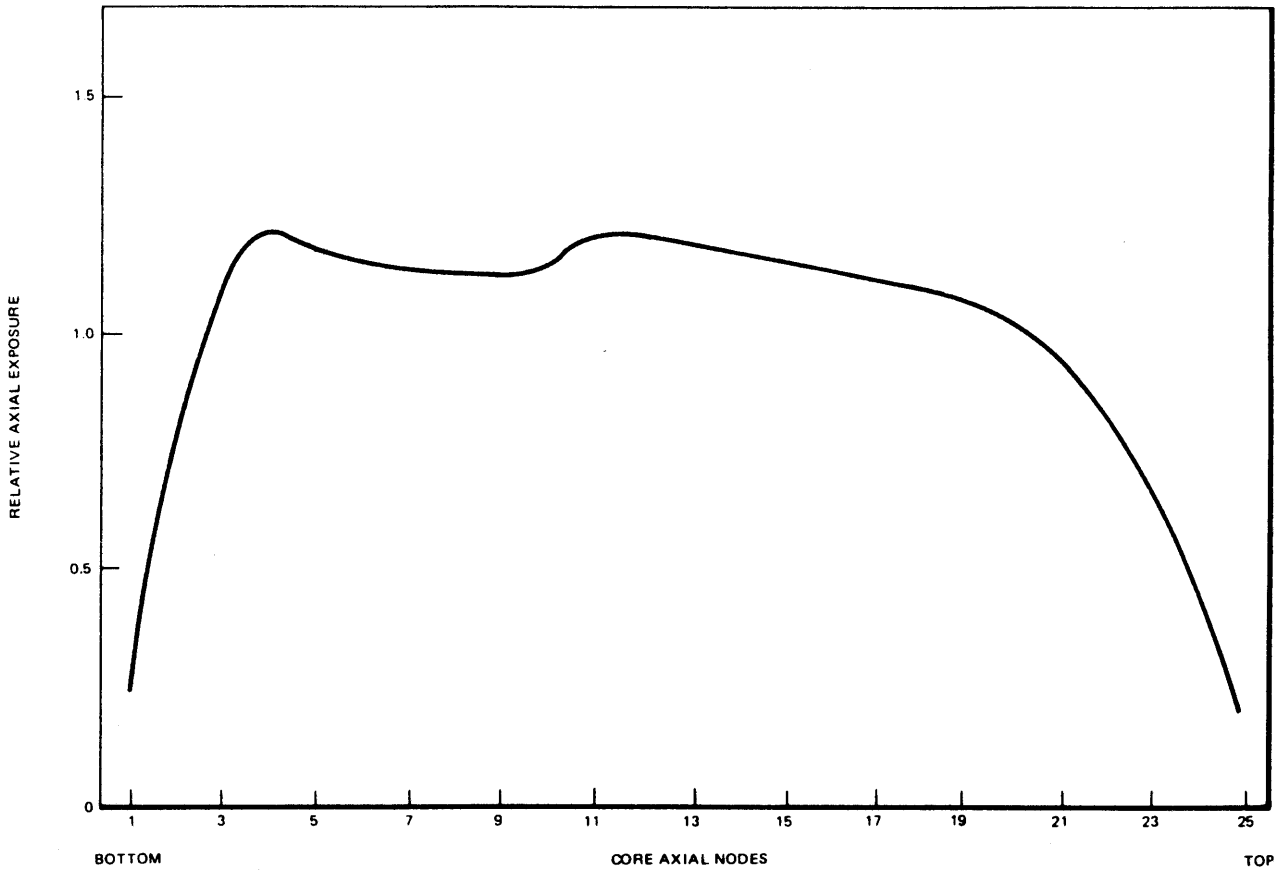

FIGURE 4A-4C

RELATIVE AXIAL EXPOSURE AT 2000 MWd/t CORE AVERAGE EXPOSURE

RIVER BEND STATION
UPDATED SAFETY ANALYSIS REPORT

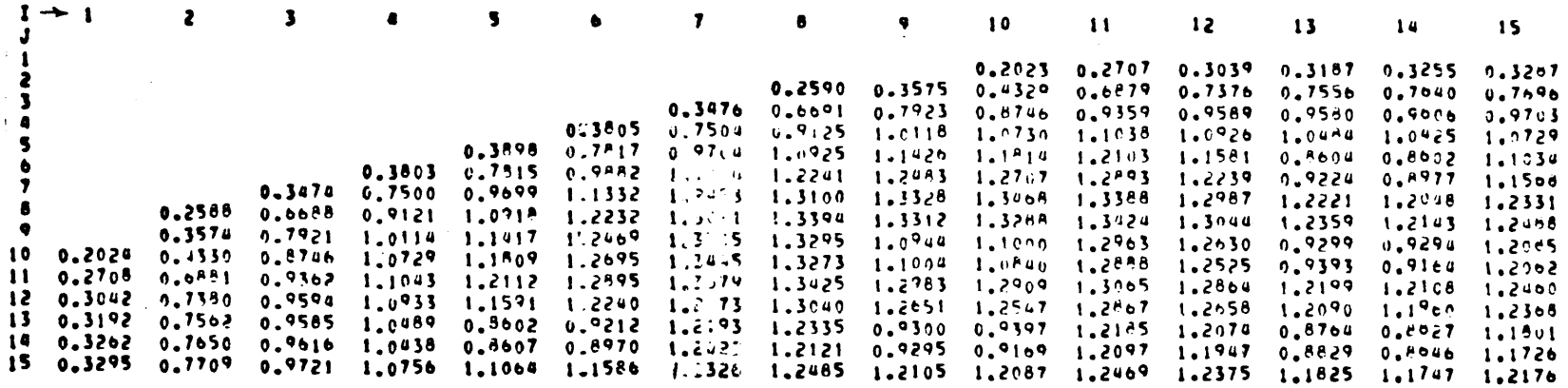

I → / J	1	2	3	4	5	6	7	8	9	10	11	12	13	14	15
1										0.2023	0.2707	0.3039	0.3187	0.3255	0.3287
2								0.2590	0.3575	0.4320	0.6879	0.7376	0.7556	0.7640	0.7696
3							0.3476	0.6691	0.7923	0.8746	0.9359	0.9589	0.9580	0.9606	0.9703
4						0.3805	0.7504	0.9125	1.0118	1.0730	1.1038	1.0926	1.0484	1.0425	1.0729
5					0.3898	0.7817	0.9764	1.0925	1.1426	1.1814	1.2103	1.1581	0.8604	0.8602	1.1034
6				0.3803	0.7515	0.9882	1.0	1.2241	1.2483	1.2707	1.2893	1.2239	0.9224	0.8977	1.1506
7			0.3474	0.7500	0.9699	1.1332	1.2	1.3100	1.3328	1.3468	1.3388	1.2987	1.2221	1.2048	1.2331
8		0.2588	0.6688	0.9121	1.0918	1.2232	1.3	1.3394	1.3312	1.3288	1.3424	1.3044	1.2359	1.2143	1.2488
9		0.3574	0.7921	1.0114	1.1417	1.2469	1.3	1.3295	1.0944	1.1000	1.2963	1.2630	0.9299	0.9294	1.2065
10	0.2024	0.4330	0.8746	1.0729	1.1809	1.2695	1.2	1.3273	1.1004	1.0840	1.2888	1.2525	0.9393	0.9164	1.2062
11	0.2708	0.6881	0.9362	1.1043	1.2112	1.2995	1.3	1.3425	1.2783	1.2909	1.3065	1.2864	1.2199	1.2108	1.2460
12	0.3042	0.7380	0.9594	1.0933	1.1591	1.2240	1.2	1.3040	1.2651	1.2547	1.2867	1.2658	1.2090	1.1960	1.2368
13	0.3192	0.7562	0.9585	1.0489	0.8602	0.9212	1.2	1.2335	0.9300	0.9397	1.2185	1.2078	0.8764	0.8627	1.1801
14	0.3262	0.7650	0.9616	1.0438	0.8607	0.8970	1.2	1.2121	0.9295	0.9169	1.2097	1.1947	0.8829	0.8646	1.1726
15	0.3295	0.7709	0.9721	1.0756	1.1064	1.1586	1.3	1.2485	1.2105	1.2087	1.2469	1.2375	1.1825	1.1747	1.2176

FIGURE 4A-4D

INTEGRATED POWER PER
BUNDLE, 2000 MWd/t

RIVER BEND STATION
UPDATED SAFETY ANALYSIS REPORT

I →	1	2	3	4	5	6	7	8	9	10	11	12	13	14	15
J															
1										377.2	516.2	590.1	627.9	645.0	650.7
2								474.0	661.8	815.2	1357.9	1486.2	1547.1	1572.4	1578.5
3							633.6	1211.2	1528.6	1709.6	1860.4	1955.4	2008.3	2022.6	2013.8
4						685.6	1414.9	1746.8	1966.1	2112.6	2207.6	2270.2	2304.1	2294.8	2254.3
5					698.5	1462.6	1835.3	2096.0	2267.0	2371.7	2407.1	2440.9	2459.2	2425.9	2195.0
6				684.2	1401.1	1856.2	2139.3	2339.5	2467.9	2530.8	2520.6	2519.0	2552.8	2478.7	2225.2
7			631.7	1411.4	1830.9	2135.1	2323.5	2471.3	2577.0	2607.3	2484.0	2488.1	2558.6	2504.9	2198.8
8		472.9	1270.0	1741.8	2087.9	2326.6	2454.9	2548.4	2643.3	2610.0	2460.0	2424.2	2537.5	2470.0	2175.4
9		660.7	1525.6	1960.9	2256.8	2444.5	2496.2	2577.2	2636.4	2579.9	2188.9	2181.0	2458.0	2432.9	2071.9
10	377.5	815.0	1708.3	2111.0	2367.9	2513.0	2533.2	2563.7	2629.3	2529.8	2146.8	2096.3	2414.3	2360.6	2043.2
11	517.1	1358.9	1861.7	2212.4	2436.0	2538.7	2468.9	2505.5	2583.8	2506.5	2103.7	2088.4	2367.6	2360.0	2072.9
12	592.2	1489.1	1958.3	2275.5	2465.2	2516.8	2425.7	2423.8	2503.7	2459.2	2101.4	2051.7	2353.6	2330.0	2054.7
13	631.9	1552.9	2008.5	2303.8	2455.5	2485.6	2180.8	2204.2	2469.0	2435.1	2075.5	2065.4	2325.7	2310.1	1952.9
14	652.1	1585.7	2036.5	2320.2	2465.6	2451.3	2154.1	2136.2	2440.9	2401.2	2087.7	2044.3	2326.2	2291.8	1966.0
15	660.7	1599.9	2052.3	2331.8	2458.0	2447.4	2168.4	2165.1	2416.5	2392.8	2096.8	2073.6	2311.7	2280.2	1975.4

FIGURE 4A-4E

AVERAGE BUNDLE
EXPOSURE, 2000 MWd/t

RIVER BEND STATION
UPDATED SAFETY ANALYSIS REPORT

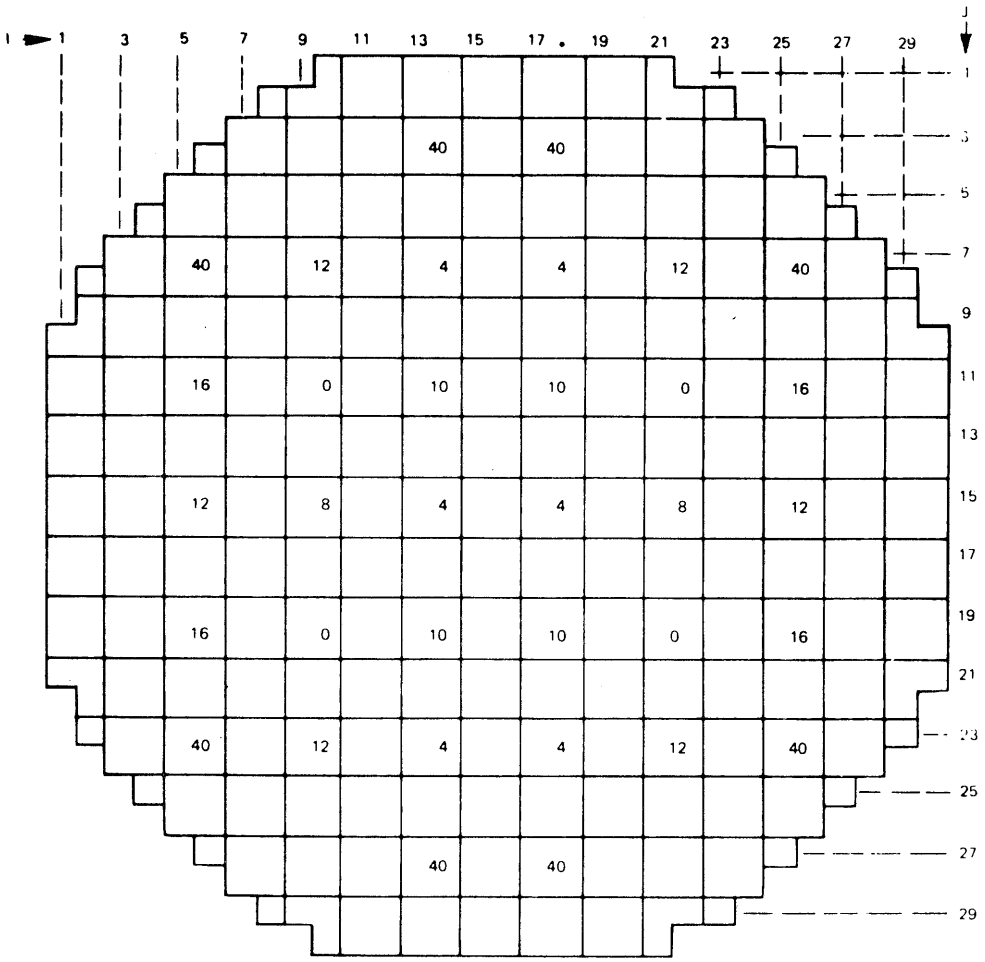

CONTROL ROD PATTERN (NOTCHES WITHDRAWN)

EXPOSURE	3000 MWd/t			
K_{eff}	0.9969			
ROD SEQUENCE	B-2			
POWER DISTRIBUTIONS		LOCATION		
		I	J	K
AXIAL	1.2825	–	–	4
RADIAL	1.3038	15	5	–
GROSS	1.8573	11	5	4
MCPR	1.3971	15	5	–
MLHGR	11.9915	11	5	4

I, J, K CODE COORDINATES
K = 1 BOTTOM OF CORE
K = 25 TOP OF CORE

FIGURE 4 A-5A

SUMMARY OF 3000 MWd/t CONDITION

RIVER BEND STATION
UPDATED SAFETY ANALYSIS REPORT

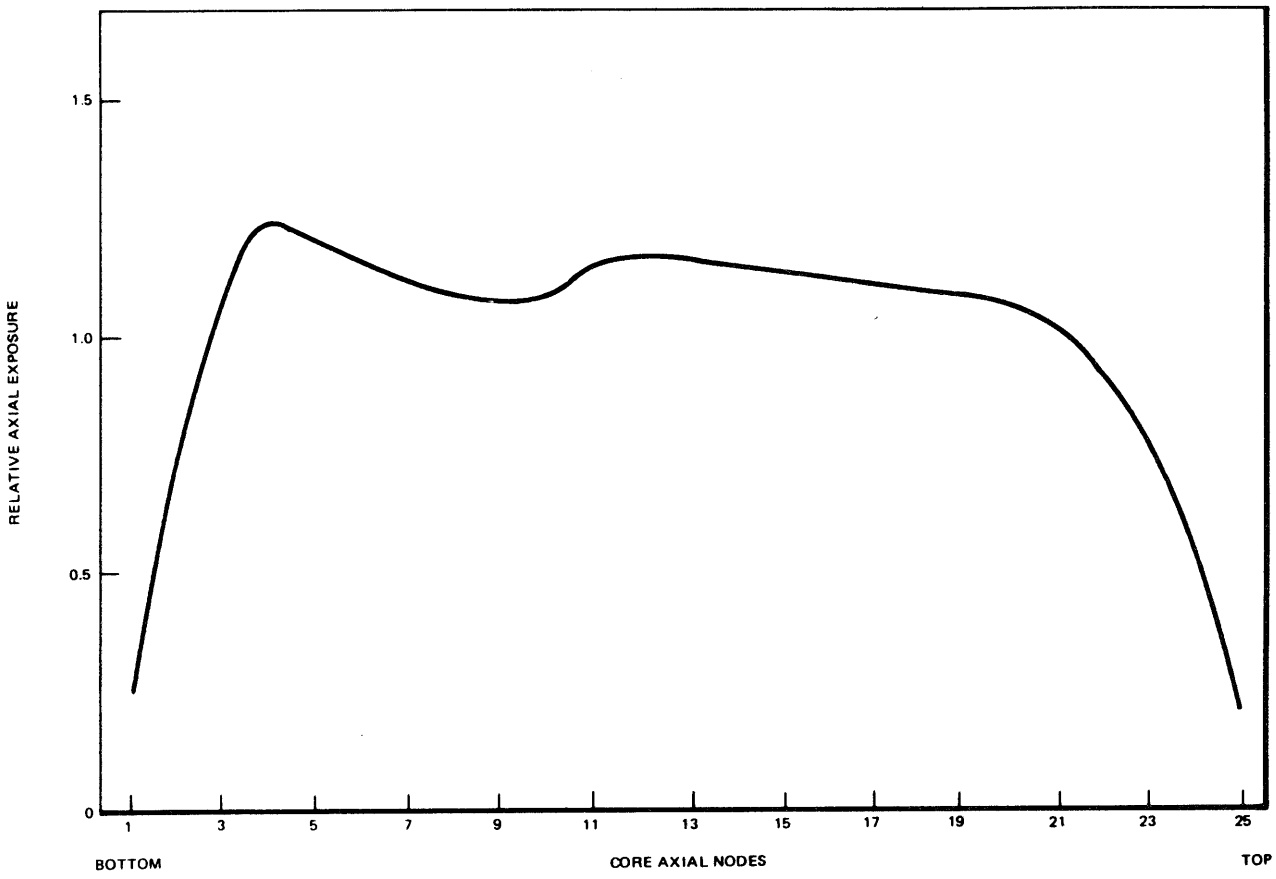

FIGURE 4A-5B

RELATIVE AXIAL POWER AT 3000 MWd/t CORE AVERAGE EXPOSURE

RIVER BEND STATION
UPDATED SAFETY ANALYSIS REPORT

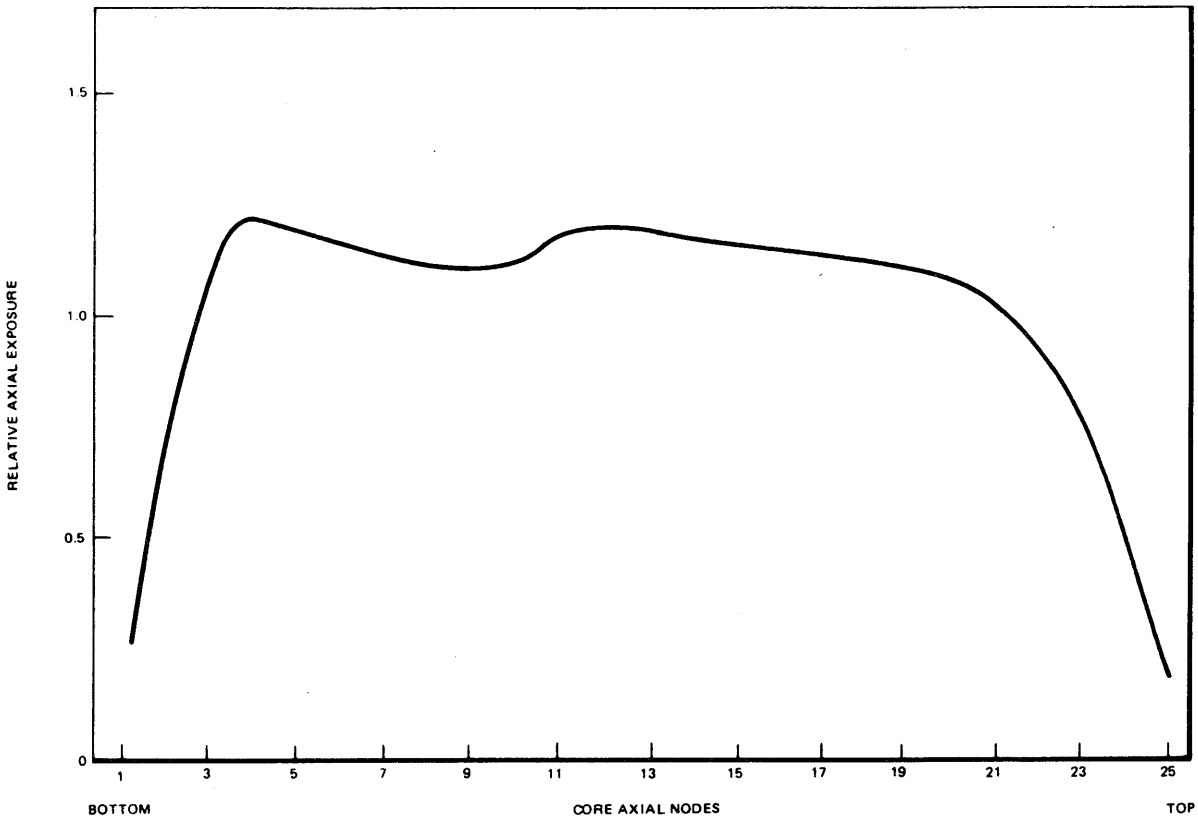

FIGURE 4A-5C

RELATIVE AXIAL EXPOSURE AT 3000 MWd/t CORE AVERAGE EXPOSURE

RIVER BEND STATION

UPDATED SAFETY ANALYSIS REPORT

I →	1	2	3	4	5	6	7	8	9	10	11	12	13	14	15
J															
1										0.2269	0.3057	0.3482	0.3704	0.3830	0.3898
2								0.27[illegible]	0.3818	0.4690	0.7446	0.8097	0.8404	0.8597	0.8733
3							0.3555	0.6[illegible]2	0.8166	0.9163	0.9999	1.0473	1.0482	1.0661	1.1053
4						0.3801	0.7461	0.9[illegible]29	1.0258	1.1081	1.1689	1.2012	1.1873	1.2012	1.2436
5					0.3832	0.7645	0.9488	1.0704	1.1472	1.2085	1.2581	1.2800	1.2747	1.2863	1.3039
6				0.3726	0.7566	0.9524	1.0870	1.1581	1.1779	1.2178	1.2748	1.2764	1.2467	1.2472	1.2919
7			0.3443	0.7290	0.9158	1.0599	1.1735	1.1882	0.9371	0.9659	1.2322	1.2321	0.8674	0.8829	1.2279
8		0.2608	0.6606	0.8905	1.0350	1.1480	1.2381	1.2231	0.9768	0.9635	1.2430	1.2254	0.8811	0.8955	1.2219
9		0.3615	0.7851	0.9919	1.1275	1.2230	1.2734	1.2917	1.2311	1.2392	1.2791	1.2826	1.2264	1.2318	1.2779
10	0.2091	0.4387	0.8659	1.0416	1.1371	1.2151	1.2781	1.2668	1.2187	1.2126	1.2755	1.2777	1.2422	1.2401	1.2872
11	0.2823	0.6971	0.9295	1.0548	0.9546	1.0078	1.2307	1.2185	0.8204	0.8349	1.2104	1.2347	0.9504	0.9690	1.2459
12	0.3224	0.7606	0.9756	1.0835	0.9684	1.0023	1.2373	1.2095	0.8332	0.8167	1.2110	1.2254	0.9617	0.9535	1.2413
13	0.3444	0.7953	1.0091	1.1264	1.1668	1.2200	1.2693	1.2680	1.2028	1.2053	1.2564	1.2707	1.2259	1.2338	1.2758
14	0.3553	0.8112	1.0216	1.1313	1.1676	1.2082	1.2728	1.2062	1.2193	1.2102	1.2632	1.2575	1.2134	1.2093	1.2608
15	0.3591	0.8153	1.0181	1.1014	0.9172	0.9542	1.2250	1.2218	0.9111	0.9072	1.2092	1.2019	0.8515	0.8513	1.1999

FIGURE 4A-5D

INTEGRATED POWER PER
BUNDLE, 3000 MWd/t

RIVER BEND STATION

UPDATED SAFETY ANALYSIS REPORT

I →	1	2	3	4	5	6	7	8	9	10	11	12	13	14	15
J															
1										579.1	786.3	893.4	946.0	969.8	978.7
2								732.5	1018.6	1247.2	2046.4	2224.5	2303.3	2337.1	2348.7
3							980.5	1942.8	2321.6	2584.9	2797.1	2915.2	2967.2	2984.0	2984.9
4						1065.4	2165.8	2660.1	2978.7	3186.6	3312.3	3363.7	3353.4	3330.1	3328.1
5					1087.5	2245.0	2806.4	3169.4	3410.5	3554.1	3618.4	3600.0	3319.0	3266.8	3297.5
6				1063.8	2243.3	2845.2	3273.8	3564.6	3717.3	3802.5	3811.0	3742.1	3476.0	3375.8	3381.2
7			978.4	2162.0	2801.7	3269.2	3569.9	3782.4	3908.8	3955.1	3821.8	3787.9	3779.9	3710.7	3431.1
8		731.2	1939.3	2654.6	3180.6	3550.8	3765.0	3886.8	3975.6	3937.9	3803.5	3727.7	3774.4	3683.4	3423.3
9		1017.4	2318.4	2973.1	3329.5	3692.5	3825.7	3937.8	3730.0	3680.8	3884.3	3445.1	3387.3	3363.1	3279.5
10	579.4	1247.1	2563.6	3184.8	3549.8	3783.6	3878.8	3890.1	3730.6	3613.0	3436.6	3347.9	3354.4	3290.4	3248.5
11	787.4	2047.6	2798.6	3317.6	3648.2	3829.2	3805.8	3849.2	3881.1	3798.5	3409.2	3375.9	3586.6	3577.8	3317.7
12	895.8	2227.8	2918.5	3369.7	3625.2	3740.0	3724.2	3726.9	3809.8	3713.0	3389.2	3316.5	3563.6	3525.2	3290.6
13	950.4	2309.7	2967.8	3353.6	3315.0	3407.5	3399.3	3438.8	3398.4	3375.7	3293.2	3273.9	3201.4	3201.6	3162.1
14	977.7	2351.3	2998.9	3364.8	3327.0	3347.6	3357.3	3347.4	3371.2	3317.4	3298.4	3238.1	3209.9	3155.8	3137.8
15	989.6	2371.5	3025.3	3408.3	3563.6	3605.2	3400.1	3412.7	3626.2	3600.6	3342.8	3310.2	3493.3	3460.0	3192.0

FIGURE 4A-5E

AVERAGE BUNDLE EXPOSURE,
3000 MWd/t

RIVER BEND STATION

UPDATED SAFETY ANALYSIS REPORT

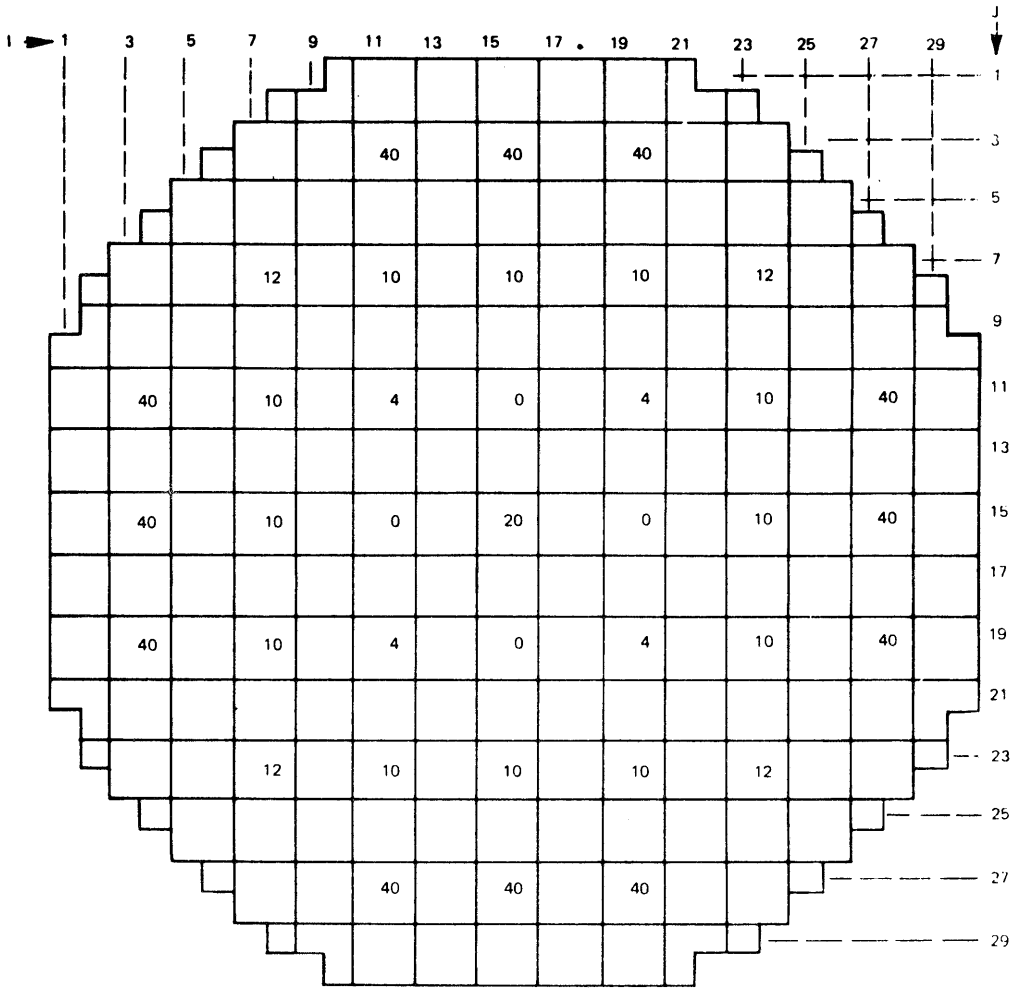

CONTROL ROD PATTERN (NOTCHES WITHDRAWN)

EXPOSURE	4000 MWd/t			
K_{eff}	0.9997			
ROD SEQUENCE	A-2			
POWER DISTRIBUTIONS		LOCATION		
		I	J	K
AXIAL	1.3029	–	–	4
RADIAL	1.3265	14	5	–
GROSS	1.8594	14	5	4
MCPR	1.3659	14	5	–
MLHGR	12.0828	14	5	4

I, J, K CODE COORDINATES
K = 1 = BOTTOM OF CORE
K = 25 TOP OF CORE

FIGURE 4 A-6A

SUMMARY OF 4000 MWd/t CONDITION

RIVER BEND STATION
UPDATED SAFETY ANALYSIS REPORT

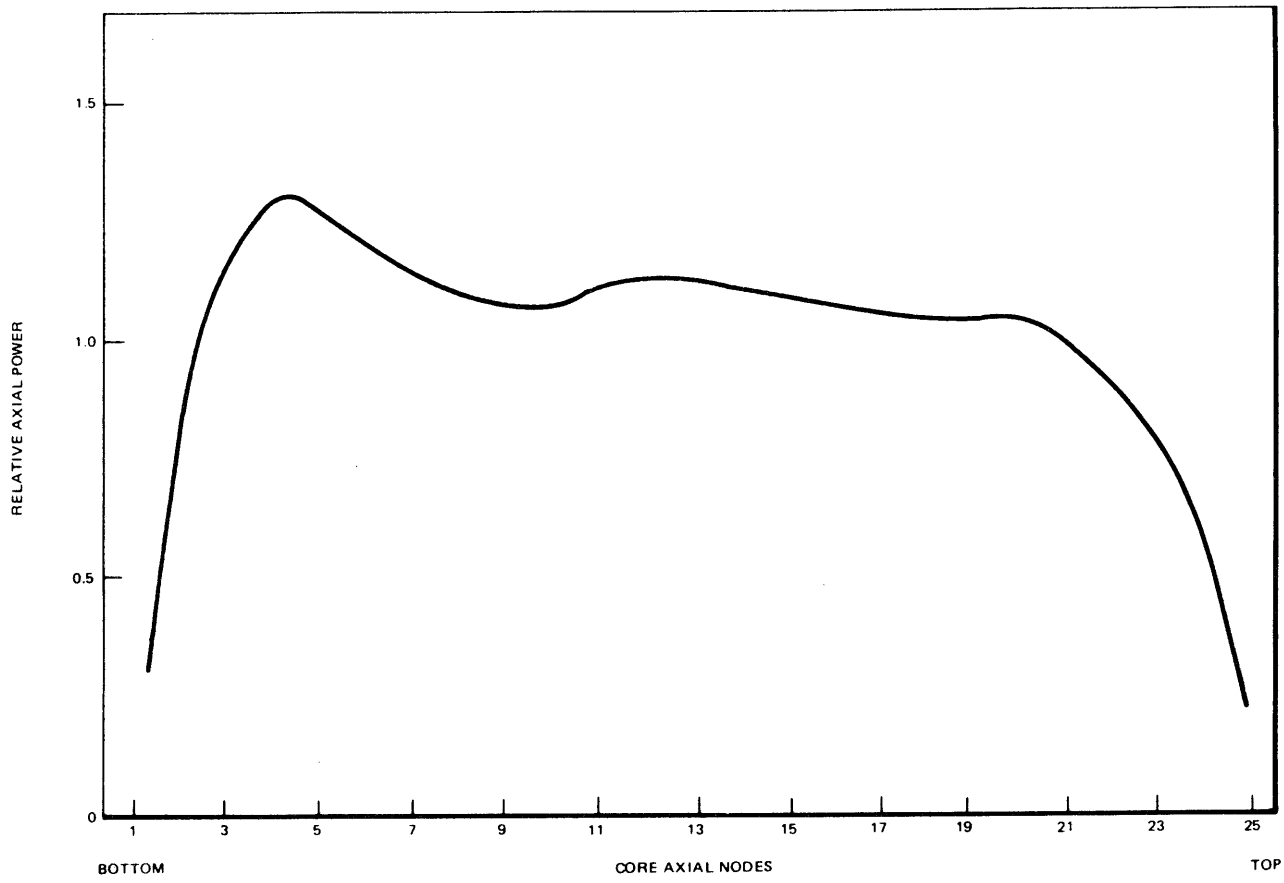

FIGURE 4A-6B

RELATIVE AXIAL POWER AT 4000 MWd/t CORE AVERAGE EXPOSURE

RIVER BEND STATION
UPDATED SAFETY ANALYSIS REPORT

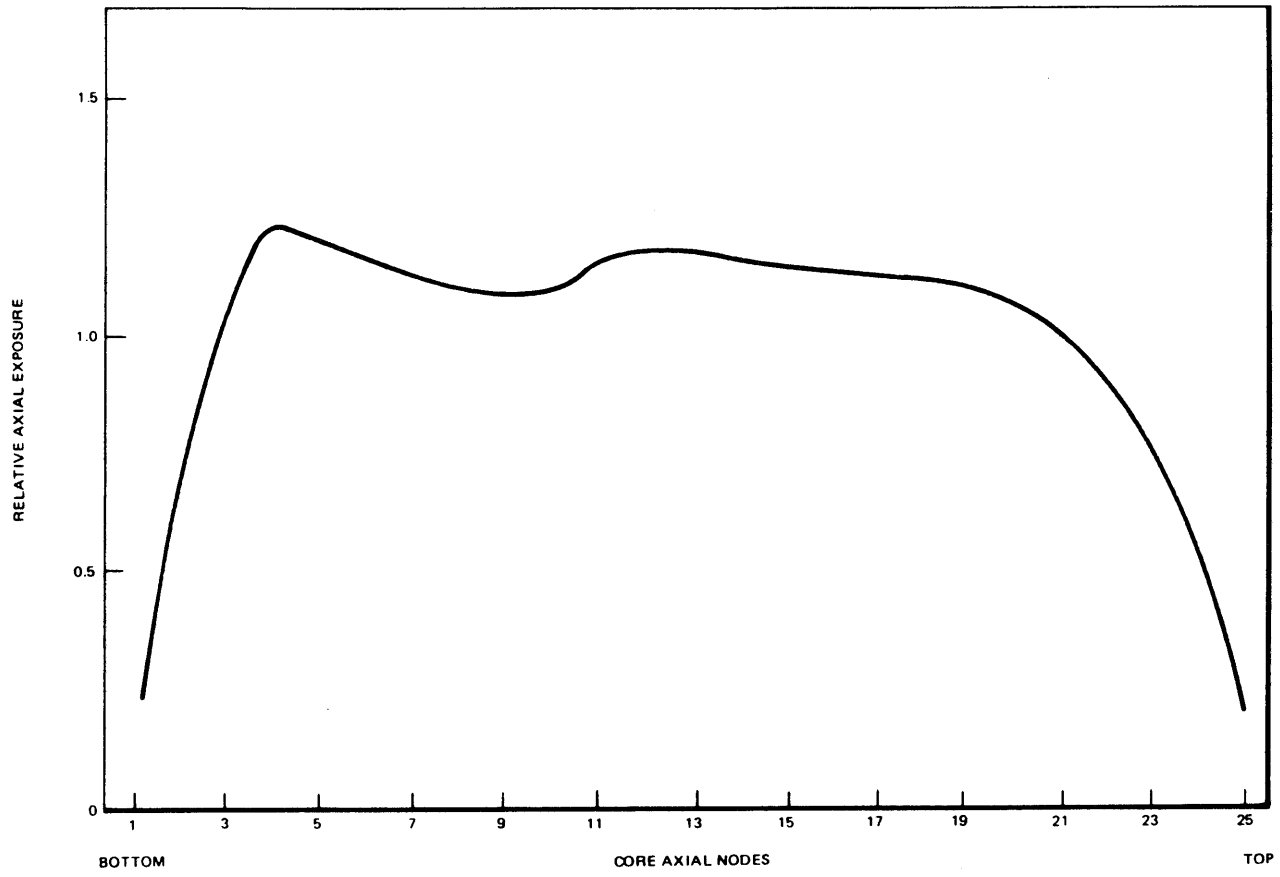

FIGURE 4A-6C

RELATIVE AXIAL EXPOSURE AT 4000 MWd/t CORE AVERAGE EXPOSURE

RIVER BEND STATION

UPDATED SAFETY ANALYSIS REPORT

I → 1 J	1	2	3	4	5	6	7	8	9	10	11	12	13	14	15
1										0.2282	0.3079	0.3542	0.3818	0.3961	0.4010
2								0.2706	0.3792	0.4654	0.7377	0.8112	0.8572	0.8795	0.8844
3							0.3440	0.6659	0.8055	0.9047	0.9668	1.0268	1.0922	1.1135	1.0940
4						0.3577	0.7124	0.8874	1.0125	1.0966	1.1293	1.1762	1.2410	1.2564	1.2365
5					0.3575	0.7128	0.8893	1.0286	1.1372	1.2066	1.2440	1.2787	1.3020	1.3263	1.3038
6				0.3565	0.7117	0.8753	0.9769	1.0805	1.1864	1.2371	1.2366	1.2457	1.3121	1.3062	1.2649
7			0.3822	0.7097	0.8865	0.9750	0.9321	0.8898	1.1656	1.2087	0.9304	0.9612	1.2443	1.2593	0.9506
8		0.2688	0.6627	0.8835	1.0245	1.0775	0.8691	0.9988	1.2028	1.2033	0.9479	0.9360	1.2424	1.2292	0.9345
9		0.3768	0.8014	1.0075	1.1322	1.1826	1.1620	1.2024	1.2422	1.2634	1.2082	1.2239	1.2507	1.2066	1.2032
10	0.2263	0.4620	0.8999	1.0906	1.2003	1.2321	1.2061	1.2003	1.2629	1.2437	1.2053	1.1903	1.2493	1.2314	1.1738
11	0.3057	0.7338	0.9619	1.1230	1.2362	1.2330	0.9240	0.9468	1.2082	1.2050	0.8397	0.8519	1.1722	1.1760	0.7898
12	0.3518	0.8073	1.0218	1.1699	1.2711	1.2408	0.9584	0.9344	1.2226	1.1905	0.8517	0.8283	1.1788	1.1928	0.7907
13	0.3796	0.8537	1.0480	1.2357	1.2765	1.3064	1.2394	1.2392	1.2548	1.2482	1.1716	1.1788	1.2227	1.2482	1.1817
14	0.3940	0.8762	1.1098	1.2541	1.3218	1.3018	1.2552	1.2252	1.2648	1.2301	1.1755	1.1625	1.2402	1.2914	1.2255
15	0.3990	0.8812	1.0902	1.2263	1.3007	1.2669	0.9479	0.9321	1.2011	1.1726	0.7893	0.7906	1.1625	1.2263	1.0594

FIGURE 4A-6D

INTEGRATED POWER PER BUNDLE,
4000 MWd/t

RIVER BEND STATION
UPDATED SAFETY ANALYSIS REPORT

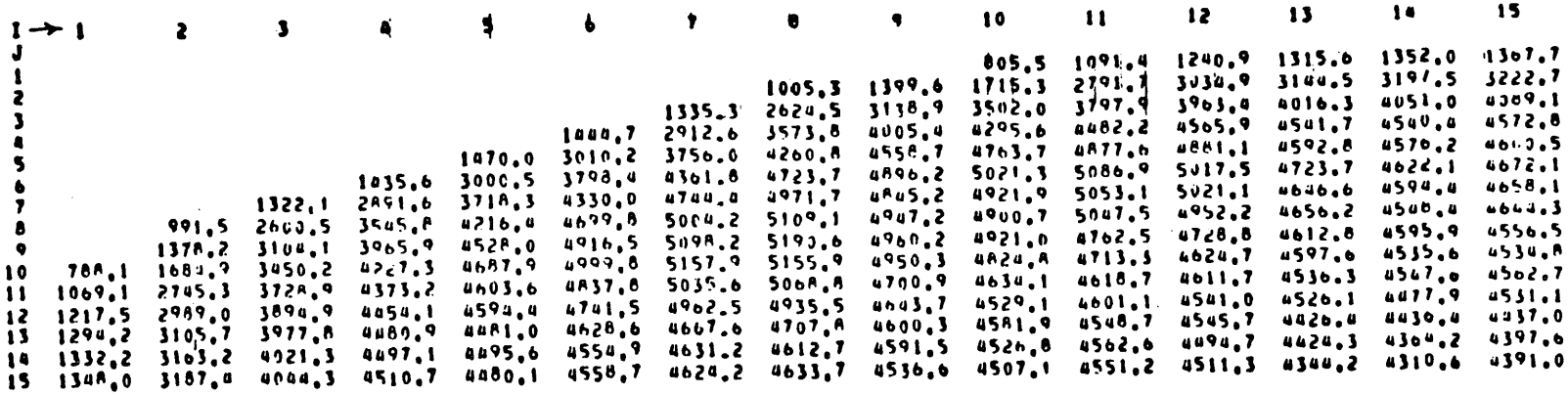

I →	1	2	3	4	5	6	7	8	9	10	11	12	13	14	15
J															
1										805.5	1091.4	1240.9	1315.6	1352.0	1367.7
2								1005.3	1399.6	1716.3	2791.1	3034.9	3144.5	3197.5	3222.7
3							1335.3	2624.5	3138.9	3502.0	3797.9	3963.4	4016.3	4051.0	4069.1
4						1444.7	2912.6	3573.8	4005.4	4295.6	4482.2	4565.9	4541.7	4540.4	4572.8
5					1470.0	3010.2	3756.0	4260.8	4558.7	4763.7	4877.6	4881.1	4592.8	4570.2	4600.5
6				1435.6	3000.5	3798.4	4361.8	4723.7	4896.2	5021.3	5086.9	5017.5	4723.7	4622.1	4672.1
7			1322.1	2891.6	3718.3	4330.0	4744.4	4971.7	5045.2	4921.9	5053.1	5021.1	4646.6	4594.4	4658.1
8		991.5	2603.5	3545.8	4216.4	4699.8	5004.2	5109.1	4947.2	4900.7	5047.5	4952.2	4656.2	4548.4	4644.3
9		1378.2	3104.1	3965.9	4528.0	4916.5	5098.2	5193.6	4960.2	4921.0	4762.5	4728.8	4612.8	4595.9	4556.5
10	788.1	1684.9	3450.2	4227.3	4687.9	4999.8	5157.9	5155.9	4950.3	4824.8	4713.3	4624.7	4597.6	4535.6	4534.8
11	1069.1	2745.3	3728.9	4373.2	4603.6	4837.8	5035.6	5068.8	4700.9	4634.1	4618.7	4611.7	4536.3	4547.0	4562.7
12	1217.5	2989.0	3894.9	4454.1	4594.4	4741.5	4962.5	4935.5	4643.7	4529.1	4601.1	4541.0	4526.1	4477.9	4531.1
13	1294.2	3105.7	3977.8	4480.9	4481.0	4628.6	4667.6	4707.8	4600.3	4581.9	4548.7	4545.7	4426.4	4430.4	4437.0
14	1332.2	3163.2	4021.3	4497.1	4495.6	4554.9	4631.2	4612.7	4591.5	4526.8	4562.6	4494.7	4424.3	4364.2	4397.6
15	1348.0	3187.4	4044.3	4510.7	4480.1	4558.7	4624.2	4633.7	4536.6	4507.1	4551.2	4511.3	4344.2	4310.6	4391.0

FIGURE 4A-6E

AVERAGE BUNDLE EXPOSURE,
4000 MWd/t

RIVER BEND STATION
UPDATED SAFETY ANALYSIS REPORT

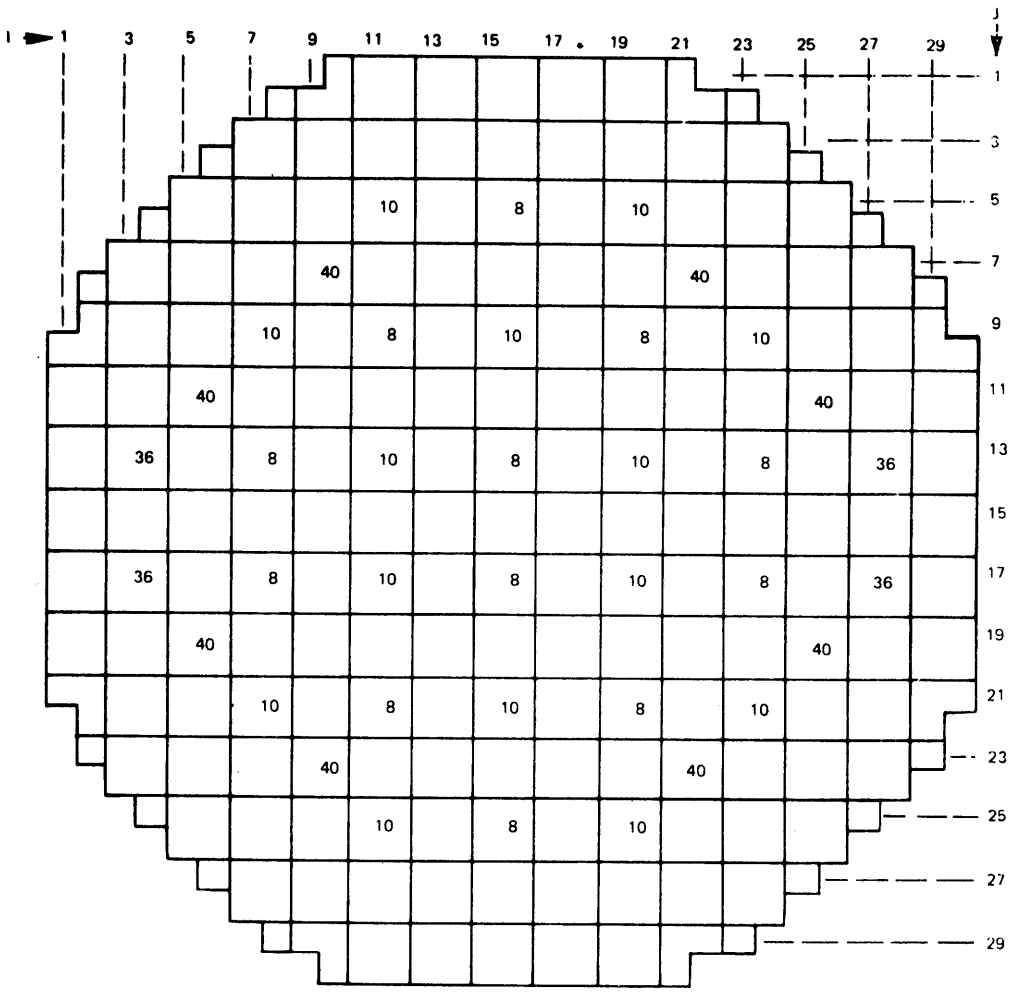

CONTROL ROD PATTERN (NOTCHES WITHDRAWN)

EXPOSURE		5000 MWd/t		
K_{eff}		1.0005		
ROD SEQUENCE		B-1		
POWER DISTRIBUTIONS		LOCATION		
		I	J	K
AXIAL	1.2735	–	–	5
RADIAL	1.3076	5	14	–
GROSS	1.8362	8	6	4
MCPR	1.3827	5	14	–
MLHGR	12.0664	8	6	4

I, J, K CODE COORDINATES
K = 1 = BOTTOM OF CORE
K = 25 TOP OF CORE

FIGURE 4 A-7A

SUMMARY OF 5000 MWd/t CONDITION

RIVER BEND STATION
UPDATED SAFETY ANALYSIS REPORT

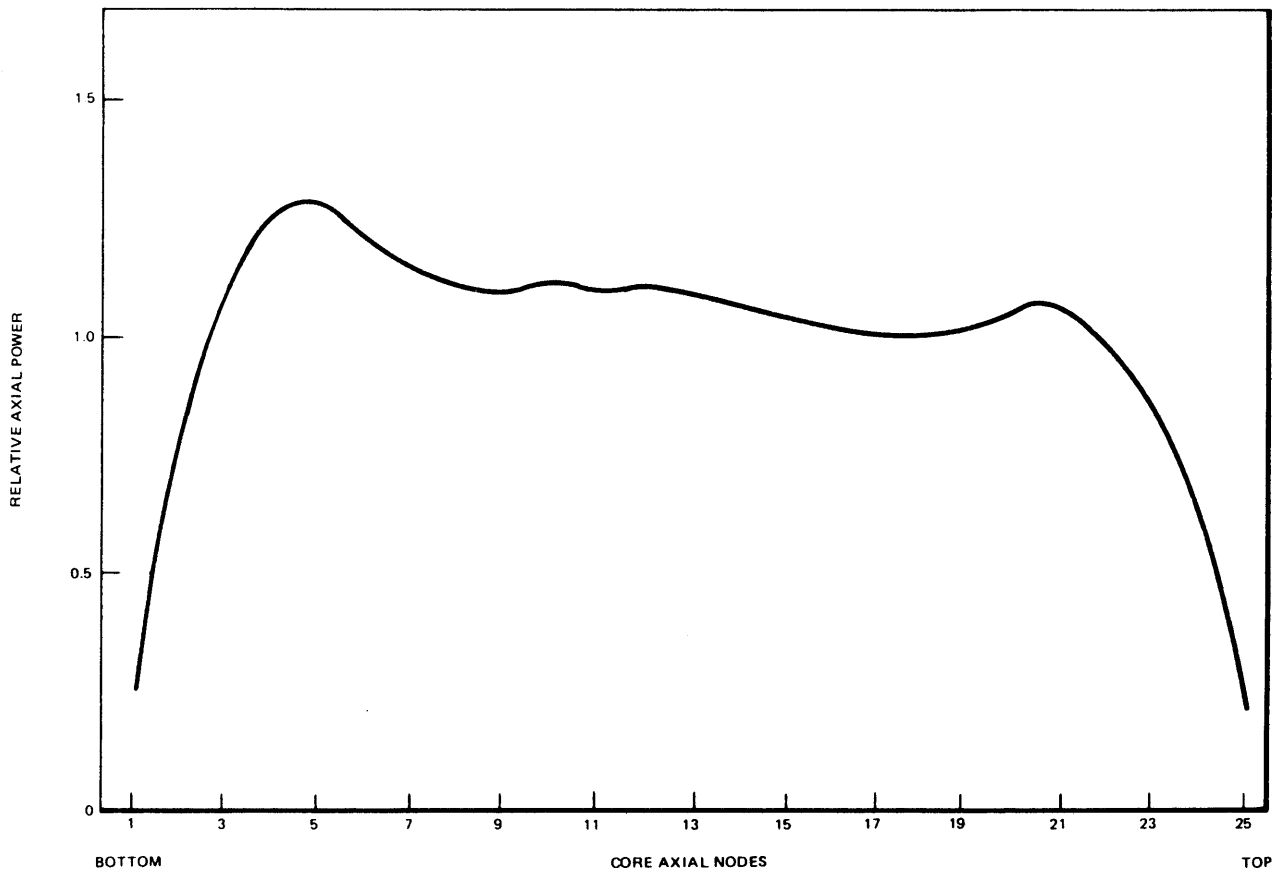

FIGURE 4A-7B

RELATIVE AXIAL POWER AT 5000 MWd/t CORE AVERAGE EXPOSURE

RIVER BEND STATION
UPDATED SAFETY ANALYSIS REPORT

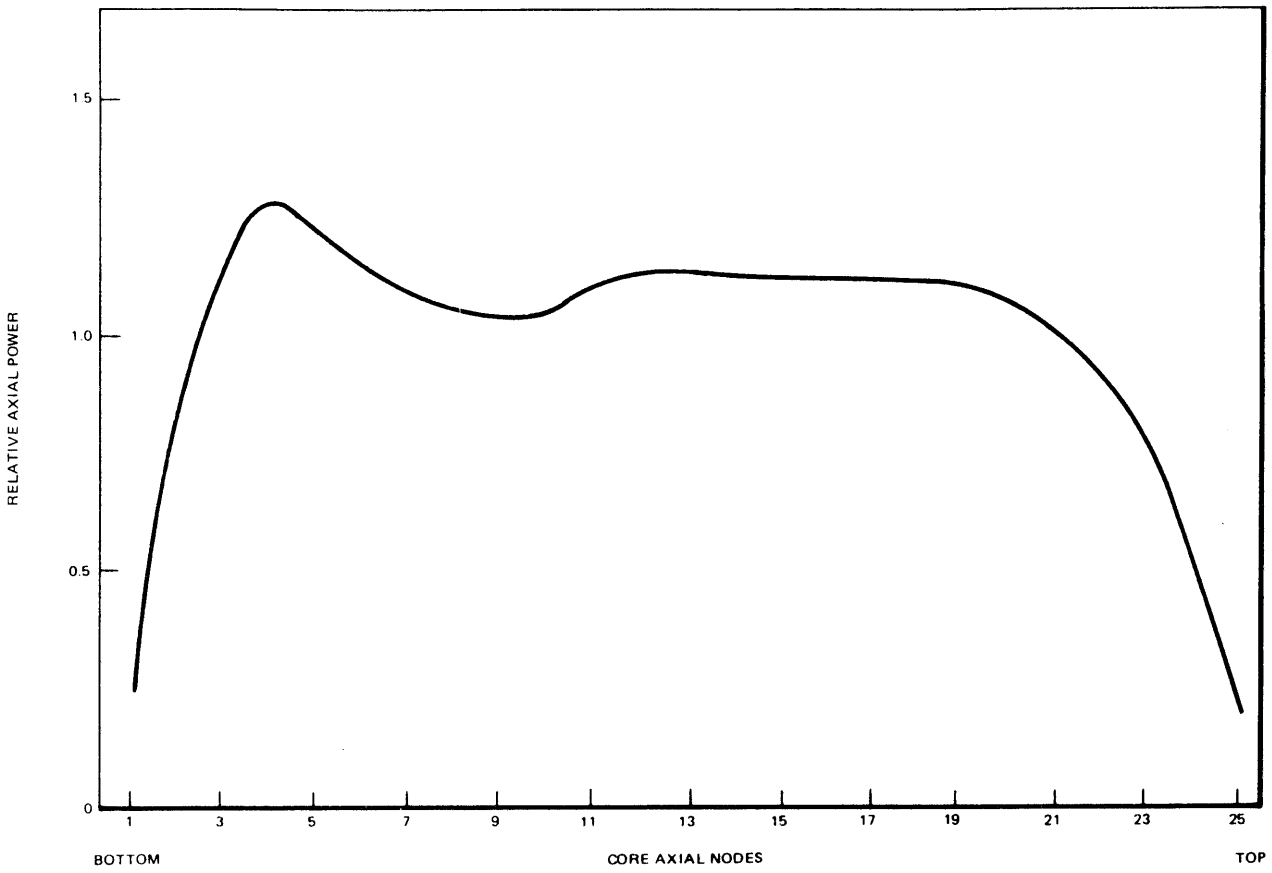

FIGURE 4A-7C

RELATIVE AXIAL EXPOSURE AT 5000 MWd/t CORE AVERAGE EXPOSURE

RIVER BEND STATION
UPDATED SAFETY ANALYSIS REPORT

I →	1	2	3	4	5	6	7	8	9	10	11	12	13	14	15
J															
1										0.2136	0.2852	0.3235	0.3444	0.3544	0.3578
2								0.2706	0.3677	0.4376	0.6882	0.7482	0.7812	0.7961	0.7991
3							0.3595	0.6714	0.7882	0.8593	0.9134	0.9546	0.9871	0.9983	0.9925
4						0.3926	0.7542	0.9108	0.9985	1.0306	1.0244	1.0441	1.0680	1.0923	1.0557
5					0.4031	0.7862	0.9691	1.0840	1.1351	1.1153	0.6533	0.8548	1.0872	1.1056	0.8048
6				0.3984	0.7900	0.9859	1.1176	1.1952	1.2185	1.1822	0.9006	0.8716	1.1553	1.1229	0.8360
7			0.3737	0.7704	0.9773	1.1164	1.1971	1.2410	1.2047	1.2141	1.1678	1.1906	1.2056	1.2261	1.1467
8		0.2911	0.7050	0.9419	1.1008	1.1827	1.1971	1.1942	1.2305	1.1989	1.2042	1.1831	1.2493	1.2613	1.1713
9		0.4021	0.8444	1.0575	1.1770	1.1966	0.9063	0.9451	1.1977	1.2205	0.9028	0.9269	1.1961	1.2172	0.9164
10	0.2434	0.4842	0.9455	1.1379	1.2311	1.2295	0.9496	0.9307	1.2407	1.2119	0.9386	0.9139	1.2305	1.2056	0.9280
11	0.3246	0.7690	1.0275	1.1918	1.2453	1.2536	1.2156	1.2475	1.2706	1.2945	1.2271	1.2427	1.2612	1.2786	1.2093
12	0.3674	0.8341	1.0720	1.2197	1.2658	1.2405	1.2444	1.2266	1.2996	1.2783	1.2554	1.2330	1.2892	1.2581	1.2078
13	0.3891	0.8631	1.0580	1.1930	1.2695	1.2641	0.9224	0.9473	1.2312	1.2562	0.9566	0.9784	1.2258	1.2357	0.9095
14	0.4021	0.8836	1.0775	1.2100	1.3076	1.2516	0.9488	0.9221	1.2521	1.2328	0.9792	0.9527	1.2444	1.2100	0.9062
15	0.4100	0.9007	1.1319	1.2696	1.3046	1.2903	1.2340	1.2252	1.2697	1.2711	1.2320	1.2271	1.2016	1.2506	1.1976

FIGURE 4A-7D

INTEGRATED POWER
PER BUNDLE, 5000 MWd/t

RIVER BEND STATION
UPDATED SAFETY ANALYSIS REPORT

I → 1	2	3	4	5	6	7	8	9	10	11	12	13	14	15
J														
1									1033.3	1398.7	1594.3	1696.6	1747.3	1768.0
2							1[illegible]	1778.1	2179.8	3530.0	3846.7	4002.4	4077.7	4107.8
3						1678.5	3[illegible]	3945.0	4407.5	4765.5	4991.0	5109.4	5165.4	5184.0
4					1801.7	3625.5	4[illegible]	5018.8	5393.1	5612.5	5743.1	5783.7	5799.9	5804.3
5				1826.7	3723.6	4646.0	5[illegible]	5696.9	5971.3	6122.6	6180.9	5893.8	5903.6	5903.4
6			1791.4	3712.8	4674.4	5339.5	5[illegible]	6083.5	6259.4	6324.5	6262.3	6036.9	5927.3	5941.0
7		1663.6	3601.9	4605.5	5305.6	5977.2	5862.2	6009.9	6131.5	5962.9	5983.1	5890.0	5854.7	5608.0
8	1259.7	3263.8	4430.1	5241.8	5778.2	5894.0	6017.2	6151.1	6103.0	5996.2	5887.5	5899.7	5776.6	5578.2
9	1754.2	3906.2	4974.3	5661.1	6100.1	6259.3	6393.9	6201.4	6185.5	5969.9	5953.7	5808.6	5863.6	5758.[illegible]
10 1014.0	2146.5	4350.8	5318.7	5887.1	6232.9	6365.0	6355.3	6214.3	6067.6	5919.6	5814.1	5848.0	5766.0	5707.7
11 1374.2	3479.7	4691.6	5497.2	5840.8	6068.9	5963.0	6016.3	5908.2	5840.1	5457.7	5464.3	5707.7	5724.6	5351.9
12 1568.7	3797.0	4917.6	5625.0	5866.5	5981.4	5921.7	5869.2	5867.4	5718.8	5453.6	5368.7	5705.9	5639.9	5521.1
13 1673.0	3960.1	5066.7	5717.7	5776.5	5936.1	5906.0	5948.1	5854.2	5831.2	5719.5	5725.5	5648.2	5677.6	5617.9
14 1725.4	4040.2	5132.0	5752.2	5818.1	5855.8	5887.4	5837.0	5857.0	5755.9	5739.0	5656.3	5665.6	5614.7	5622.2
15 1746.2	4069.4	5135.3	5738.0	5779.8	5824.6	5571.4	5565.1	5736.9	5678.8	5339.9	5301.3	5525.9	5536.1	5449.7

FIGURE 4A-7E

AVERAGE BUNDLE
EXPOSURE, 5000 MWd/t

RIVER BEND STATION

UPDATED SAFETY ANALYSIS REPORT

C(9/79)

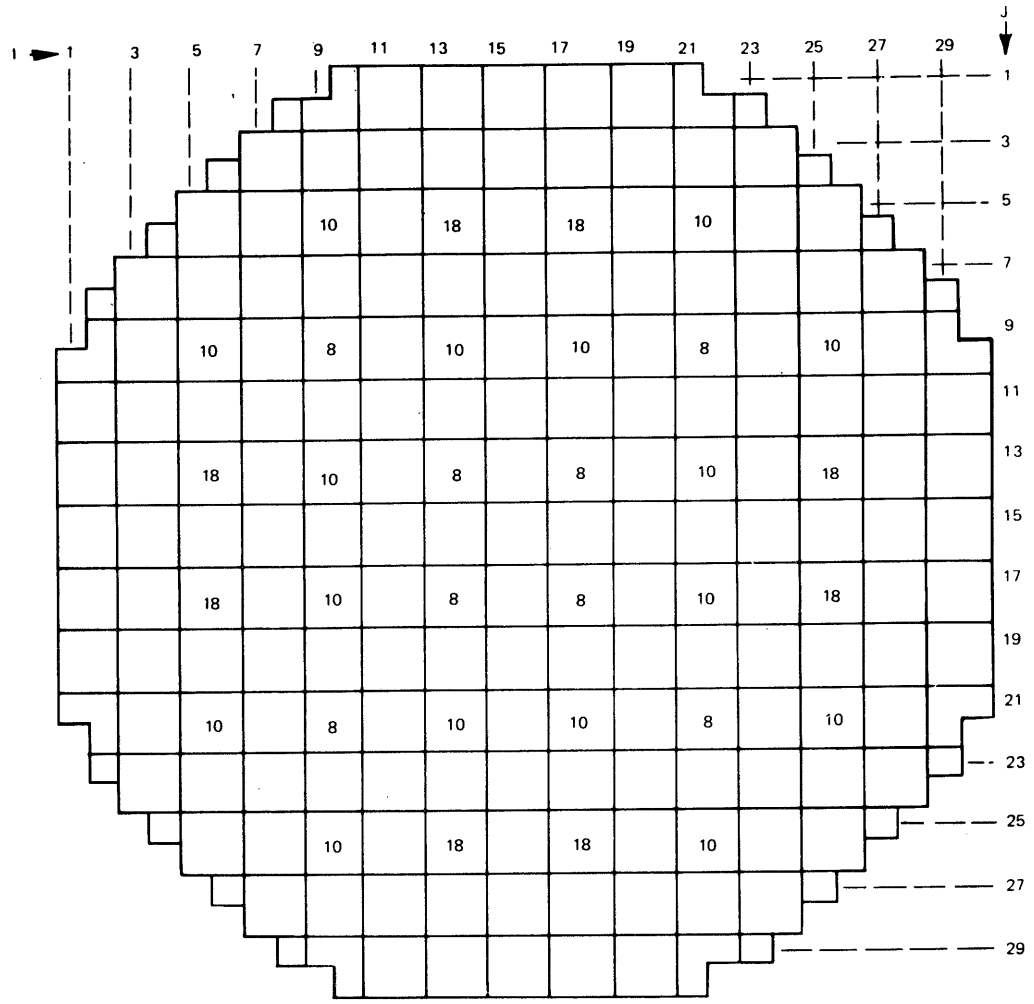

CONTROL ROD PATTERN (NOTCHES WITHDRAWN)

EXPOSURE	6000 MWd/t			
K_{eff}	0.9981			
ROD SEQUENCE	A-1			
POWER DISTRIBUTIONS		LOCATION		
		I	J	K
AXIAL	1.2749	–	–	4
RADIAL	1.3069	12	7	–
GROSS	1.7815	7	7	4
MCPR	1.3919	12	7	–
MLHGR	11.7399	7	7	4

I, J, K CODE COORDINATES
K = 1 = BOTTOM OF CORE
K = 25 = TOP OF CORE

FIGURE 4 A-8A

SUMMARY OF 6000 MWd/t CONDITION

RIVER BEND STATION
UPDATED SAFETY ANALYSIS REPORT

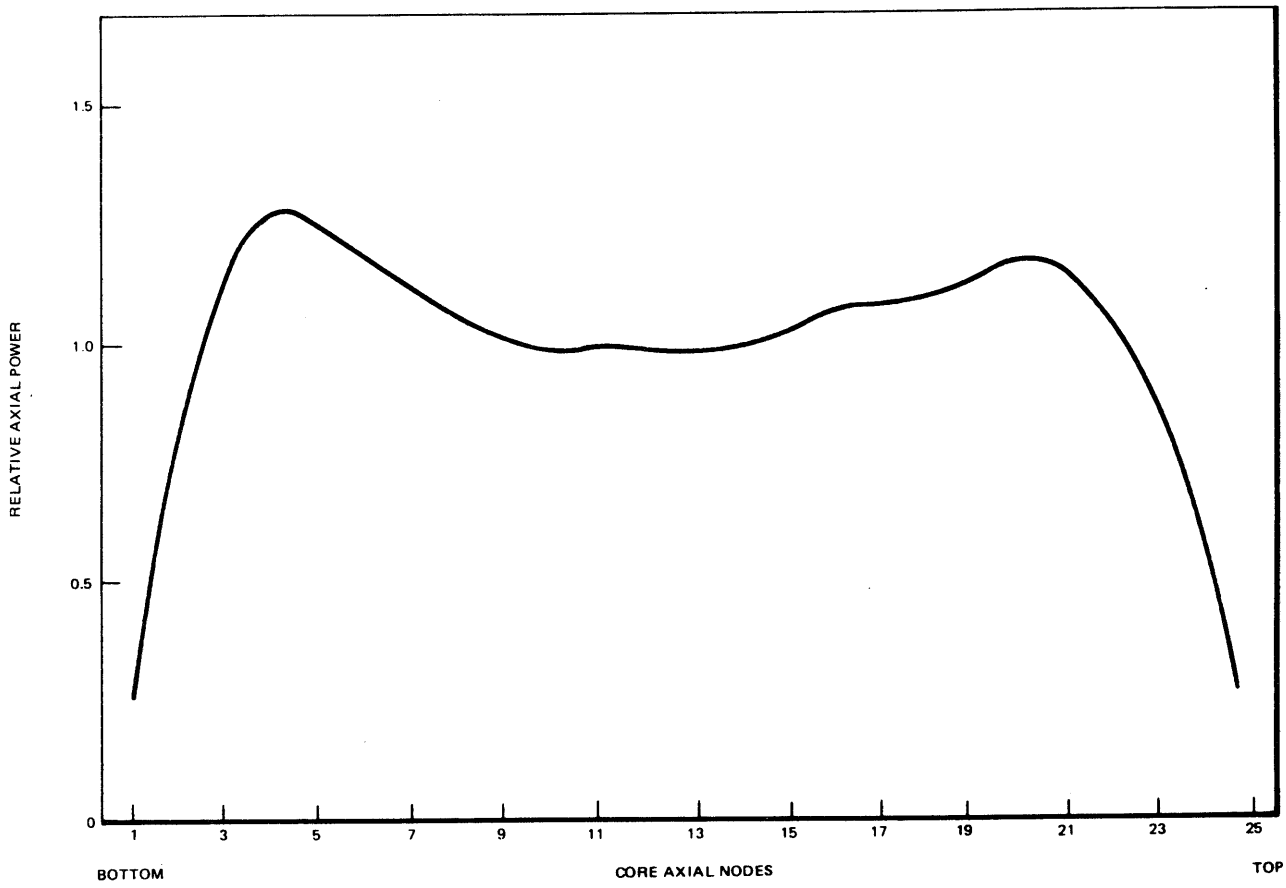

FIGURE 4A-8B

RELATIVE AXIAL POWER AT 6000 MWd/t CORE AVERAGE EXPOSURE

RIVER BEND STATION

UPDATED SAFETY ANALYSIS REPORT

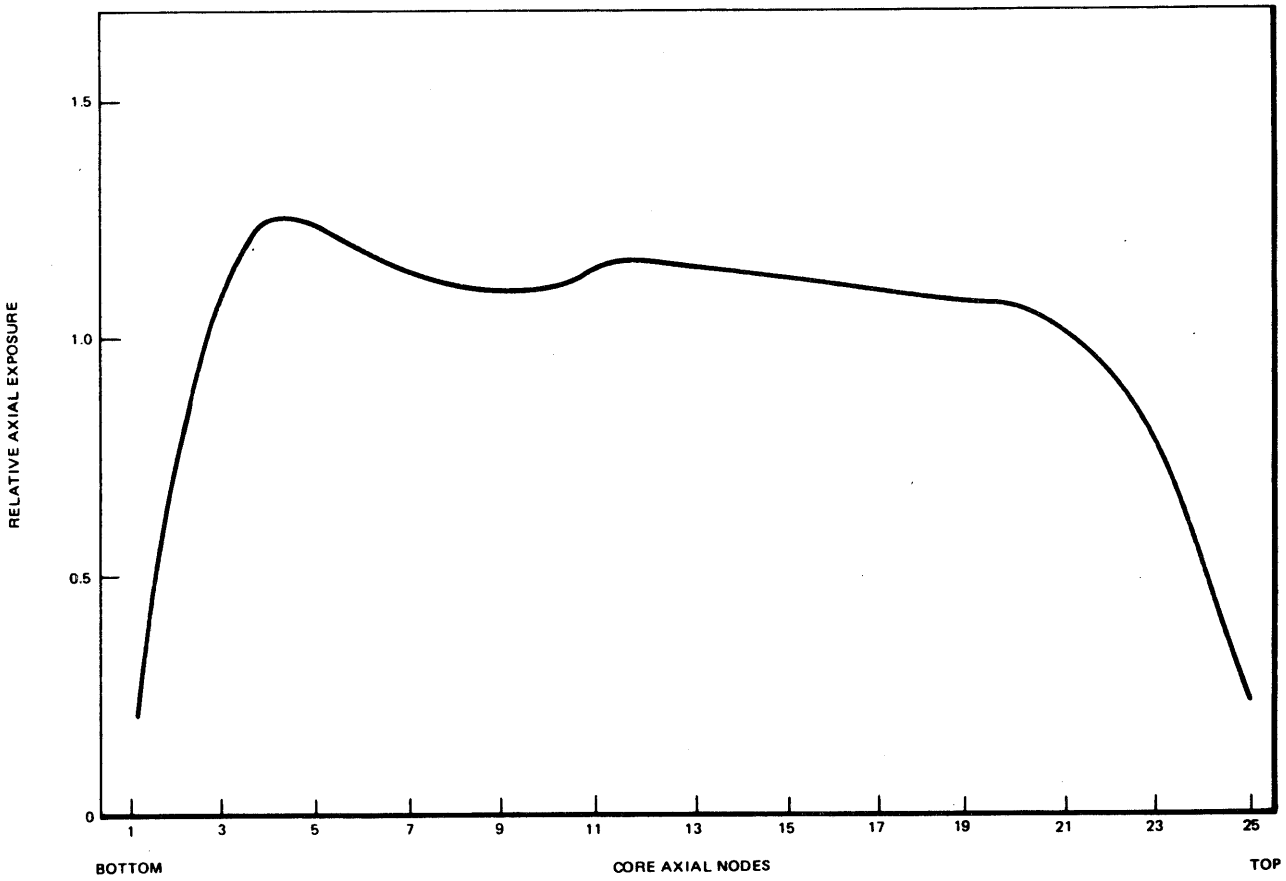

FIGURE 4A-8C

RELATIVE AXIAL EXPOSURE AT 6000 MWd/t CORE AVERAGE EXPOSURE

RIVER BEND STATION
UPDATED SAFETY ANALYSIS REPORT

I → 1	2	3	4	5	6	7	8	9	10	11	12	13	14	15
J														
1									0.2340	0.3195	0.3689	0.3970	0.4129	0.4204
2							0.2662	0.3690	0.4586	0.7529	0.8354	0.8808	0.9072	0.9208
3						0.3424	0.6492	0.7751	0.8847	0.9951	1.0664	1.1036	1.1294	1.1473
4					0.3718	0.7185	0.8571	0.9301	1.0168	1.1283	1.1858	1.1947	1.2171	1.2494
5				0.3820	0.7546	0.9177	0.9849	0.8100	0.8638	1.1759	1.2212	1.0224	1.0702	1.2265
6			0.3718	0.7547	0.9476	1.0656	1.0962	0.8782	0.9170	1.2221	1.2172	1.0843	1.0572	1.2440
7		0.3424	0.7185	0.9185	1.0670	1.1631	1.1927	1.1393	1.2112	1.2408	1.3069	1.2486	1.2913	1.2823
8	0.2661	0.6491	0.8575	0.9867	1.0982	1.1934	1.1787	1.1972	1.1803	1.2683	1.2672	1.2750	1.2367	1.2703
9	0.3688	0.7749	0.9305	0.8105	0.6767	1.1403	1.1972	0.8855	0.9342	1.2135	1.2622	0.9541	0.9854	1.2208
10	0.2338	0.4582	0.8843	1.0189	0.8636	0.9165	1.2105	1.1797	0.9333	0.9067	1.2528	1.2275	0.9821	0.9940	1.2103
11	0.3190	0.7520	0.9944	1.1277	1.1744	1.2198	1.2383	1.2856	1.2070	1.2515	1.2675	1.3024	1.2175	1.2455	1.2463
12	0.3681	0.8341	1.0650	1.1843	1.2183	1.2123	1.3039	1.2638	1.2592	1.2219	1.3015	1.2644	1.2433	1.1969	1.2336
13	0.3959	0.8791	1.1015	1.1924	1.0175	1.0800	1.2485	1.2716	0.9510	0.9900	1.2197	1.2426	0.9052	0.9264	1.1781
14	0.4116	0.9052	1.1268	1.2136	1.0650	1.0504	1.2861	1.2347	0.9811	0.9403	1.2426	1.1988	0.9257	0.8837	1.1643
15	0.4191	0.9188	1.1445	1.2442	1.2135	1.2307	1.2741	1.2629	1.2092	1.1998	1.2417	1.2307	1.1724	1.1597	1.1964

FIGURE 4A-8D

INTEGRATED POWER
PER BUNDLE, 6000 MWd/t

RIVER BEND STATION
UPDATED SAFETY ANALYSIS REPORT

I →	1	2	3	4	5	6	7	8	9	10	11	12	13	14	15
J										1246.5	1683.3	1917.2	2040.3	2101.0	2125.0
1								1545.5	2145.0	2616.5	4218.7	4595.6	4784.2	4874.5	4907.6
2							2037.3	3962.9	4733.9	5267.5	5679.7	5946.4	6097.4	6164.6	6177.2
3						2193.5	4360.4	5373.6	6018.1	6424.8	6637.7	6768.0	6872.5	6893.1	6860.9
4					2229.0	4510.5	5615.9	6375.3	6832.9	7087.6	6976.7	7016.4	6980.3	7010.1	6707.6
5				2189.0	4503.5	5661.1	6458.1	7001.2	7303.1	7442.6	7226.1	7133.3	7193.2	7049.4	6776.4
6			2036.5	4372.9	5563.6	6423.2	6775.3	7104.2	7213.8	7346.7	7149.8	7174.7	7094.8	7077.9	6755.8
7		1550.3	3969.5	5372.8	6343.6	6961.9	7097.2	7210.5	7332.6	7301.1	7201.4	7069.7	7150.0	6997.0	6748.6
8		2155.5	4751.3	6032.6	6839.1	7297.7	7165.0	7339.8	7398.3	7407.0	6871.9	6861.4	7063.9	7081.8	6676.6
9	1256.9	2633.7	5297.1	6457.6	7121.3	7463.4	7315.5	7285.3	7456.0	7278.6	6859.0	6727.3	7079.5	6970.8	6635.1
10	1696.1	4249.3	5720.0	6690.0	7087.2	7323.6	7177.8	7264.9	7177.9	7135.7	6683.9	6708.1	6966.6	7004.3	6566.3
11	1935.3	4631.8	5990.5	6845.7	7133.4	7221.1	7167.1	7094.9	7168.1	6998.1	6710.0	6660.8	6996.2	6897.1	6528.0
12	2061.3	4823.9	6125.6	6911.7	7045.1	7201.3	6827.8	6896.2	7084.5	7090.5	6675.4	6704.7	6873.1	6914.4	6526.7
13	2126.7	4924.6	6210.5	6963.2	7126.8	7106.5	6837.0	6758.5	7110.1	6987.8	6719.1	6666.4	6911.0	6823.6	6527.8
14	2155.4	4970.8	6268.2	7008.7	7083.5	7114.0	6804.5	6789.4	7005.7	6949.0	6571.0	6527.5	6786.6	6785.8	6646.4
15															

FIGURE 4A-8E

AVERAGE BUNDLE
EXPOSURE, 6000 MWd/t

RIVER BEND STATION
UPDATED SAFETY ANALYSIS REPORT

C(9/79)

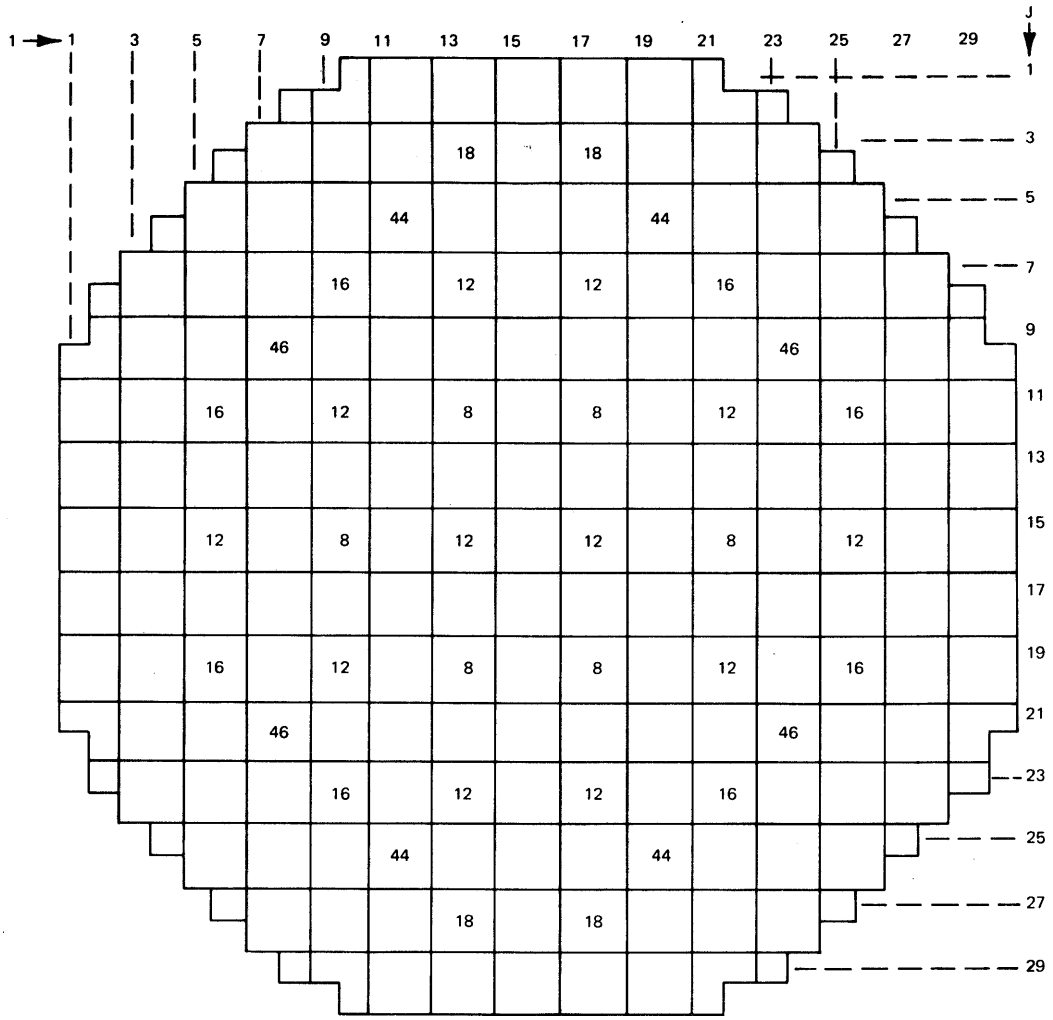

CONTROL ROD PATTERN (NOTCHES WITHDRAWN)

EXPOSURE	7000 MWd/t			
K_{eff}	0.9981			
ROD SEQUENCE	B-2			
POWER DISTRIBUTIONS		LOCATION		
		I	J	K
AXIAL	1.2220	–	–	19
RADIAL	1.3174	7	8	–
GROSS	1.8384	6	8	4
MCPR	1.3779	7	8	–
MLHGR	12.1453	6	8	4

I, J, K CODE COORDINATES
K = 1 = BOTTOM OF CORE
K = 25 = TOP OF CORE

FIGURE 4 A-9A

SUMMARY OF 7000 MWd/t CONDITION

RIVER BEND STATION
UPDATED SAFETY ANALYSIS REPORT

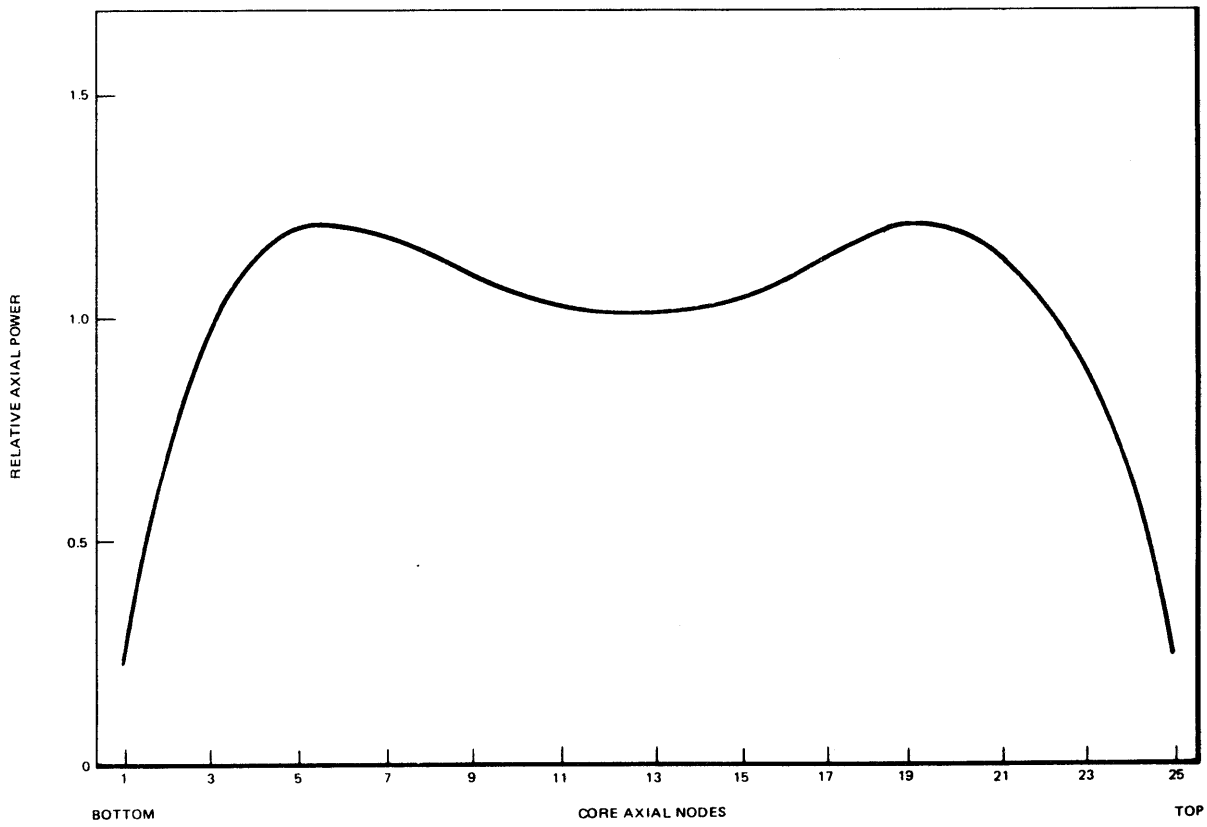

FIGURE 4A-9B

RELATIVE AXIAL POWER AT 7000 MWd/t CORE AVERAGE EXPOSURE

RIVER BEND STATION
UPDATED SAFETY ANALYSIS REPORT

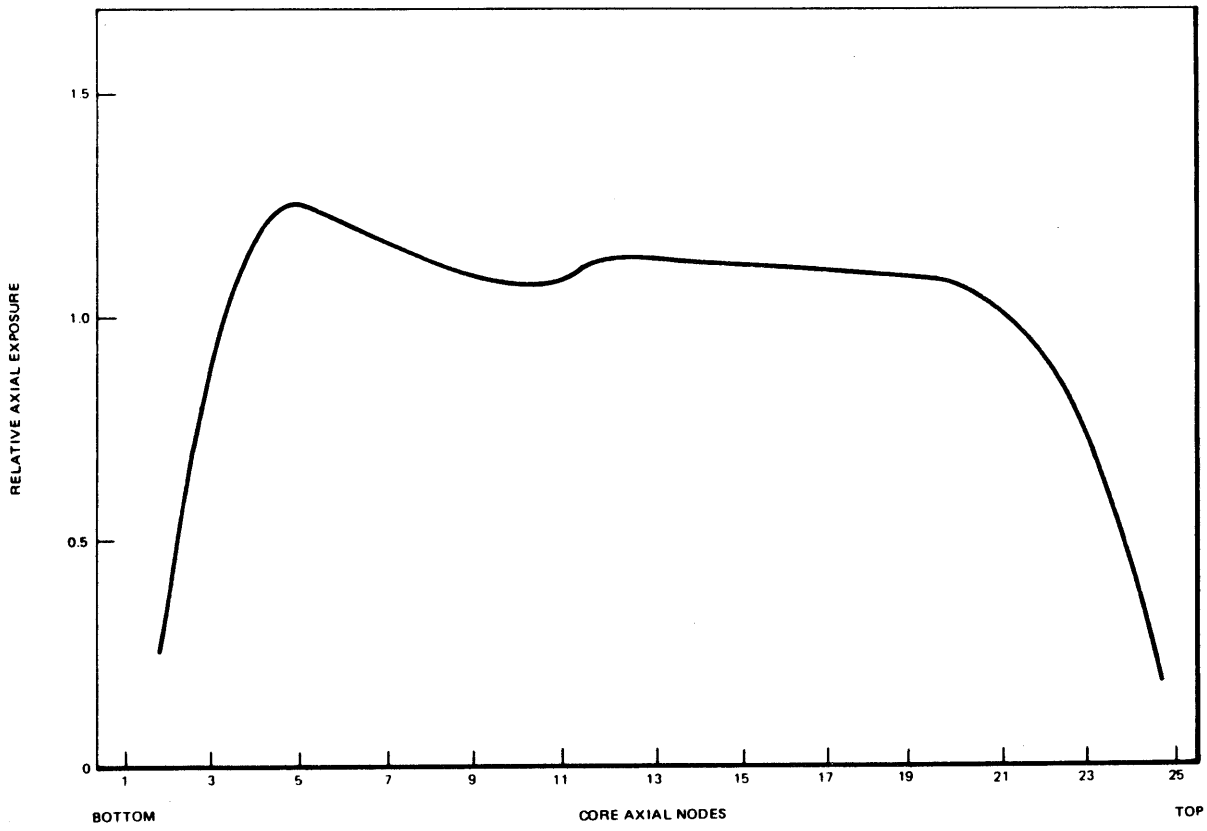

FIGURE 4A-9C

RELATIVE AXIAL EXPOSURE AT 7000 MWd/t CORE AVERAGE EXPOSURE

RIVER BEND STATION
UPDATED SAFETY ANALYSIS REPORT

I → 1	2	3	4	5	6	7	8	9	10	11	12	13	14	15
J														
1									0.2511	0.3230	0.3486	0.3516	0.3547	0.3618
2							0.3167	0.4228	0.4984	0.7722	0.8057	0.7917	0.7956	0.8200
3						0.4080	0.7604	0.9965	0.9822	1.0344	1.0246	0.8007	0.8072	1.0107
4					0.4380	0.8395	1.0145	1.1189	1.1772	1.1973	1.1660	0.9786	0.9737	1.1202
5				0.4463	0.8678	1.0012	1.1763	1.2408	1.2755	1.2769	1.2470	1.1537	1.1832	1.1491
6			0.4392	0.8687	1.0767	1.2006	1.2556	1.2624	1.2781	1.2864	1.2088	1.2067	1.1389	1.1522
7		0.4061	0.8356	1.0657	1.2091	1.2861	1.2707	1.2094	1.0561	1.2051	1.2305	0.9302	0.9520	1.1186
8	0.3134	0.7544	1.0108	1.1827	1.2821	1.3173	1.2347	1.0567	1.0098	1.2509	1.1806	0.9671	0.9087	1.1142
9	0.4181	0.8846	1.1042	1.2358	1.3063	1.2745	1.3097	1.2176	1.2577	1.2334	1.2619	1.1562	1.1776	1.1489
10	0.4953	0.9648	1.1359	1.2194	1.2718	1.3037	1.2408	1.2491	1.1931	1.2675	1.2029	1.1639	1.1166	1.1349
11	0.5316	0.7798	1.0239	1.1343	0.9970	1.0281	1.1959	1.2366	0.9430	0.9774	1.1681	1.1919	0.8506	0.8695	1.0837
12	0.3715	0.8433	1.0617	1.1445	0.9856	0.9657	1.2228	1.1683	0.9673	0.9230	1.1965	1.1356	0.8779	0.8246	1.0739
13	0.3917	0.8757	1.0866	1.1709	1.1292	1.1931	1.1899	1.2335	1.1452	1.1847	1.1739	1.2063	1.1094	1.1325	1.1139
14	0.4068	0.8868	1.0922	1.1607	1.1569	1.1196	1.2094	1.1592	1.1002	1.1127	1.1959	1.1476	1.1442	1.0862	1.1081
15	0.4035	0.8907	1.0835	1.1270	0.8630	0.8664	1.0983	1.0896	0.8209	0.8184	1.0897	1.0908	0.8616	0.8514	1.0626

FIGURE 4A-9D

INTEGRATED POWER
PER BUNDLE, 7000 MWd/t

RIVER BEND STATION
UPDATED SAFETY ANALYSIS REPORT

I →	1	2	3	4	5	6	7	8	9	10	11	12	13	14	15
J															
1										1480.0	2002.2	2285.3	2436.5	2513.0	2544.6
2								1811.2	2513.3	3074.2	4972.3	5431.7	5665.7	5782.4	5829.2
3							2379.0	4612.7	5509.6	6152.9	6675.7	7013.7	7201.9	7294.9	7325.4
4						2554.5	5099.4	6231.4	6949.0	7444.4	7767.0	7974.8	8068.3	8111.2	8111.4
5					2610.2	5255.8	6534.4	7361.0	7843.7	7952.1	8153.6	8236.6	8001.9	8081.2	7933.2
6				2560.0	5258.8	6609.5	7524.6	8098.3	8182.0	8360.4	8449.2	8349.6	8278.4	8105.8	8019.5
7			2375.2	5092.1	6502.9	7491.1	7939.3	8296.0	8352.2	8558.9	8389.7	8482.7	8342.5	8370.3	8037.2
8		1815.8	4619.1	6231.0	7331.1	8001.0	8285.5	8368.3	8580.8	8460.5	8490.8	8330.1	8420.1	8232.9	8018.1
9		2523.5	5526.8	6963.9	7650.3	8177.1	8504.5	8538.0	8263.2	8341.9	8084.8	8144.7	8017.3	8066.1	7896.5
10	1490.2	3091.0	6162.1	7477.4	7985.5	8360.7	8527.0	8404.1	8390.1	8186.6	8112.9	7953.8	8062.5	7914.1	7844.5
11	2016.5	5002.0	6715.2	7818.6	8262.6	8544.4	8415.1	8551.6	8384.0	8388.2	7950.5	8011.5	8184.6	8250.8	7805.7
12	2302.7	5406.7	7056.4	8031.0	8352.8	8432.5	8472.1	8357.8	8429.4	8217.1	8012.7	7864.2	8240.5	8095.1	7760.7
13	2450.4	5703.7	7228.0	8105.0	8061.9	8252.2	8075.4	8168.9	8034.7	8071.3	7894.5	7946.5	7777.6	7841.5	7703.9
14	2537.4	5830.5	7339.2	8177.8	8192.7	8156.1	8124.1	7992.2	8092.0	7927.4	7952.8	7806.3	7837.5	7706.9	7691.3
15	2573.6	5890.4	7413.7	8254.0	8290.1	8343.8	8077.9	8051.8	8214.0	8148.0	7811.7	7757.3	7958.2	7944.7	7844.0

FIGURE 4A-9E

AVERAGE BUNDLE
EXPOSURE, 7000 MWd/t

RIVER BEND STATION

UPDATED SAFETY ANALYSIS REPORT

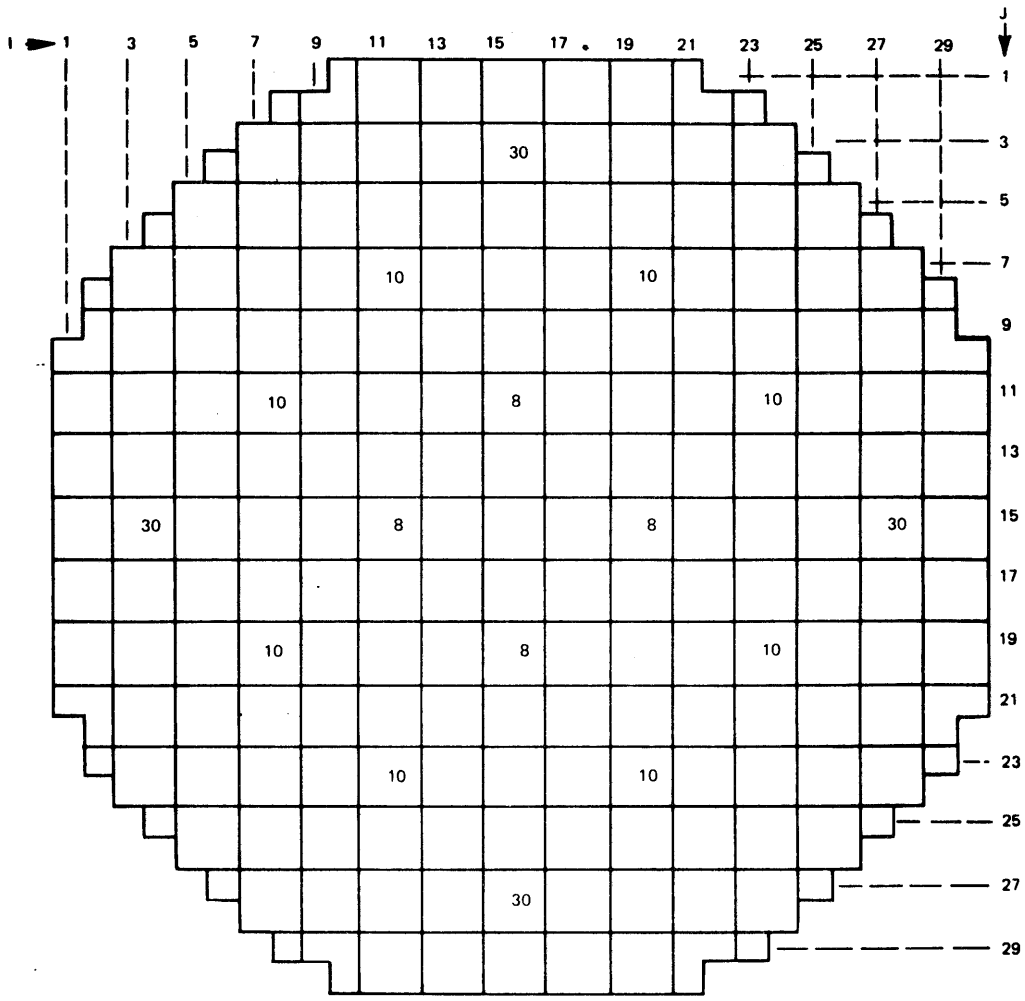

CONTROL ROD PATTERN (NOTCHES WITHDRAWN)

EXPOSURE	8000 MWd/t			
K_{eff}	1.0028			
ROD SEQUENCE	A-2			
POWER DISTRIBUTIONS		LOCATION		
		I	J	K
AXIAL	1.3890	–	–	7
RADIAL	1.2789	12	11	–
GROSS	1.8360	11	12	6
MCPR	1.4166	12	11	–
MLHGR	12.1033	11	12	6

I, J, K CODE COORDINATES
K = 1 = BOTTOM OF CORE
K = 25 = TOP OF CORE

FIGURE 4 A-10A

SUMMARY OF 8000 MWd/t CONDITION

RIVER BEND STATION
UPDATED SAFETY ANALYSIS REPORT

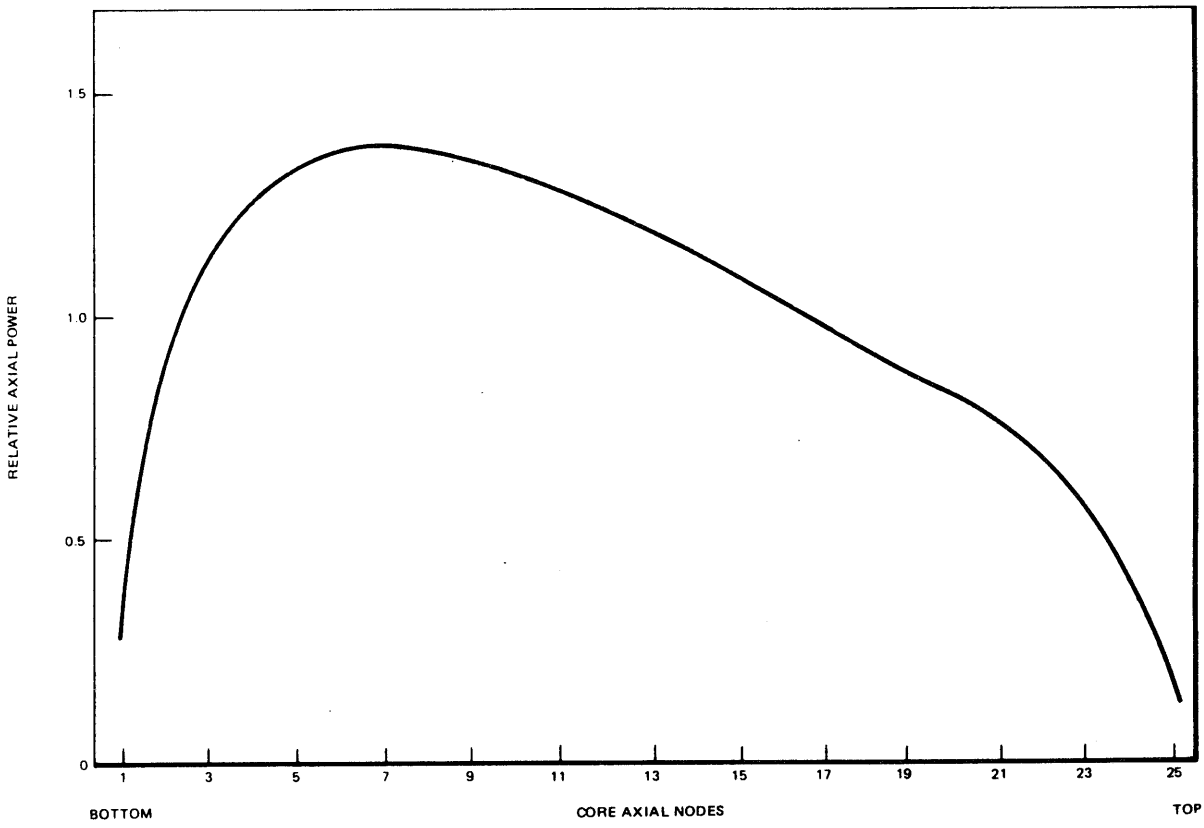

FIGURE 4A-10B

RELATIVE AXIAL POWER AT 8000 MWd/t CORE AVERAGE EXPOSURE

RIVER BEND STATION

UPDATED SAFETY ANALYSIS REPORT

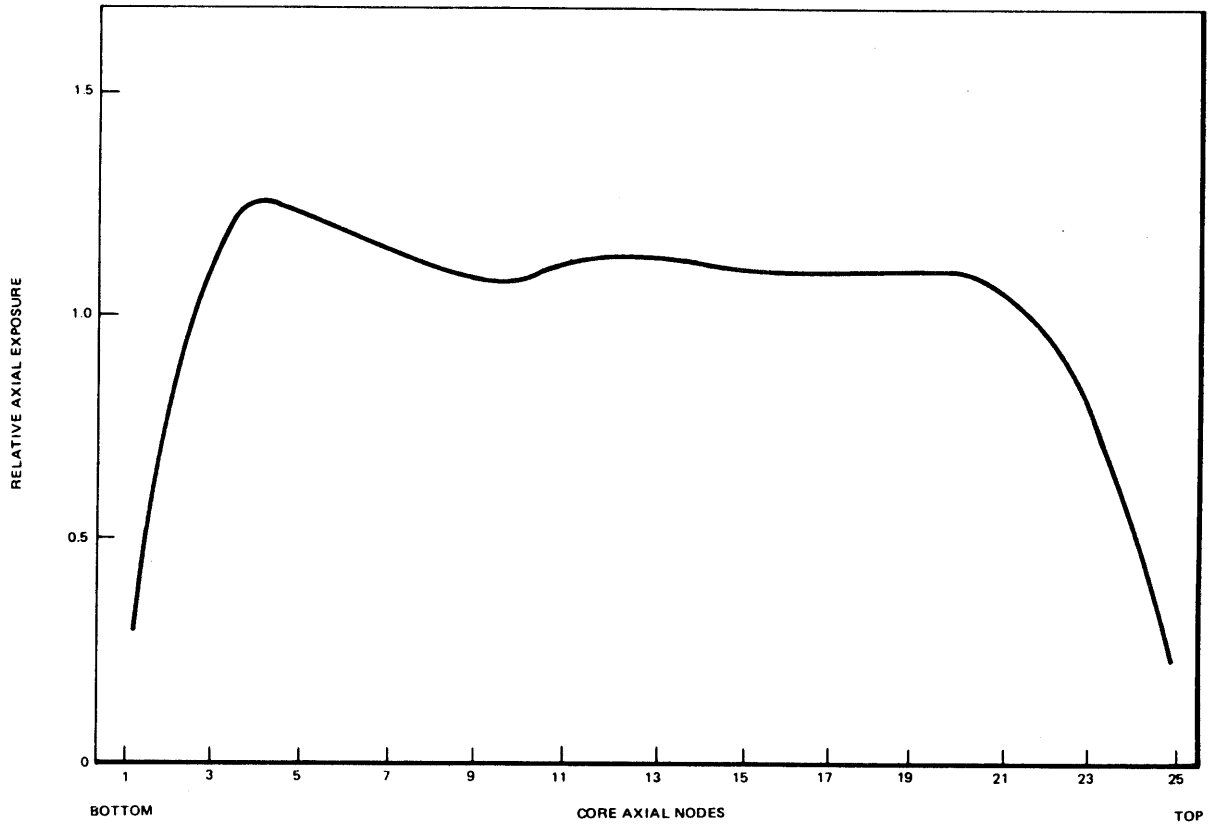

FIGURE 4A-10C

RELATIVE AXIAL EXPOSURE AT
8000 MWd/t CORE AVERAGE EXPOSURE

RIVER BEND STATION
UPDATED SAFETY ANALYSIS REPORT

I → 1	1	2	3	4	5	6	7	8	9	10	11	12	13	14	15
J															
1										0.2451	0.3225	0.3609	0.3778	0.3812	0.3779
2								0.2959	0.3991	0.4797	0.7691	0.8336	0.8592	0.8599	0.8446
3							0.3780	0.7184	0.8528	0.9413	1.0116	1.0514	1.0674	1.0550	0.9628
4						0.4041	0.7894	0.9531	1.0498	1.1070	1.1426	1.1631	1.1717	1.1596	1.0568
5					0.4106	0.8129	0.9911	1.0988	1.1618	1.1887	1.1932	1.1963	1.1579	1.2125	1.1398
6				0.4042	0.8130	1.0011	1.1166	1.1810	1.2086	1.2008	1.1568	1.1026	1.2018	1.1731	1.1675
7			0.3779	0.7844	0.9915	1.1169	1.1907	1.2191	1.1642	1.1661	0.8252	0.8652	1.1191	1.2268	1.1797
8		0.2956	0.7180	0.9532	1.0989	1.1603	1.2174	1.1747	1.2230	1.1196	0.8712	0.8321	1.1752	1.1751	1.1751
9		0.3987	0.8523	1.0495	1.1612	1.2064	1.1579	1.2180	1.1789	1.2209	1.1348	1.1866	1.1732	1.2321	1.1599
10	0.2445	0.4769	0.9404	1.1066	1.1886	1.1994	1.1605	1.1134	1.2190	1.1961	1.2552	1.2035	1.2492	1.1612	1.0968
11	0.3214	0.7675	1.0098	1.1418	1.1959	1.1590	0.8235	0.8692	1.1330	1.2545	1.2268	1.2788	1.1991	1.1705	0.7929
12	0.3593	0.8311	1.0472	1.1660	1.1975	1.1048	0.8038	0.8305	1.1851	1.2025	1.2782	1.2243	1.2476	1.1171	0.7884
13	0.3757	0.8555	1.0590	1.1735	1.1541	1.1999	1.1175	1.1735	1.1716	1.2477	1.1976	1.2466	1.1895	1.2054	1.0903
14	0.3788	0.8556	1.0456	1.1500	1.2065	1.1693	1.2243	1.1732	1.2305	1.1597	1.1689	1.1157	1.2030	1.1569	1.1391
15	0.3754	0.8402	0.9561	1.0500	1.1337	1.1633	1.1767	1.1730	1.1586	1.0958	0.7919	0.7877	1.0698	1.1390	1.1469

FIGURE 4A-10D

INTEGRATED POWER
PER BUNDLE, 8000 MWd/t

RIVER BEND STATION
UPDATED SAFETY ANALYSIS REPORT

I →	1	2	3	4	5	6	7	8	9	10	11	12	13	14	15
J										1730.6	2324.5	2633.2	2787.3	2867.0	2905.6
1								2127.2	2935.2	3571.6	5745.1	6230.1	6456.1	6576.7	6649.8
2							2786.2	5373.7	6400.6	7136.0	7711.0	8039.2	8069.4	8162.8	8337.0
3						3001.6	5939.7	7240.7	8058.9	8622.6	8965.3	9141.8	9047.6	9085.7	9238.5
4					3055.7	6134.3	7590.5	8538.3	8885.4	9228.7	9431.0	9486.6	9154.7	9265.4	9081.4
5				2997.3	6128.2	7667.1	8726.2	9354.9	9445.4	9639.6	9736.6	9557.5	9486.1	9243.9	9170.9
6			2783.5	5931.4	7569.5	8701.2	9220.5	9569.7	9360.9	9615.9	9593.9	9714.2	9272.1	9323.1	9155.0
7		2126.7	5374.2	7242.7	8514.8	9344.1	9605.0	9622.2	9636.3	9489.6	9742.8	9516.0	9394.0	9140.9	9131.4
8		2940.7	6412.1	8069.1	8867.1	9464.4	9578.1	9848.8	9499.9	9600.7	9317.1	9407.7	9172.6	9240.7	9044.5
9	1742.5	3585.3	7147.7	8617.2	9206.0	9653.6	9831.8	9704.0	9640.3	9378.8	9381.4	9155.8	9247.4	9029.9	8976.5
10	2347.4	5782.4	7739.9	8953.6	9260.4	9573.3	9610.2	9789.2	9326.3	9366.5	9117.6	9204.5	9034.6	9121.1	8888.6
11	2673.4	6310.7	8118.9	9176.5	9339.4	9397.5	9695.9	9525.3	9396.5	9139.5	9210.2	8999.0	9119.1	8917.1	8833.8
12	2847.4	6580.1	8315.5	9276.9	9190.3	9476.3	9264.4	9403.5	9179.0	9257.0	9067.3	9155.6	8866.2	8975.0	8817.0
13	2937.4	6720.1	8431.4	9345.4	9350.6	9274.9	9334.6	9150.6	9253.2	9039.3	9159.7	8953.1	8982.6	8792.3	8798.5
14	2976.3	6781.9	8498.0	9381.9	9159.1	9209.7	9175.2	9140.2	9034.3	8965.8	8900.7	8847.3	8819.2	8795.5	8905.9
15															

FIGURE 4A-10E

AVERAGE BUNDLE
EXPOSURE, 8000 MWd/t

RIVER BEND STATION
UPDATED SAFETY ANALYSIS REPORT

C(9/79)

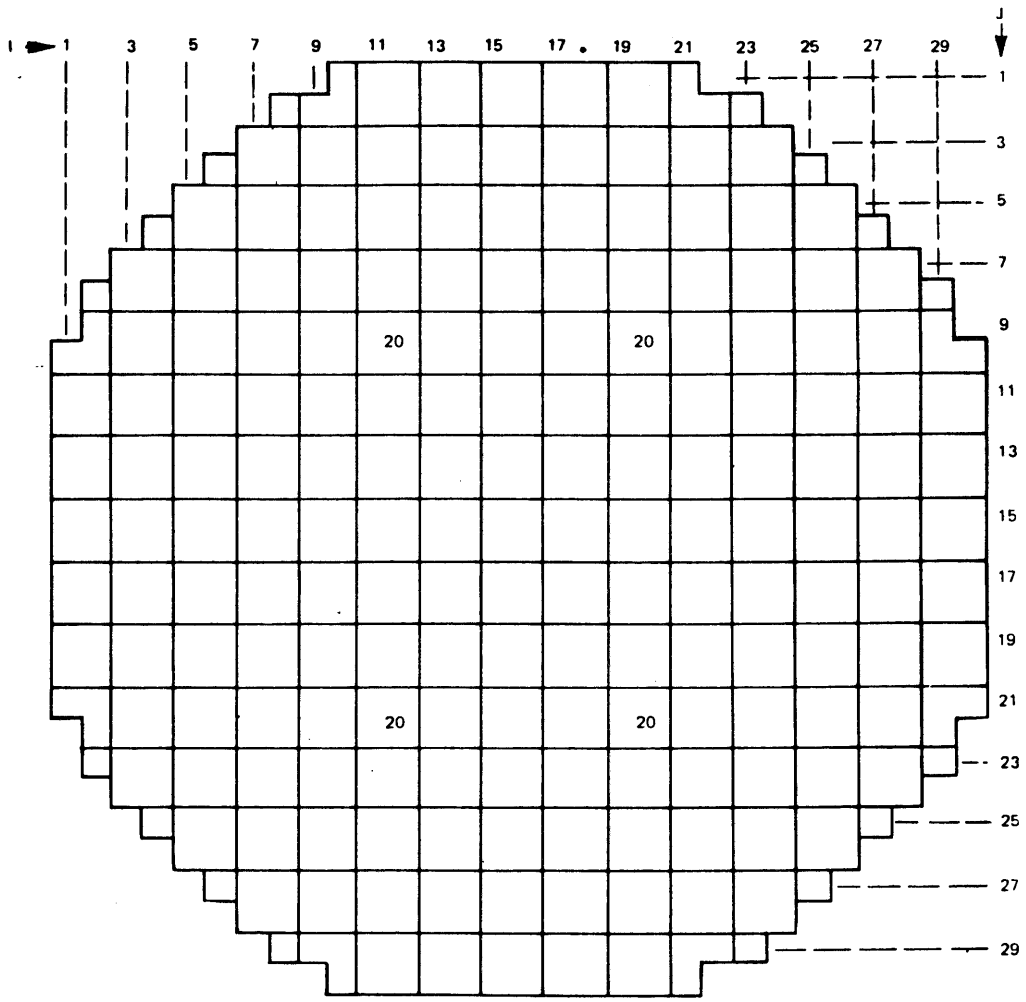

CONTROL ROD PATTERN (NOTCHES WITHDRAWN)

EXPOSURE	9000 MWd/t			
K_{eff}	1.0062			
ROD SEQUENCE	B-1			
POWER DISTRIBUTIONS		LOCATION		
		I	J	K
AXIAL	1.3943	–	–	8
RADIAL	1.2760	13	14	–
GROSS	1.7894	13	14	9
MCPR	1.4121	13	14	–
MLHGR	11.7324	11	14	8

I, J, K CODE COORDINATES
K = 1 = BOTTOM OF CORE
K = 25 = TOP OF CORE

FIGURE 4.A-11A

SUMMARY OF 9000 MWd/t CONDITION

RIVER BEND STATION
UPDATED SAFETY ANALYSIS REPORT

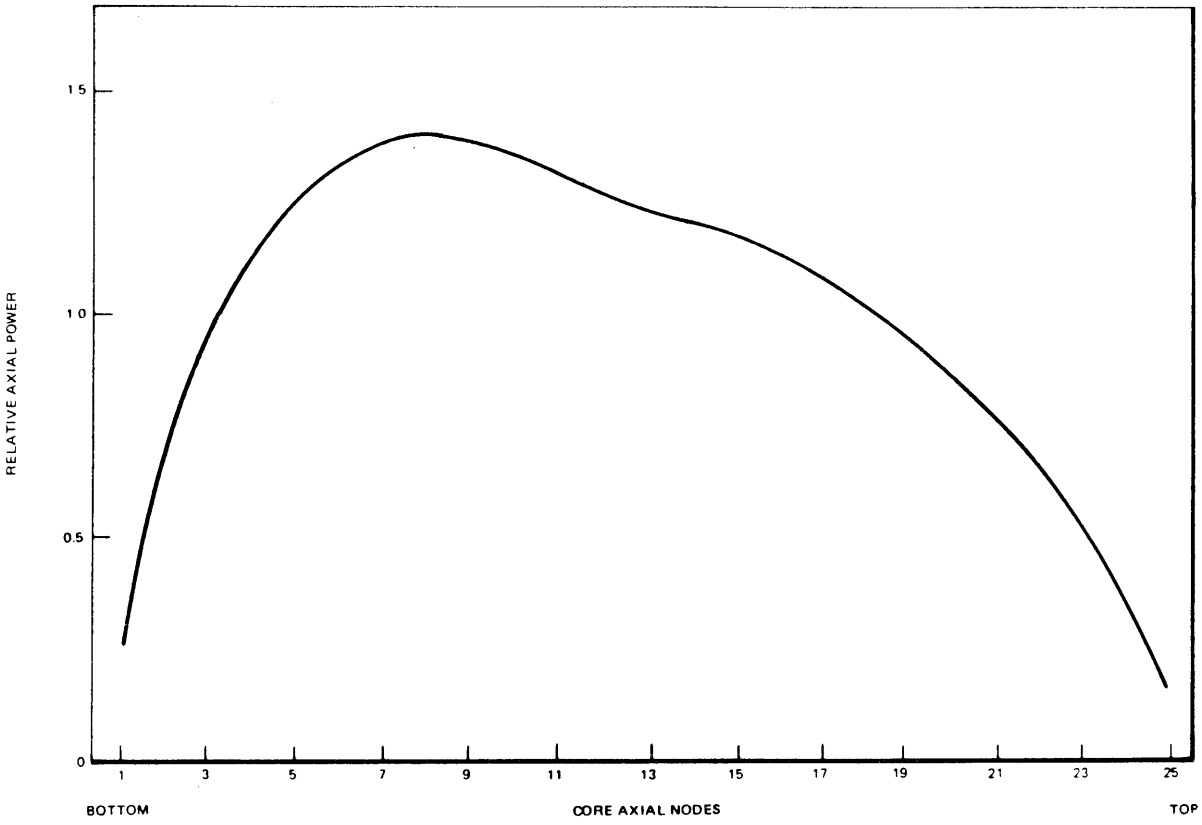

FIGURE 4A-11B

RELATIVE AXIAL POWER AT 9000 MWd/t CORE AVERAGE EXPOSURE

RIVER BEND STATION

UPDATED SAFETY ANALYSIS REPORT

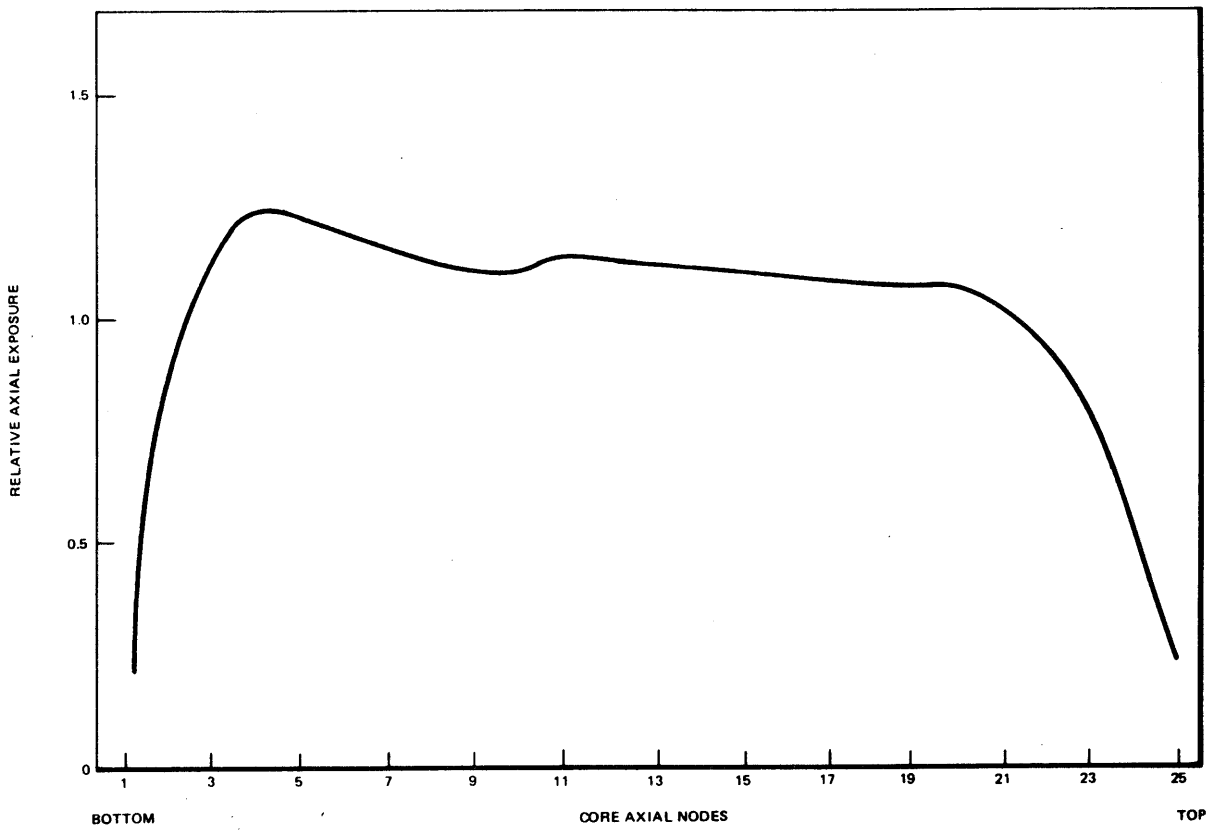

FIGURE 4A-11C

RELATIVE AXIAL EXPOSURE AT 9000 MWd/t CORE AVERAGE EXPOSURE

RIVER BEND STATION
UPDATED SAFETY ANALYSIS REPORT

I →	1	2	3	4	5	6	7	8	9	10	11	12	13	14	15
J															
1										0.2267	0.3006	0.3395	0.3595	0.3692	0.3730
2								0.2727	0.3699	0.4462	0.7303	0.7933	0.8240	0.8385	0.8437
3							0.3503	0.6781	0.8024	0.8636	0.9506	0.9907	1.0142	1.0252	1.0270
4						0.3732	0.7425	0.8922	0.9828	1.0401	1.0782	1.0997	1.1118	1.1190	1.1143
5					0.3791	0.7622	0.9245	1.0256	1.0912	1.1299	1.1495	1.1535	1.1632	1.1555	1.0914
6				0.3747	0.7635	0.9333	1.0400	1.1048	1.1458	1.1704	1.1744	1.1192	1.1749	1.1164	1.1013
7			0.3526	0.7461	0.9278	1.0422	1.1127	1.1467	1.1137	1.1764	1.1216	1.1759	1.1302	1.1027	1.1152
8		0.2751	0.6825	0.8975	1.0316	1.1105	1.1508	1.1139	1.1744	1.1123	1.1424	1.0935	1.1740	1.1317	1.1214
9		0.3732	0.8084	0.9906	1.1015	1.1580	1.1247	1.1854	1.1287	1.1471	0.9250	0.9726	1.1040	1.1905	1.1354
10	0.2259	0.4501	0.8910	1.0512	1.1468	1.1936	1.2060	1.1536	1.2005	1.1110	0.9825	0.9400	1.1709	1.1515	1.1503
11	0.3030	0.7357	0.9586	1.0919	1.1745	1.2110	1.1730	1.2344	1.1760	1.2141	1.1343	1.1896	1.1663	1.2350	1.1791
12	0.3415	0.7974	0.9971	1.1168	1.1798	1.1582	1.2373	1.1943	1.2534	1.1956	1.2454	1.1931	1.2559	1.2006	1.1932
13	0.3607	0.8202	1.0103	1.1197	1.1232	1.2101	1.1617	1.2528	1.2075	1.2681	1.2154	1.2730	1.2197	1.2063	1.1978
14	0.3699	0.8394	1.0255	1.1244	1.1729	1.1450	1.2265	1.1877	1.2588	1.2113	1.2759	1.2206	1.2760	1.2071	1.1918
15	0.3735	0.8444	1.0286	1.1269	1.1066	1.1271	1.1518	1.1677	1.1869	1.1975	1.2137	1.2139	1.2078	1.1950	1.1835

FIGURE 4A-11D

INTEGRATED POWER
PER BUNDLE, 9000 MWd/t

RIVER BEND STATION
UPDATED SAFETY ANALYSIS REPORT

I → / J	1	2	3	4	5	6	7	8	9	10	11	12	13	14	15
1										1975.2	2646.3	2993.3	3164.3	3247.5	3282.8
2								2422.5	3333.6	4050.3	6514.9	7072.3	7318.0	7439.3	7495.1
3							3163.4	6092.8	7260.4	8078.1	8723.5	9091.5	9137.7	9218.7	9300.5
4						3404.9	6729.7	8200.6	9119.5	9730.6	10108.8	10305.6	10220.4	10246.5	10296.2
5					3465.5	6947.9	8588.4	9636.0	10048.3	10418.3	10625.8	10663.9	10311.6	10479.0	10220.4
6				3400.6	6941.9	8669.1	9843.6	10536.9	10655.0	10841.4	10894.4	10659.3	10668.9	10416.1	10337.6
7			3160.6	6721.5	8562.2	9819.0	10412.3	10789.6	10524.2	10783.0	10418.5	10560.1	10390.3	10550.9	10333.9
8		2423.7	6092.8	8196.7	9614.6	10525.4	10823.5	10796.0	10862.4	10608.3	10614.7	10547.5	10570.3	10315.2	10305.7
9		3338.6	7265.1	9119.4	10049.3	10691.9	10735.1	11067.8	10677.9	10822.7	10451.0	10595.3	10344.9	10479.8	10203.6
10	1986.5	4063.2	8089.0	9724.7	10395.6	10854.0	10993.3	10816.7	10860.3	10574.1	10637.7	10356.5	10497.6	10190.2	10074.5
11	2668.1	6550.6	8750.5	10096.6	10457.3	10733.3	10433.1	10659.2	10456.5	10622.1	10343.7	10484.4	10232.6	10292.6	9660.9
12	3032.0	7142.4	9167.1	10337.5	10538.0	10501.5	10560.4	10355.2	10582.6	10341.1	10469.5	10222.4	10367.7	10033.3	9621.7
13	3222.3	7436.3	9375.4	10441.3	10343.5	10677.2	10381.1	10577.9	10349.8	10505.7	10264.0	10403.3	10074.8	10179.4	9906.4
14	3315.4	7576.3	9477.8	10496.4	10556.1	10443.4	10559.9	10322.9	10484.7	10196.2	10329.6	10060.0	10186.6	9948.4	9936.8
15	3350.9	7622.8	9455.0	10432.7	10291.9	10372.1	10351.0	10312.4	10192.0	10060.8	9892.0	9834.4	9908.2	9933.6	10052.0

FIGURE 4A-11E

AVERAGE BUNDLE
EXPOSURE, 9000 MWd/t

RIVER BEND STATION
UPDATED SAFETY ANALYSIS REPORT

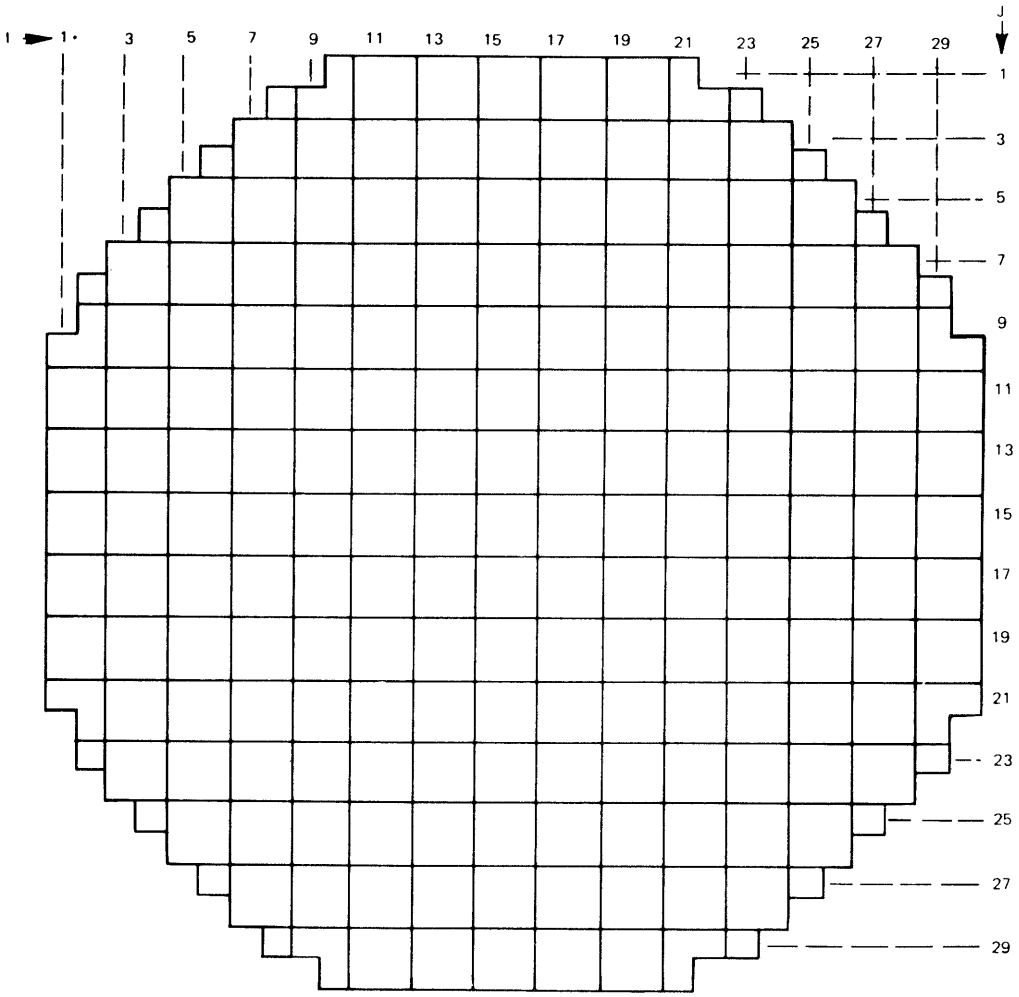

CONTROL ROD PATTERN (NOTCHES WITHDRAWN)

EXPOSURE	9200 MWd/t			
K_{eff}	1.0066			
ROD SEQUENCE	ALL RODS OUT			
POWER DISTRIBUTIONS		LOCATION		
		I	J	K
AXIAL	1.4413	–	–	8
RADIAL	1.2751	12	11	–
GROSS	1.8341	13	12	8
MCPR	1.4137	13	12	–
MLHGR	12.0184	13	12	8

I, J, K CODE COORDINATES
K = 1 = BOTTOM OF CORE
K = 25 = TOP OF CORE

FIGURE 4 A-12A

SUMMARY OF 9200 MWd/t CONDITION

RIVER BEND STATION
UPDATED SAFETY ANALYSIS REPORT

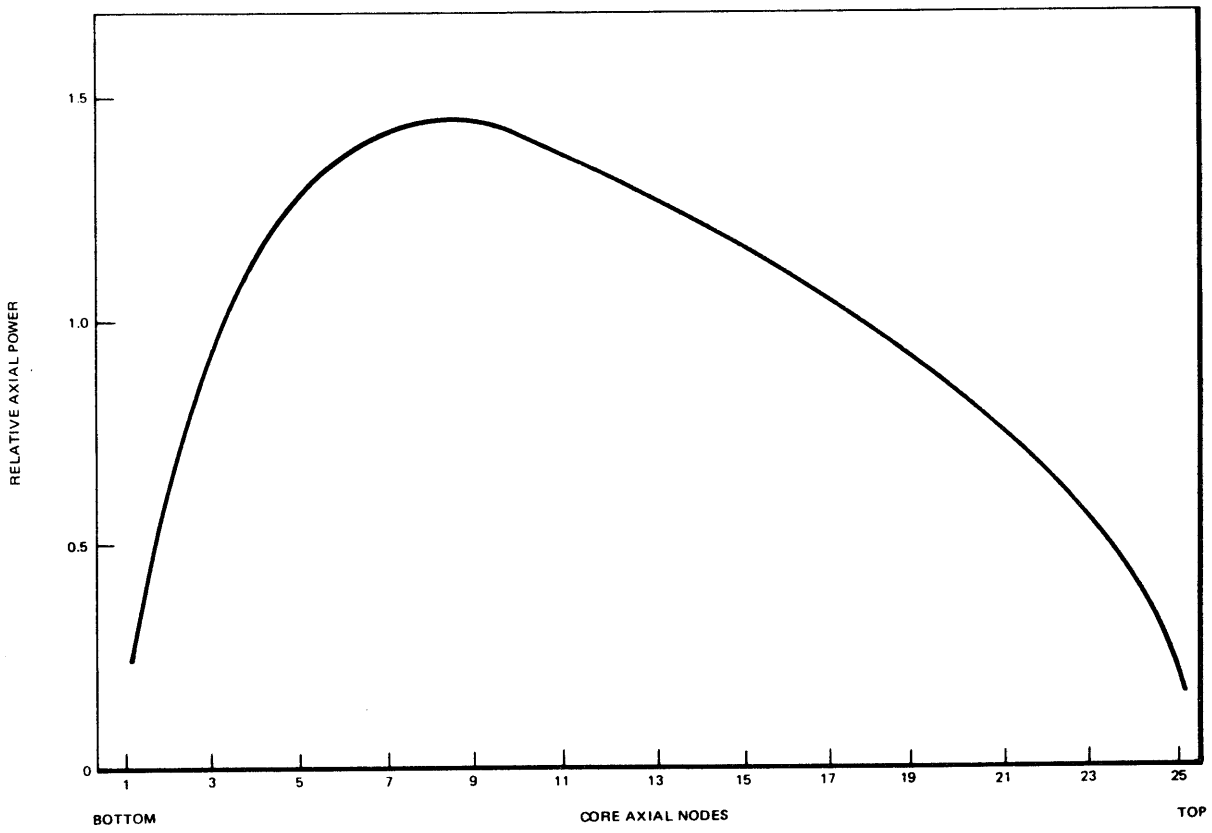

FIGURE 4A-12B

RELATIVE AXIAL POWER AT 9200 MWd/t CORE AVERAGE EXPOSURE

RIVER BEND STATION

UPDATED SAFETY ANALYSIS REPORT

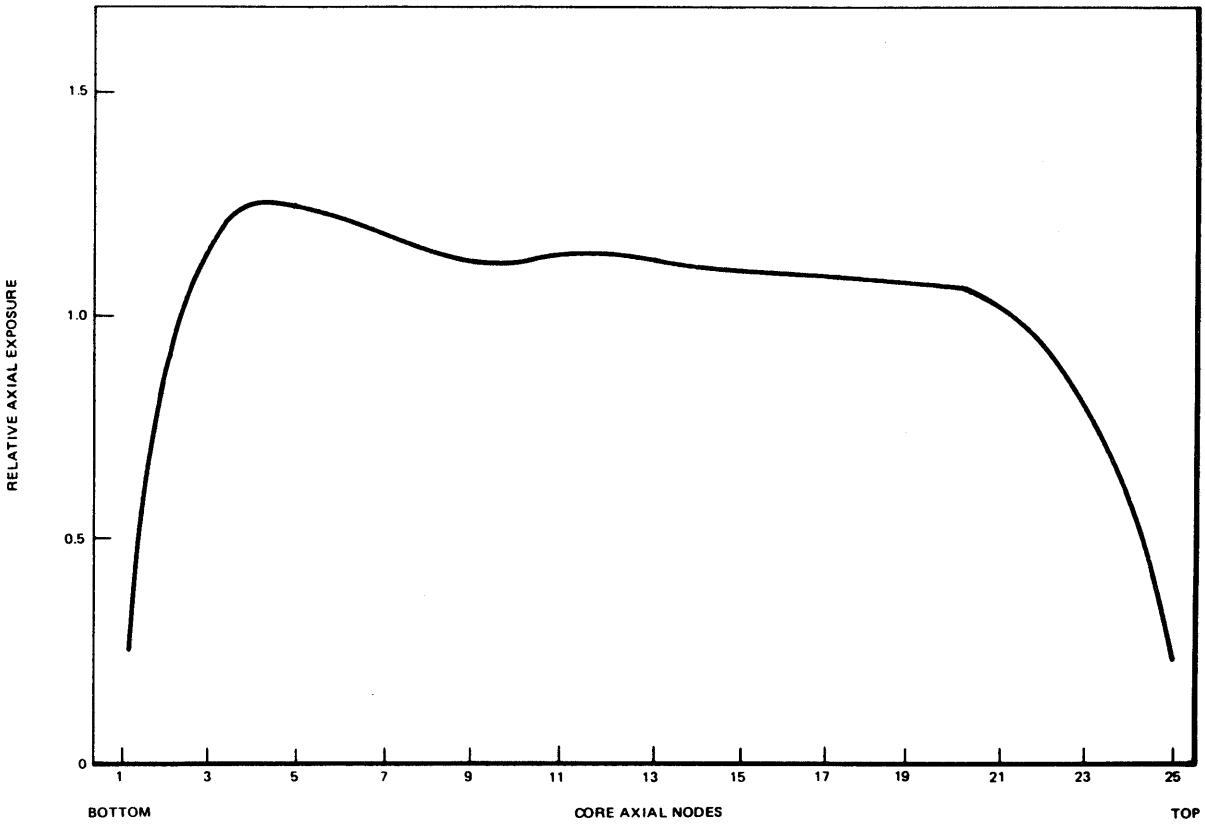

FIGURE 4A-12C

RELATIVE AXIAL EXPOSURE AT 9200 MWd/t CORE AVERAGE EXPOSURE

RIVER BEND STATION
UPDATED SAFETY ANALYSIS REPORT

I →	1	2	3	4	5	6	7	8	9	10	11	12	13	14	15
J															
1										0.2222	0.2950	0.3330	0.3522	0.3615	0.3650
2								0.2678	0.3634	0.4385	0.7196	0.7812	0.8106	0.8241	0.8288
3							0.3443	0.6690	0.7912	0.8706	0.9363	0.9752	0.9975	1.0075	1.0086
4						0.5664	0.7316	0.8794	0.9692	1.0263	1.0641	1.0850	1.0958	1.1016	1.0959
5					0.3714	0.7502	0.9104	1.0114	1.0786	1.1198	1.1414	1.1455	1.0934	1.1431	1.0774
6				0.3661	0.7499	0.9173	1.0241	1.0919	1.1386	1.1706	1.1806	1.1258	1.1778	1.1136	1.0951
7			0.3436	0.7369	0.9096	1.0233	1.0967	1.1378	1.1167	1.1959	1.1547	1.2123	1.1531	1.1946	1.1197
8		0.2671	0.6678	0.8760	1.0097	1.0897	1.1356	1.1105	1.1919	1.1594	1.2303	1.1800	1.2298	1.1596	1.1373
9		0.3624	0.7895	0.9673	1.0764	1.1351	1.1099	1.1659	1.1573	1.2316	1.1918	1.2529	1.1929	1.2352	1.1591
10	0.2210	0.4364	0.8082	1.0244	1.1155	1.1679	1.1884	1.1521	1.2290	1.1909	1.2010	1.2102	1.2023	1.1930	1.1730
11	0.2930	0.7102	0.9327	1.0620	1.1432	1.1821	1.1515	1.2257	1.1877	1.2556	1.2139	1.2751	1.2100	1.2616	1.1920
12	0.3300	0.7757	0.9697	1.0862	1.1457	1.1268	1.2100	1.1764	1.2487	1.2070	1.2736	1.2217	1.2750	1.2070	1.1929
13	0.3481	0.8025	0.9860	1.0851	1.0881	1.1746	1.1503	1.2205	1.1896	1.2593	1.2135	1.2735	1.2157	1.2596	1.1857
14	0.3565	0.8144	0.9940	1.0804	1.1349	1.1065	1.1908	1.1566	1.2321	1.1902	1.2588	1.2050	1.2590	1.1890	1.1713
15	0.3597	0.8187	0.9964	1.0842	1.0691	1.0894	1.1154	1.1340	1.1566	1.1708	1.1897	1.1911	1.1848	1.1710	1.1508

FIGURE 4A-12D

INTEGRATED POWER
PER BUNDLE, 9200 MWd/t

RIVER BEND STATION

UPDATED SAFETY ANALYSIS REPORT

I → 1	1	2	3	4	5	6	7	8	9	10	11	12	13	14	15
J															
1										2020.5	2706.3	3061.1	3236.1	3321.2	3357.3
2								2477.0	3407.4	4139.3	5061.1	7231.1	7483.0	7607.2	7664.0
3							3233.3	6228.5	7421.0	8254.9	8913.8	9289.8	9340.7	9423.9	9506.1
4						3479.4	6878.4	9379.2	9316.3	9938.8	10324.6	10525.9	10442.9	10470.4	10519.3
5					3541.2	7100.4	8773.4	9843.3	10260.7	10644.5	10855.9	10914.8	10552.3	10710.3	10438.5
6				3475.4	7094.8	8875.9	10052.0	10758.0	10864.4	11075.7	11129.5	10863.0	10924.1	10639.3	10557.7
7			3231.0	6870.8	8747.9	10027.6	10635.0	11019.3	10746.8	11016.5	10842.6	10815.5	10816.2	10787.7	10556.7
8		2478.6	6229.4	8379.4	9421.1	10747.7	11053.4	11018.6	11097.4	10830.6	10843.4	10566.0	10605.3	10541.3	10529.8
9		3413.1	7420.9	9317.8	10209.8	10923.7	10959.9	11305.1	10903.5	11052.3	10635.9	10769.9	10505.6	10710.2	10430.5
10	2032.2	4153.0	8267.3	9935.1	10625.2	11042.9	11234.7	11047.2	11100.6	10796.1	10834.4	10546.4	10732.0	10420.4	10304.4
11	2728.6	6697.9	8942.4	10315.1	10692.4	10975.7	10867.5	10996.3	10693.5	10865.1	10570.4	10722.5	10465.9	10539.8	9916.6
12	3100.2	7302.0	9366.6	10560.2	10774.1	10733.0	10806.1	10593.9	10833.5	10580.1	10738.8	10460.9	10619.1	10273.3	9860.1
13	3294.3	7601.7	9578.9	10665.5	10568.0	10919.5	10617.2	10828.7	10591.1	10759.6	10506.9	10658.1	10316.6	10433.3	10145.8
14	3369.2	7744.4	9683.1	10721.5	10792.0	10672.2	10805.4	10560.3	10736.7	10440.3	10585.0	10312.0	10442.0	10169.6	10175.0
15	3425.5	7791.8	9660.9	10657.1	10513.1	10597.3	10581.2	10545.8	10429.2	10300.1	9934.6	9877.1	10149.6	10172.4	10288.5

FIGURE 4A-12E

AVERAGE BUNDLE
EXPOSURE, 9200 MWd/t

RIVER BEND STATION
UPDATED SAFETY ANALYSIS REPORT

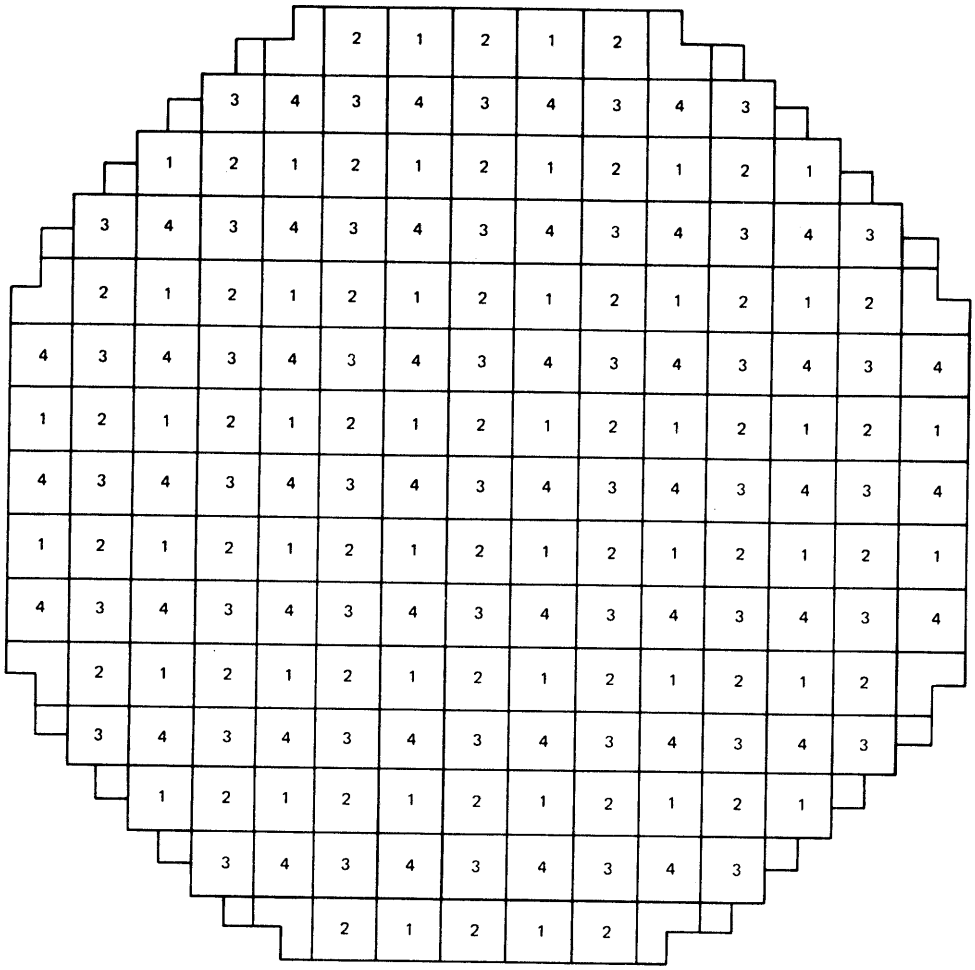

SEQUENCE:

A-1 = ROD TYPE 1 DEEP; TYPE 3 SHALLOW; 2 AND 4 OUT
A-2 = ROD TYPE 3 DEEP; TYPE 1 SHALLOW; 2 AND 4 OUT
B-1 = ROD TYPE 2 DEEP; TYPE 4 SHALLOW; 1 AND 3 OUT
B-2 = ROD TYPE 4 DEEP; TYPE 2 SHALLOW; 1 AND 3 OUT

FIGURE 4A-13

A AND B SEQUENCE DESIGNATIONS

RIVER BEND STATION
UPDATED SAFETY ANALYSIS REPORT

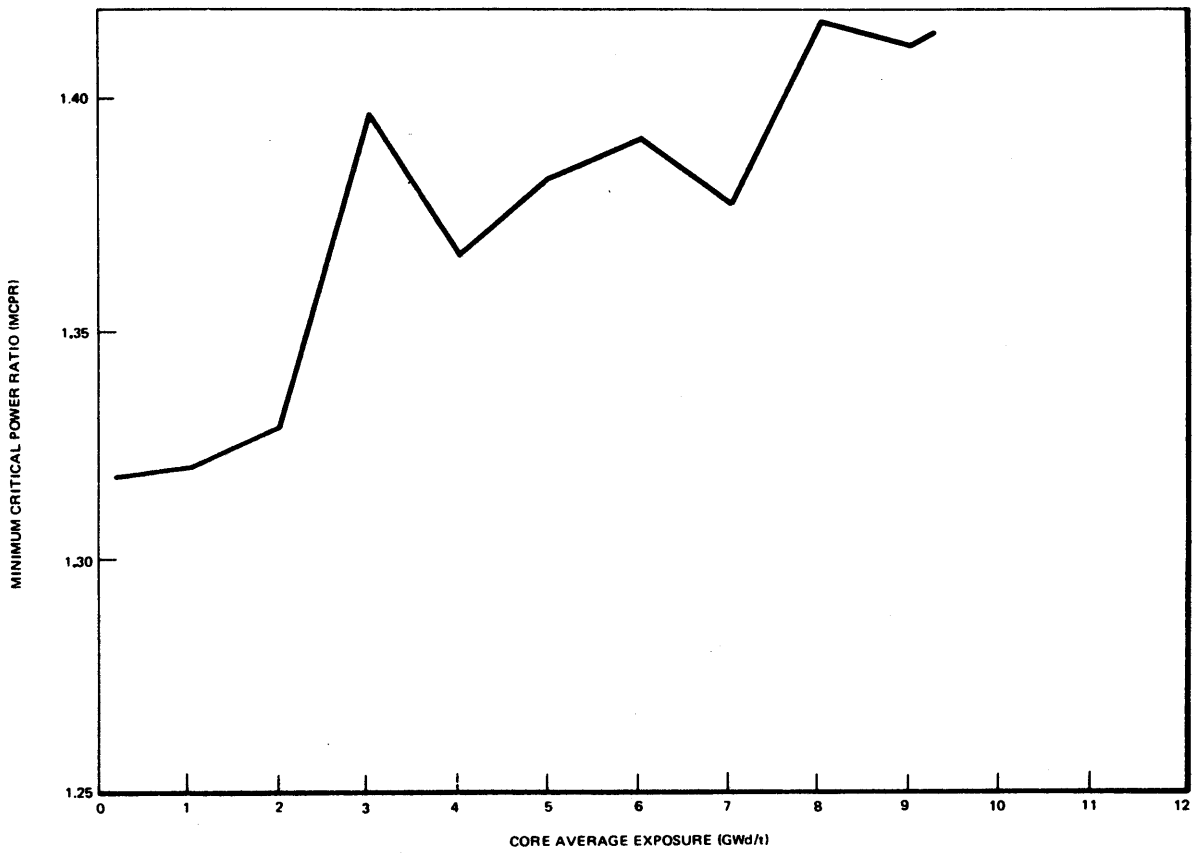

FIGURE 4A-14

MINIMUM CRITICAL POWER RATIO AS A FUNCTION OF CORE AVERAGE EXPOSURE

RIVER BEND STATION

UPDATED SAFETY ANALYSIS REPORT

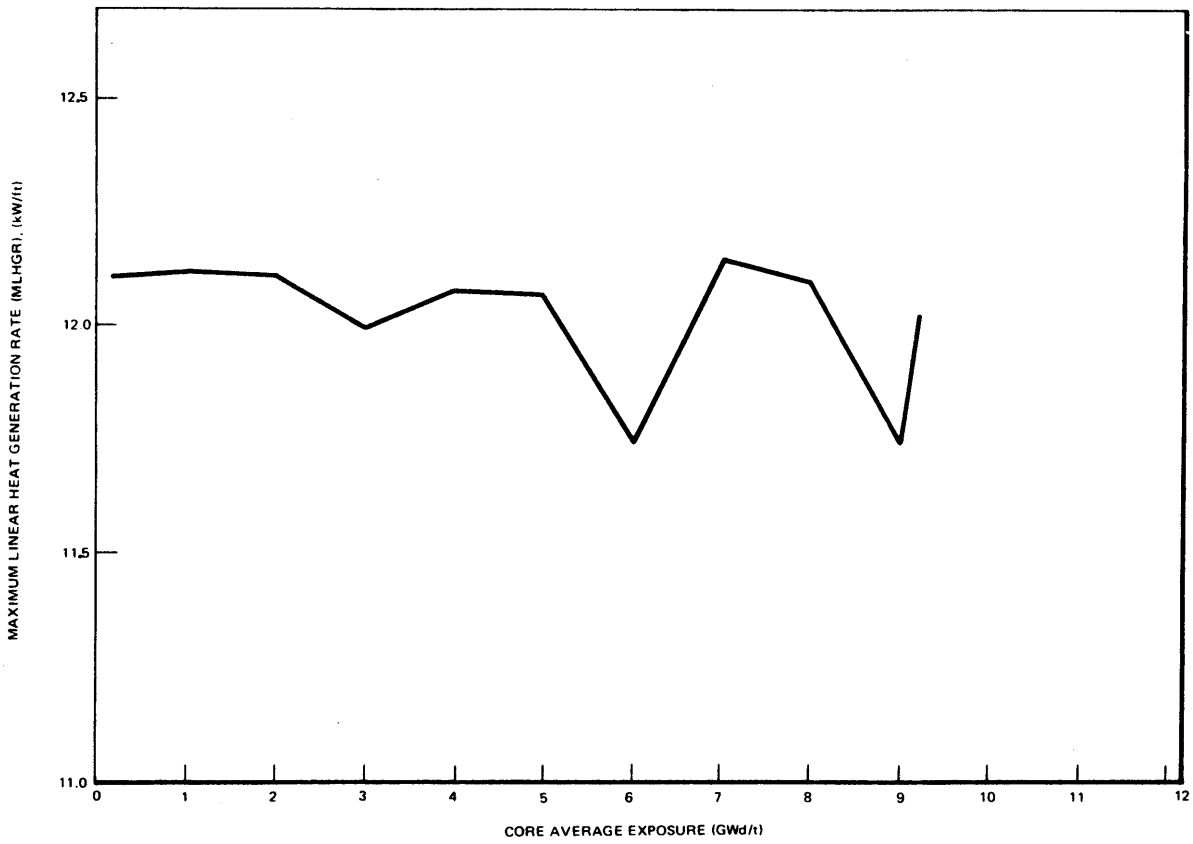

FIGURE 4A-15

MAXIMUM LINEAR HEAT GENERATION RATE AS A FUNCTION OF CORE AVERAGE EXPOSURE

RIVER BEND STATION

UPDATED SAFETY ANALYSIS REPORT

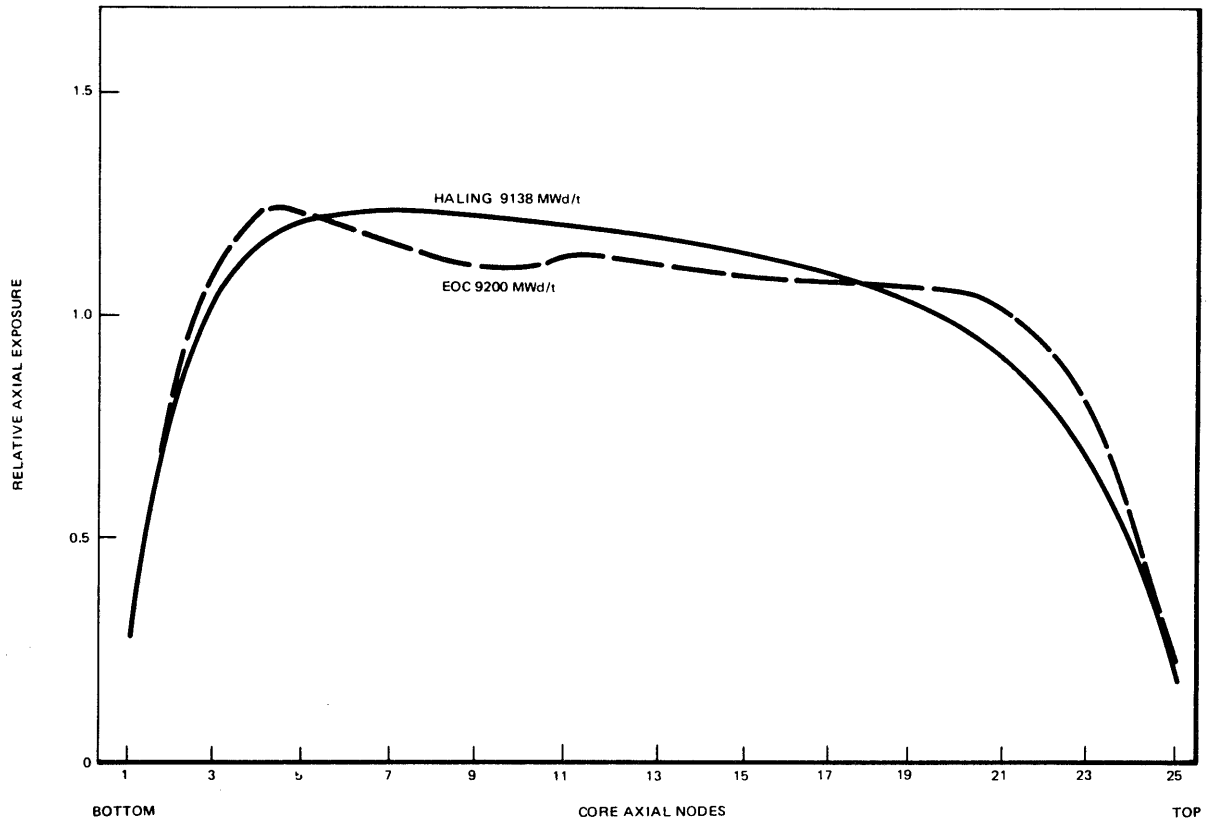

FIGURE 4A-16

A COMPARISON OF PREDICTED END-OF-CYCLE EXPOSURE AND TARGET HALING DISTRIBUTION

RIVER BEND STATION

UPDATED SAFETY ANALYSIS REPORT

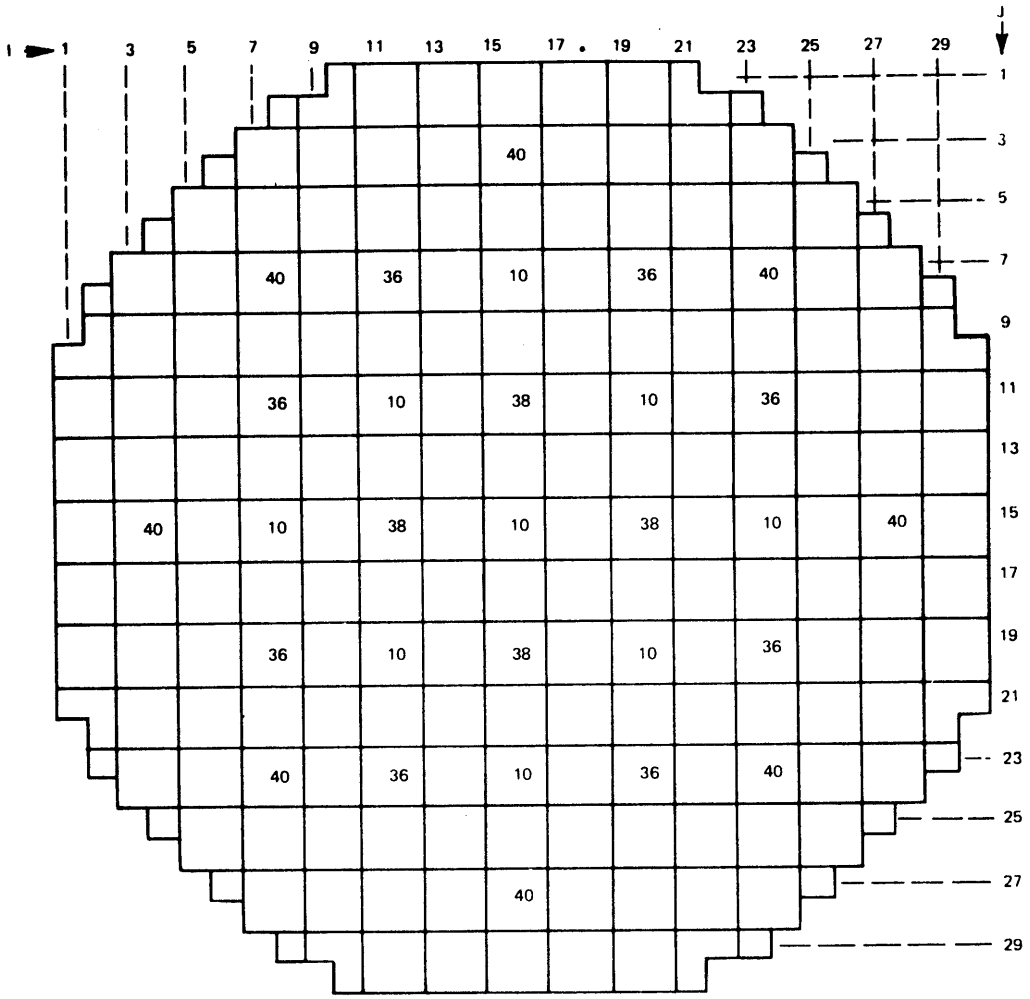

CONTROL ROD PATTERN (NOTCHES WITHDRAWN)

EXPOSURE	200 MWd/t			
K_{eff}	1.0037			
ROD SEQUENCE	A-2			
POWER DISTRIBUTIONS		LOCATION		
		I	J	K
AXIAL	1.3007	–	–	11
RADIAL	1.3253	13	14	–
GROSS	1.8304	8	11	11
MCPR	1.3308	14	13	–
MLHGR	12.0847	8	11	11

I, J, K CODE COORDINATES
K = 1 = BOTTOM OF CORE
K = 25 = TOP OF CORE

FIGURE 4A-17

UNDER-REACTIVE
MODEL, 200 MWd/t

RIVER BEND STATION
UPDATED SAFETY ANALYSIS REPORT

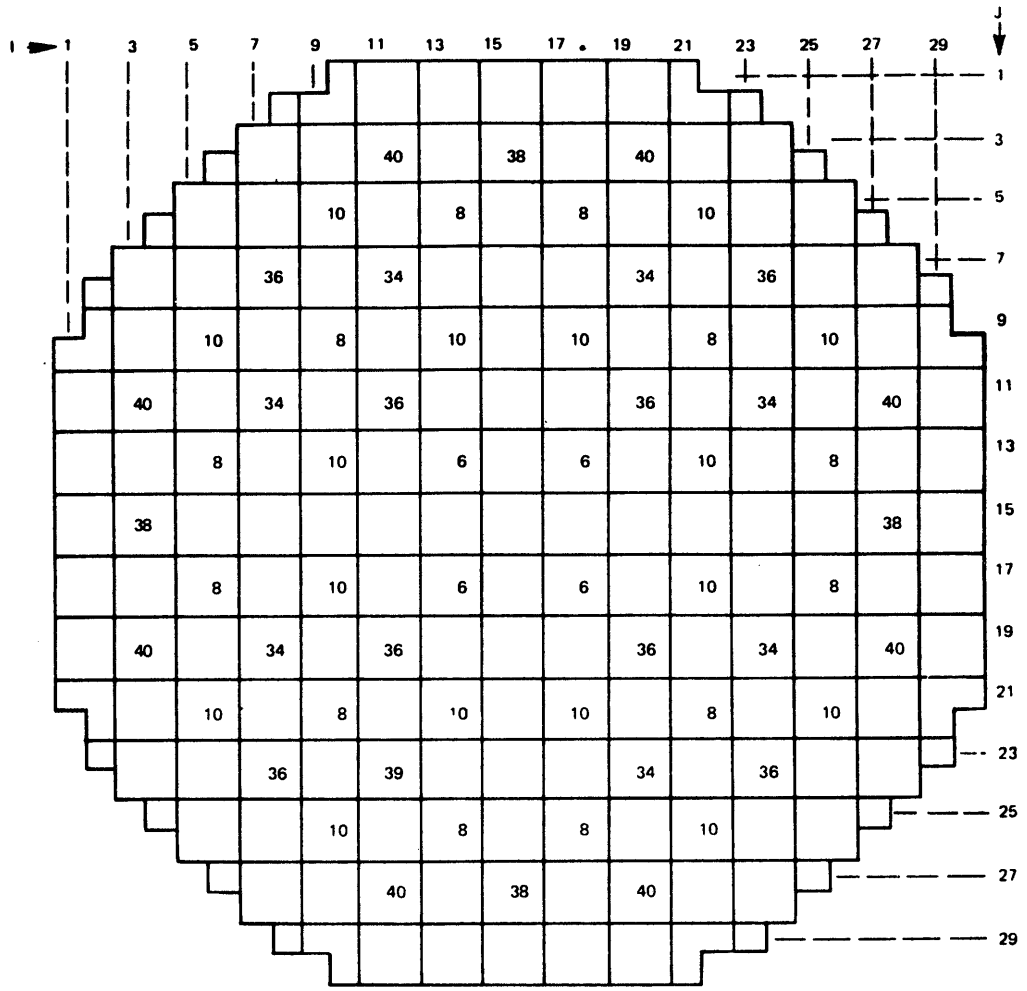

CONTROL ROD PATTERN (NOTCHES WITHDRAWN)

EXPOSURE		6000 MWd/t		
K_{eff}		0.9913		
ROD SEQUENCE		A-1		
POWER DISTRIBUTIONS		LOCATION		
		I	J	K
AXIAL	1.2829	–	–	8
RADIAL	1.3050	15	11	–
GROSS	1.8599	11	8	9
MCPR	1.3197	12	11	
MLHGR	12.2062	11	8	9

I, J, K CODE COORDINATES
K = 1 = BOTTOM OF CORE
K = 25 = TOP OF CORE

FIGURE 4A-18

OVER-REACTIVE
MODEL, 6000 MWd/t

RIVER BEND STATION
UPDATED SAFETY ANALYSIS REPORT

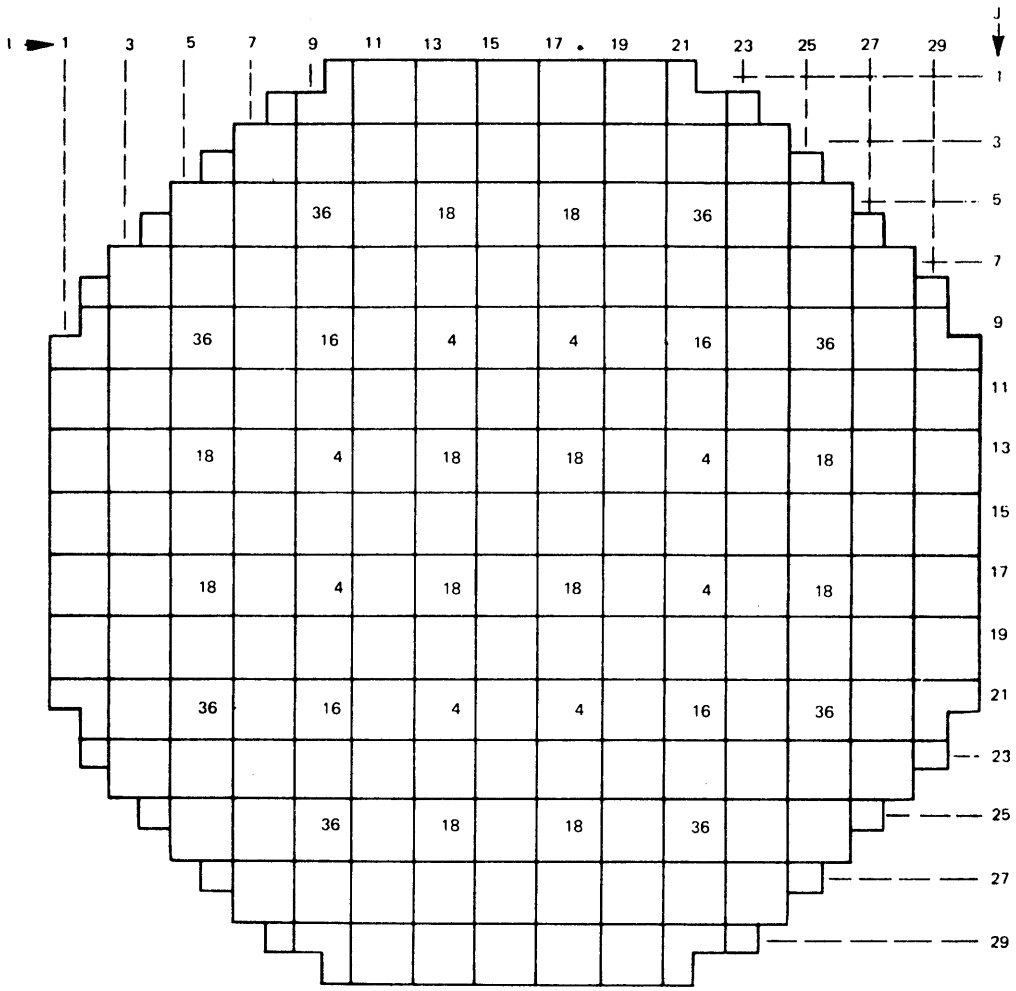

CONTROL ROD PATTERN (NOTCHES WITHDRAWN)

EXPOSURE	6000 MWd/t			
K_{eff}	1.0077			
ROD SEQUENCE	A-2			
POWER DISTRIBUTIONS		LOCATION		
		I	J	K
AXIAL	1.2299	–	–	17
RADIAL	1.3144	10	7	–
GROSS	1.8541	10	6	7
MCPR	1.3743	10	7	–
MLHGR	12.1932	10	6	7

I, J, K CODE COORDINATES
K = 1 = BOTTOM OF CORE
K = 25 = TOP OF CORE

FIGURE 4A-19

UNDER-REACTIVE
MODEL, 6000 MWd/t

RIVER BEND STATION
UPDATED SAFETY ANALYSIS REPORT

4B.0 CURRENT CYCLE FUEL AND CORE DESIGN

This appendix previously contained information regarding the following:

- Reload Fuel Bundles
- Reference Core Loading Pattern
- Calculated Core Effective Multiplication and Control System Worth with No Voids, 20°C
- Standby Liquid Control System Shutdown Capability
- Stability Analysis Results
- Loss of Coolant Accident Results

This information has been relocated to Appendix 15B.